

Circularly polarized-thermally activated delayed fluorescent materials based on chiral bicarbazole donors

Laurélie Poulard,^a Sitthichok Kasemthaveechok,^b Max Coehlo,^a Ramar Arun Kumar,^{a,c} Lucas Frédéric,^a Patthira Sumsalee,^b Timothée d'Anfray,^a Sen Wu,^d Jingxiang Wang,^d Tomas Matulaitis,^d Jeanne Crassous,^b Eli Zysman-Colman,^d Ludovic Favereau*^b and Grégory Pieters*^a

-
- a. *Université Paris-Saclay, CEA, INRAE, Département Médicaments et Technologies pour la Santé (DMTS), SCBM, 91191 Gif-sur-Yvette, France. E-mail: Gregory.pieters@cea.fr*
- b. *Univ Rennes, CNRS, ISCR-UMR 6226, ScanMAT–UMS 2001, F-35000 Rennes, France. E-mail: ludovic.favereau@univ-rennes1.fr*
- c. *SRM Research Institute, Department of Chemistry, SRM Institute of Science and Technology, Kattankulathur, 603203 Chennai, Tamilnadu, India.*
- d. *Organic Semiconductor Centre, EaStCHEM School of Chemistry, University of St Andrews, St Andrews, Fife, UK, KY16 9ST.*

The research data supporting this publication can be accessed at <https://doi.org/10.17630/16db897f-026e-4ae1-ab0c-5ef416aa8ed8>

Table of contents	
General Information	3
Synthetic procedures and characterizations	5
NMR spectra	11
SFC purification	21
B²TPNF₂	21
B²CNPyrF₂	22
UV-vis spectra.....	23
Absorption spectra in DCM	23
Absorption spectra in toluene	25
Emission spectra.....	27
CV and DPV	29
TCSPC experiments.....	31
Rate constants.....	39
ΔE_{ST} determination.....	39
ECD spectra	42
B¹TPNF₂	42
B²TPNF₂	42
B²CNPyrF₂	43
Circularly polarized luminescence spectra	45
B¹TPNF₂	45
B²TPNF₂	46
B²CNPyrF₂	47
Theoretical calculations.....	48
Cartesian coordinates of the optimized geometry of ground state B¹TPNF₂ (M06-2X/6-31+G(d,p)/CPCM(DCM)):	48
Simulated UV spectrum of B¹TPNF₂ :	49
Cartesian coordinates of the optimized geometry of ground state B²TPNF₂ (M06-2X/6-31+G(d,p)/CPCM(DCM)):	50
Simulated UV spectrum of B²TPNF₂ :	51
Cartesian coordinates of the optimized geometry of ground state B²CNPyrF₂ (M06-2X/6-31+G(d,p)/CPCM(DCM)):	52
Simulated UV spectrum of B²CNPyrF₂	53
Theoretical calculations of ΔE_{ST}	54
Theoretical dissymmetry factor calculations	55
Isosurfaces of LUMO+1 for B¹TPNF₂ , B²TPNF₂ and B²CNPyrF₂	59
UV-Vis spectra and computational details regarding the first excitations and oscillator strengths for each compound	60

General Information

All commercial reagents purchased from Aldrich, Alfa Aesar, TCI and Merck were used without further purification. Progress of reactions was monitored by Thin Layer Chromatography (TLC) on pre-coated Merck silica gel plates (60F-254). Visualization was accomplished by UV light (254 and 365 nm).

Flash chromatography was performed with a CombiFlash (COMBIFLASH RF, Teledyne Isco) using the appropriate normal phase silica gel columns, eluting with cyclohexane, ethyl acetate (EtOAc), dichloromethane (DCM) and methanol (MeOH) mixtures. In order to be purified through a recycling size exclusion chromatography (SEC) apparatus, the compounds were solubilized in HPLC grade chloroform (stabilized with ethanol). Prior to injection, the solution was filtered through a 0.45 μm PTFE filter. Purification was performed on a LC-9160 II NEXT system from the Japan Analytical Industry Co., Ltd. (JAI) equipped with coupled UV-vis 4 channels NEXT through a set of two JAIGEL-2H columns at an elution rate of 10 mL \cdot min⁻¹ (CHCl₃).

Chiral separation and analysis were performed on a JASCO supercritical fluid chromatography.

Analytical conditions: Column: CHIRALPAK IG 250 \times 4.6 mm, 5 μm ; Flow Rate: 4 mL/min; Temperature: 40 $^{\circ}\text{C}$; Pressure: 100 bar; Detection: UV 200-400 nm; Solvent: 80% CO₂, 20% i-PrOH for **B²TPNF₂**. 50% CO₂, 50% MeOH for **B²CNPyrF₂**.

Preparative conditions: Column: CHIRALPAK IG 250 \times 21 mm, 5 μm ; Flow rate: 70 mL/min; Temperature: 40 $^{\circ}\text{C}$; Pressure: 100 bar; Detection: UV 200-400 nm; Solvent: 80% CO₂, 20% i-PrOH for **B²TPNF₂**. 50% CO₂, 50% MeOH for **B²CNPyrF₂**.

¹H NMR (400 MHz), ¹³C NMR (101 MHz) and ¹⁹F NMR (376 MHz) were recorded on a Bruker Advance 400 spectrometer. Chemical shifts are reported in parts per million (ppm) downfield from residual solvent peaks and coupling constants are reported as Hertz (Hz). Splitting patterns are designated as singlet (s), doublet (d), triplet (t), doublet of doublets (dd), doublet of triplets (dt), triplet of doublets (td). Splitting patterns that could not be interpreted or easily visualized are designated as multiplet (m). Broad signals are designated as (br).

Electrospray ionization mass spectra were recorded using an xevo G2-XS QToF mass spectrometer.

Melting points were recorded on a Buchi B-540 melting point apparatus. Infrared spectra were recorded on a Perkin Elmer Spectrum Two FT-IR Spectrometer.

UV-visible absorption spectra were recorded on a Jasco V-750 spectrometer using a 10 mm path quartz cell.

Circular dichroism (CD) spectra were recorded on a Jasco (model J-815) spectropolarimeter equipped with a Peltier thermostated cell holder and Xe laser. Data were recorded at 20 $^{\circ}\text{C}$ using a 1 mm \times 1 cm cell. The obtained signals were processed by subtracting solvent and cell contribution.

Emission spectra and TCSPC (Time-Correlated Single Photon Counting) experiments were performed on an Edinburgh FS-5 spectrofluorimeter with a SC-20 module. A right-angle configuration was used. The absolute fluorescence quantum yields for solutions were determined using an SC-30 integrating sphere or using a reference. The relative fluorescence quantum yields for solutions were determined using quinine sulfate ($\Phi_F = 0.59$ in 0.1M HClO₄)^[S1] as reference with the following formula:

$$\Phi_F(x) = \Phi_F(0) \frac{1 - 10^{A_0 S_x} \left(\frac{n_x}{n_0}\right)^2}{1 - 10^{A_x S_0} \left(\frac{n_0}{n_x}\right)^2}$$

Where $\Phi_F(0)$ is the quantum yield of the reference, A_0 and A_x respectively absorbance of the reference and the studied compound at the excitation wavelength; S_x and S_0 respectively area under the

emission peak of the reference and the studied compound; n_0 and n_x respectively refractive index of the solvent of the reference and the studied compound.

Cyclic Voltammetry (CV) and differential pulse voltammetry (DPV) analysis were performed on an Electrochemical Analyzer potentiostat model 620E from CH Instruments. Samples were prepared as DCM solutions, which were degassed by sparging with DCM-saturated argon gas for 5 minutes prior to measurements. All measurements were performed using 0.1 M DCM solution of tetra-*n*-butylammonium hexafluorophosphate ($[n\text{Bu}_4\text{N}]\text{PF}_6$). An Ag/Ag⁺ electrode was used as the reference electrode while a platinum electrode and a platinum wire were used as the working electrode and counter electrode, respectively. The redox potentials are reported relative to a saturated calomel electrode (SCE) with a ferrocenium/ferrocene (Fc⁺/Fc) redox couple as the internal standard (0.46 V vs SCE).^[S2]

The singlet-triplet splitting energy ΔE_{ST} was determined by recording the prompt fluorescence and phosphorescence spectra at 77 K. Emission from the samples was focused onto a spectrograph (Chromex imaging, 250is spectrograph) and detected on a sensitive gated iCCD camera (Stanford Computer Optics, 4Picos) having subnanosecond resolution. Phosphorescence spectra were measured 1 ms after the excitation of the Nd:YAG laser pulse with an iCCD exposure time of 8.5 ms. Prompt fluorescence spectra were measured 1 ns after the excitation with iCCD exposure time of 100 ns.

The circularly polarized luminescence (CPL) measurements were performed using a JASCO CPL-300 instrument at room temperature in 10*10 mm cell. Excitation wavelength and instrument parameters were adapted for every sample. Data pitch was set at 1 nm and spectra displayed are mean values of a minimum of 10 accumulations.

Kohn–Sham density functional theory (DFT) as implemented in the Gaussian (G16) package was used for the computations utilizing the CAM-B3LYP functional and the def2-SV(P) basis set.^[S3] Absorption spectra were computed via time-dependent DFT (TD-DFT) response theory. Absorption spectra were simulated from the lowest 200 vertical singlet electronic excitations. The molecular orbitals were plotted with Avogadro 1.2.0 and TDDFT data generated using GaussSum 3.0. The optimized geometry in the S_1 state and transition electric and magnetic dipole moments were calculated using time-dependent DFT within the Tamm-Dancoff approximation (TDA-DFT) at the M062X/6-311G(d,p) level of theory in the gas phase in the Gaussian (G16) package. Dissymmetry factor (g) for emission was calculated by the following formula:

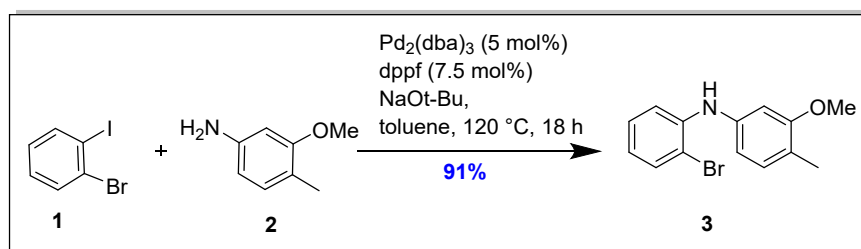
$$g = \frac{4|\boldsymbol{\mu}||\boldsymbol{m}|}{|\boldsymbol{\mu}|^2 + |\boldsymbol{m}|^2} \cos\theta$$

Where $\boldsymbol{\mu}$ and \boldsymbol{m} refer to the transition electric dipole moment and transition magnetic dipole moment vectors, respectively. θ is the angle between $\boldsymbol{\mu}$ and \boldsymbol{m} .^[S4]

Synthetic procedures and characterizations

Enantiopure **B**¹ was prepared according to the literature.^[S5] All characterized data matched those of reference S4.

Protocols for the synthesis of B²



N-(2-bromophenyl)-3-methoxy-4-methylaniline (3):

Tris(dibenzylideneacetone)dipalladium(0) (228 mg, 0.25 mmol, 2.5 mol%), sodium *tert*-butoxide (1.440 g, 15 mmol, 1.5 equiv.), 1,1'-bis(diphenylphosphino)ferrocene (dppf) (275 mg, 0.5 mmol, 5 mol%), 3-methoxy-4-methylaniline (1.370 g, 10 mmol, 1 equiv.), were placed in a round bottom flask under a argon atmosphere and dry toluene (12.5 mL) and 1-bromo-2-iodobenzene (1.275 mL, 10 mmol, 1 equiv.) were added sequentially. The reaction mixture was stirred at 110 °C for 18 h under an argon atmosphere. Consumption of 3-methoxy-4-methylaniline was monitored by TLC. After cooling to room temperature, the reaction mixture was diluted with water 100 mL and extracted with dichloromethane (4 × 125 mL). The collected organic layer was dried over anhydrous Na₂SO₄ and after filtration, concentrated in vacuum. The obtained crude product was purified by silica gel column chromatography (*n*-heptane / dichloromethane, 95/5 to 8/2) and the titled compound **3** obtained as a white solid (2.670 g, 91% yield).

TLC: R_f = 0.5 in 40% dichloromethane in *n*-heptane (UV 254 nm)

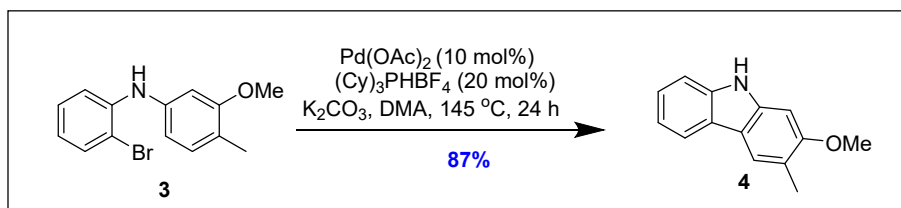
Melting point: 94-96 °C

¹H NMR (400 MHz, CDCl₃) δ 7.51 (dd, *J* = 7.9, 1.4 Hz, 1H), 7.19 – 7.12 (m, 2H), 7.09 – 7.07 (m, 1H), 6.73 – 6.66 (m, 3H), 6.01 (br, 1H), 3.81 (s, 3H), 2.20 (s, 3H).

¹³C NMR (101 MHz, CDCl₃) δ 158.4, 142.1, 140.2, 132.8, 130.9, 128.0, 121.6, 120.2, 115.2, 113.0, 111.5, 104.1, 55.3, 15.6.

IR (cm⁻¹): 3369, 2909, 1610, 1523, 1508.

HRMS (ESI) *m/z*: [M + H]⁺ calcd for C₁₄H₁₅BrNO, 292.0337; found, 292.0340



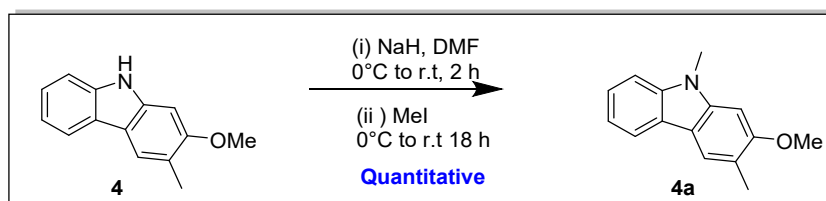
2-methoxy-3-methyl-9H-carbazole (**4**):

Under an argon atmosphere *N*-(2-bromophenyl)-3-methoxy-4-methylaniline **3** (2.4 g, 8.25 mmol, 1 equiv.), tricyclohexylphosphonium tetrafluoroborate (607 mg, 20 mol%), Pd(OAc)₂ (184 mg, 10 mol%) and K₂CO₃ (2.25 g, 2 equiv.) were taken in a round bottom flask and anhydrous *N,N*-dimethylacetamide (50 mL) was added. The reaction mixture was stirred at 145 °C for 18 hours. Then, the reaction mixture was diluted with dichloromethane and filtered through Celite using excess of dichloromethane. The filtered solution was concentrated *in vacuo* and the crude product was again dissolved with dichloromethane (100 mL) and water (100 mL) added. The mixture was extracted with another 2 × 100 mL of dichloromethane. The collected organic layer was dried over anhydrous Na₂SO₄ and after filtration, concentrated *in vacuo*. The crude product was solubilized with a minimum amount of ethyl acetate and *n*-heptane was added slowly. The obtained precipitate was filtered and washed with *n*-heptane and dried under vacuum. The desired product **4** obtained as a whitish grey colour solid, 1520 mg, 87% yield.

¹H NMR (400 MHz, Acetone-*d*₆) δ 10.06 (br, 1H), 7.96 (ddt, *J* = 7.7, 1.2, 0.6 Hz, 1H), 7.81 (s, 1H), 7.42 (dt, *J* = 8.1, 0.9 Hz, 1H), 7.26 (ddd, *J* = 8.1, 7.2, 1.2 Hz, 1H), 7.13 – 7.10 (m, 1H), 7.02 (s, 1H), 3.90 (s, 3H), 2.31 (s, 3H).

¹³C NMR (101 MHz, Acetone-*d*₆) δ 158.4, 140.9, 140.9, 124.7, 124.3, 122.1, 119.9, 119.6, 119.1, 116.9, 111.4, 111.4, 93.5, 93.5, 55.8, 17.0.

Spectral data were in agreement with those previously reported.^[S6]



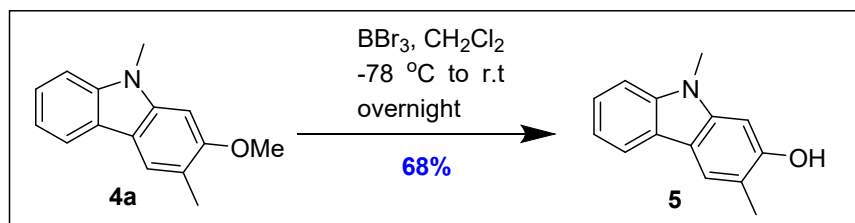
2-methoxy-3,9-dimethyl-9H-carbazole (**4a**):

Under an argon atmosphere 2-methoxy-3-methyl-9H-carbazole **4** (1.5 g, 7.10 mmol, 1 equiv.) and NaH in mineral oil (60%, 313 mg, 7.81 mmol, 1.1 equiv.) were taken in a round bottom flask and anhydrous *N,N*-dimethylformamide (30 mL) was added at 0 °C. The reaction mixture was stirred at room temperature for 2 h. Then the reaction mixture cooled again to 0 °C and MeI (0.490 mL, 7.81 mmol, 1.1 equiv.) was added dropwise, and the reaction mixture was allowed to stir at RT for 18 h. Then DMF was removed under vacuum. The crude product was diluted with 50 mL of ethyl acetate and washed with 3 × 30 mL of water and 30 mL of brine solution. The organic layer was dried over anhydrous Na₂SO₄ and concentrated under vacuum. Proton NMR of the crude product was clean, and the product was used for the next step without further purification. The desired product **4a** obtained as brown solid with quantitative yield.

^1H NMR (400 MHz, CDCl_3) δ 7.98 (d, $J = 7.7$ Hz, 1H), 7.82 (s, 1H), 7.41 – 7.34 (m, 2H), 7.20 (ddd, $J = 8.0, 6.8, 1.3$ Hz, 1H), 6.80 (s, 1H), 3.98 (s, 3H), 3.81 (s, 3H), 2.39 (s, 3H).

^{13}C NMR (101 MHz, CDCl_3) δ 157.4, 140.7, 140.7, 123.8, 122.8, 121.5, 119.2, 118.6, 118.5, 115.5, 108.0, 90.3, 55.5, 29.1, 16.6.

Spectral data were in agreement with those previously reported.^[S7]



3,9-dimethyl-9H-carbazol-2-ol (5):

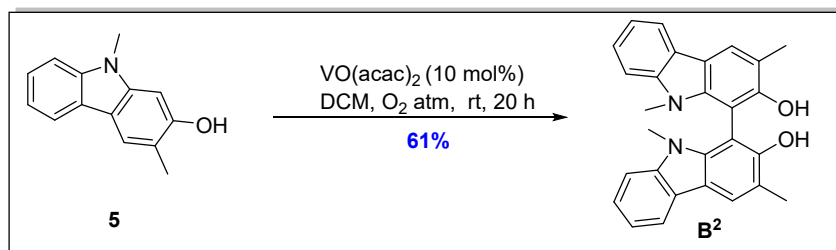
Under an argon atmosphere 2-methoxy-3,9-dimethyl-9H-carbazole **4a** (1.45 g, 6.44 mmol, 1 equiv.) was dissolved in anhydrous CH_2Cl_2 (50 mL) in a round-bottom flask and cooled to $-78\text{ }^\circ\text{C}$. Then BBr_3 (12.88 mL, 1.0 M in CH_2Cl_2 , 12.88 mmol, 2 equiv.) was added dropwise for 10 min with stirring at $-78\text{ }^\circ\text{C}$. The resulting mixture was stirred at $-78\text{ }^\circ\text{C}$ for 30 minutes, followed by warming up to room temperature and allowed to stir for overnight at room temperature. Then reaction mixture was cooled to $-78\text{ }^\circ\text{C}$ and was quenched with a saturated aqueous solution of NaHCO_3 (40 mL). The aqueous layer was extracted with ethyl acetate (80 mL \times 3). The combined organic layer was washed with brine (50 mL \times 3) and the organic layer dried over anhydrous Na_2SO_4 . After filtration and evaporation, the residue was purified by flash chromatography on silica gel (*n*-heptane /ethyl acetate= 9/1 to 4/1) to afford the desired compound **5** as a whitish grey color solid (920 mg, 68%).

TLC: $R_f = 0.4$, 30% ethyl acetate in *n*-heptane (UV 254 nm)

^1H NMR (400 MHz, CDCl_3) δ 7.98 – 7.96 (m, 1H), 7.81 (s, 1H), 7.42-7.38 (m, 1H), 7.33 (d, $J = 8.1$ Hz, 1H), 7.22-7.18 (m, 1H), 6.79 (s, 1H), 4.88 (s, 1H), 3.74 (s, 3H), 2.43 (s, 3H).

^{13}C NMR (101 MHz, CDCl_3) δ 153.1, 141.0, 140.9, 124.2, 122.8, 121.8, 119.2, 118.7, 116.5, 115.4, 108.0, 94.5, 29.0, 16.0.

Spectral data were in agreement with those previously reported.^[S7]



3,3',9,9'-tetramethyl-9H,9'H-[1,1'-bicarbazole]-2,2'-diol (**B**²):

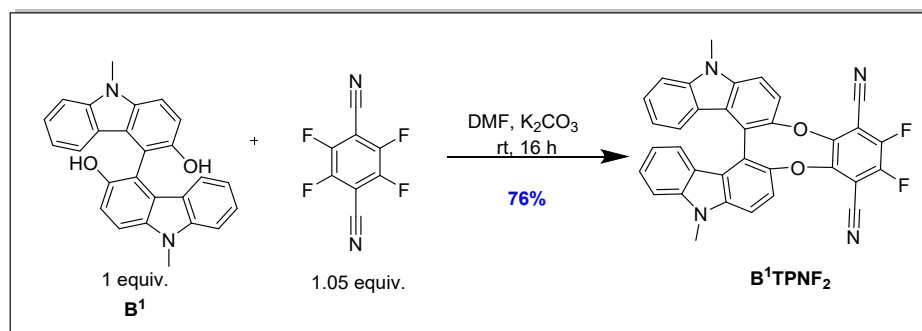
Vanadyl acetylacetonate (113 mg, 0.426 mmol, 10 mol%) was added to a solution of 3,9-dimethyl-9H-carbazol-2-ol (900 mg, 4.265 mmol, 1 equiv.) in dichloromethane (44 mL) and the mixture was stirred at room temperature for 20 h under an oxygen atmosphere (oxygen balloon). The reaction mixture was filtered through Celite and concentrated under vacuum. The crude product was purified by flash chromatography on silica gel (*n*-heptane/ethyl acetate, 95/5 to 93/7) provided the *N*-methyl BICOL **B**² as a pale yellow solid (545 mg, 61%).

TLC: R_f = 0.5 in 10% ethyl acetate in *n*-heptane (UV 254 nm)

¹H NMR (400 MHz, CDCl₃) δ 8.06 – 8.03 (m, 4H), 7.41 – 7.37 (m, 2H), 7.26-7.23 (m, 4H), 5.21 (s, 2H), 3.17 (s, 6H), 2.49 (s, 6H).

¹³C NMR (101 MHz, CDCl₃) δ 152.4, 141.5, 138.9, 124.5, 123.4, 122.6, 119.3, 119.1, 117.0, 116.8, 108.5, 98.8, 29.9, 16.6.

Spectral data were in agreement with those previously reported. ^[S7]



B¹TPNF₂:

Under an argon atmosphere, **B**¹ (40 mg, 0.102 mmol, 1 equiv.), 2,3,5,6-tetrafluoroterephthalonitrile (22 mg, 0.11 mmol, 1.05 equiv.) and anhydrous K₂CO₃ (70 mg, 0.507 mmol, 4 equiv.) were taken in an oven dried Schlenk flask. Then anhydrous DMF (5 mL) was added, and the reaction mixture was stirred at RT for 16 hours. Then the reaction mixture was diluted with 15 mL of ethyl acetate. The organic phase was washed with 3 × 10 mL of distilled water and 10 mL of brine. The organic phase dried over anhydrous Na₂SO₄ and concentrated under vacuum. The crude product was purified by SiO₂ column chromatography using (*n*-heptane/ethyl acetate, 5/5). The desired product **B**¹TPNF₂ (racemic) obtained as yellow solid (43 mg, 76%) and was later purified by size-exclusion chromatography. The *R*- and *S*- enantiomer were prepared using the same method with enantiopure **B**¹.

TLC: $R_f = 0.4$, 50% ethyl acetate/*n*-heptane (UV 254 nm, 365 nm-fluorescent yellow)

Melting point : $>260^\circ\text{C}$

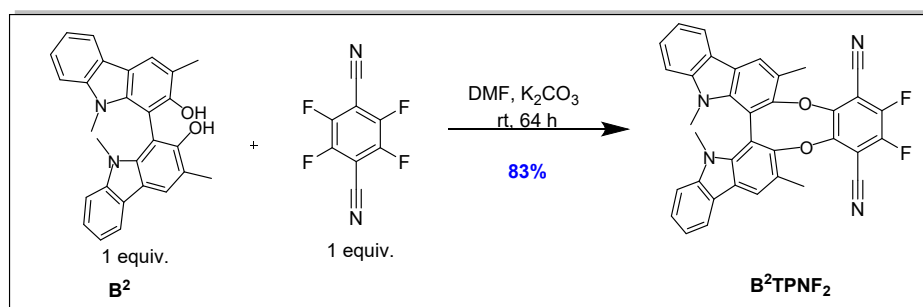
^1H NMR (400 MHz, CD_2Cl_2) δ 7.64 (d, $J = 8.8$ Hz, 2H), 7.56 (d, $J = 8.8$ Hz, 2H), 7.45 (d, $J = 8.3$ Hz, 2H), 7.34 (ddd, $J = 8.3, 7.1, 1.2$ Hz, 2H), 6.94 (d, $J = 8.0$ Hz, 2H), 6.64 (ddd, $J = 8.0, 7.0, 1.0$ Hz, 2H), 3.98 (s, 6H).

^{13}C NMR (101 MHz, CD_2Cl_2) δ 148.5, 147.8, 145.3, 145.2, 144.7, 142.2, 139.4, 126.5, 122.8, 122.0, 121.6, 120.9, 118.9, 118.6, 110.0, 109.1, 108.7, 102.8, 29.4.

^{19}F NMR (376 MHz, CD_2Cl_2) δ -135.54.

IR (cm^{-1}) : 3434, 2926, 2242, 1625, 1478, 1381, 1302, 1259, 1222, 1183.

HRMS (ESI) m/z : $[\text{M} + \text{Na}]^+$ calcd for $\text{C}_{34}\text{H}_{18}\text{N}_4\text{O}_2\text{F}_2\text{Na}$, 575.1290 ; found, 575.1288.



B²TPNF₂:

Under an argon atmosphere, *N*-Methyl BICOL **B²** (100 mg, 0.238, 1 equiv.), 2,3,5,6-tetrafluoroterephthalonitrile (48 mg, 0.238 mmol, 1 equiv.) and anhydrous K_2CO_3 (82 mg, 0.595 mmol, 2.5 equiv.) were taken in an oven dried 5 mL glass vial. Then anhydrous DMF (2 mL) was added, and the reaction mixture was stirred at rt for 64 hours. Then the reaction mixture was diluted with 15 mL of ethyl acetate. The organic phase was washed with 3×10 mL of distilled water and 10 mL of brine. The organic phase dried over anhydrous Na_2SO_4 and concentrated under vacuum. The crude product was purified by SiO_2 column chromatography (*n*-hexane/dichloromethane, 6/4). The desired product **B²TPNF₂** (racemic) obtained as yellow solid (115 mg, 83%) and was later purified by chiral SFC chromatography.

TLC: $R_f = 0.4$, 40% dichloromethane in *n*-hexane (UV 254 nm, 365 nm-fluorescent yellow)

Melting point: $380\text{-}381^\circ\text{C}$

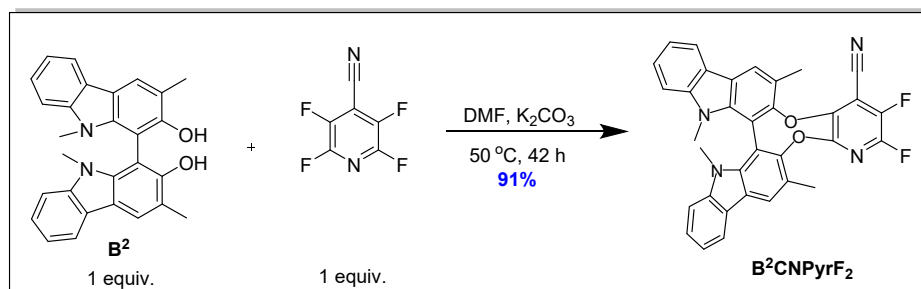
^1H NMR (400 MHz, CDCl_3) δ 8.12-8.10 (m, 2H), 8.08 (d, $J = 0.7$ Hz, 2H), 7.51 – 7.47 (m, 2H), 7.32 – 7.28 (m, 4H), 3.19 (s, 6H), 2.61 (s, 6H).

^{13}C NMR (101 MHz, CDCl_3) δ 149.3, 146.5 (dd, $J = 264.6, 15.8$ Hz), 147.1 (t, $J = 2.7$ Hz), 142.7, 137.9, 126.3, 123.1, 122.2, 121.8, 121.0, 120.1, 119.8, 111.7, 109.0, 103.3 (dd, $J = 10.3, 6.6$ Hz), 30.4, 17.8

^{19}F NMR (376 MHz, CDCl_3) δ -132.25.

IR (cm⁻¹): 3050, 2926, 2857, 2242, 1623, 1603, 1469, 1174.

HRMS (ESI) *m/z*: [M + H]⁺ calcd for C₃₆H₂₃F₂N₄O₂, 581.1784; found, 581.1781



B²CNPyrF₂:

Under an argon atmosphere, *N*-Methyl BICOL **B²** (30 mg, 0.0714, 1 equiv.), 2,3,5,6-tetrafluoroisonicotinonitrile (12.5 mg, 0.0714, 1 equiv.) and anhydrous K₂CO₃ (30 mg, 0.214 mmol, 3 equiv.) were taken in an oven dried 3 mL glass vial. Then anhydrous DMF (1 mL) was added, and the reaction mixture was stirred at 50 °C for 42 hours. After the completion of the reaction, the DMF was removed under vacuum. The crude was dissolved with 10 mL of ethyl acetate. The organic phase was washed with 3 × 10 mL of distilled water and 10 mL of brine. The organic phase was dried over anhydrous Na₂SO₄, filtered and concentrated under vacuum. The crude product was purified by SiO₂ column (*n*-hexane/dichloromethane, 8/2 to 65/35). The desired product **B²CNPyrF₂** (racemic) was obtained as pale yellowish white solid (36 mg, 91%) and was later purified by chiral SFC chromatography.

TLC: R_f = 0.4. 40% dichloromethane in *n*-hexane (UV 254 nm)

Melting point: 255-260 °C

¹H NMR (400 MHz, CDCl₃) δ 8.12 – 8.07 (m, 4H), 7.48 (t, *J* = 7.6 Hz, 2H), 7.29 (t, *J* = 7.4 Hz, 4H), 3.21 (s, 3H), 3.13 (s, 3H), 2.64 (s, 3H), 2.57 (s, 3H).

¹³C NMR (101 MHz, CDCl₃) δ 149.0, 148.3, 147.0 (dd, *J* = 11.6, 3.6 Hz), 144.1 (dd, *J* = 242.4, 14.4 Hz), 142.6, 142.55, 142.59 (d, *J* = 2.9 Hz), 141.5 (dd, *J* = 255.5, 32.0 Hz), 138.0, 137.9, 126.2, 126.1, 122.9, 122.8, 122.1, 121.95, 121.91, 121.2, 120.14, 120.12, 119.77, 119.75, 111.8, 111.6, 109.02, 109.00, 108.7 (dt, *J* = 8.4, 4.3 Hz), 30.49, 30.42, 17.7, 17.1.

¹⁹F NMR (376 MHz, CDCl₃) δ -88.10 (d, *J* = 22.9 Hz), -136.57 (d, *J* = 22.9 Hz).

IR (cm⁻¹): 3047, 2924, 2862, 1603, 1458, 1176, 936.

HRMS (ESI) *m/z*: [M + H]⁺ calcd for C₃₄H₂₃F₂N₄O₂, 557.1784; found, 557.1779

NMR spectra

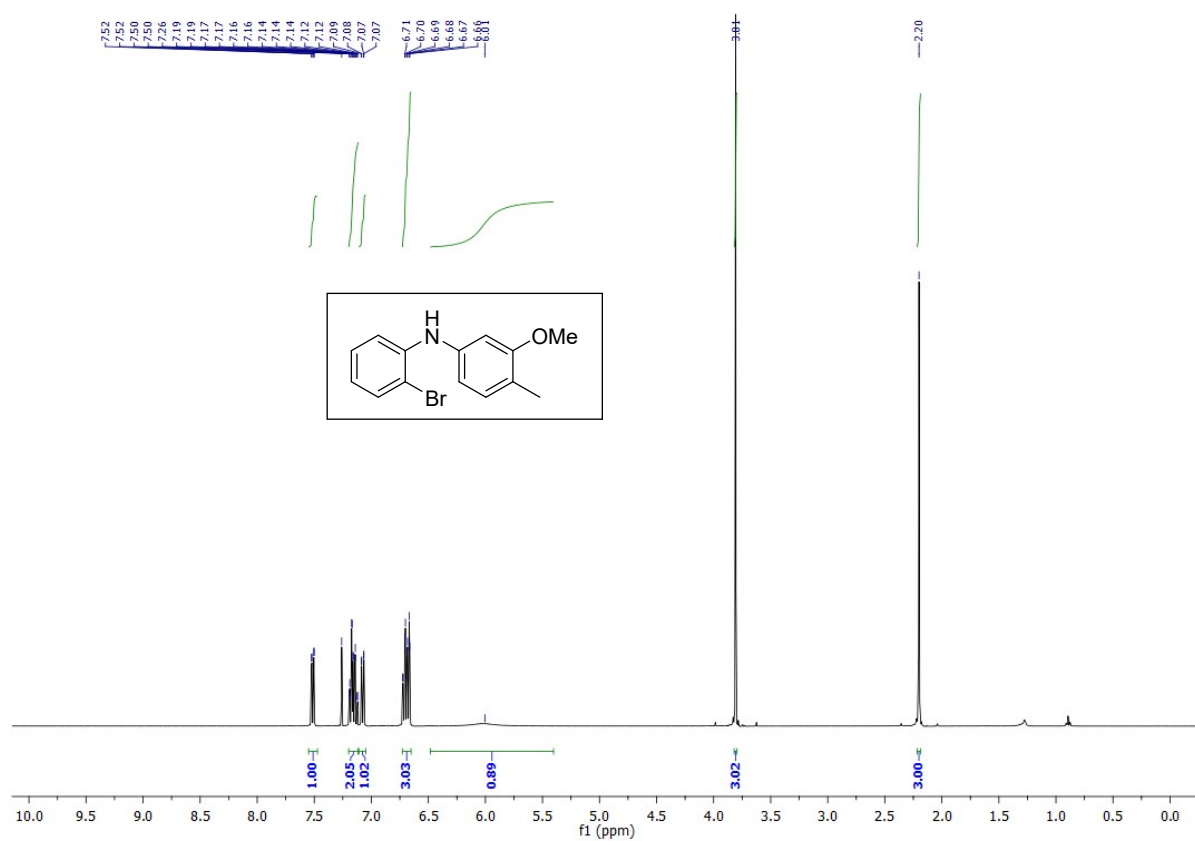


Figure S1. ¹H NMR of **3** (CDCl₃)

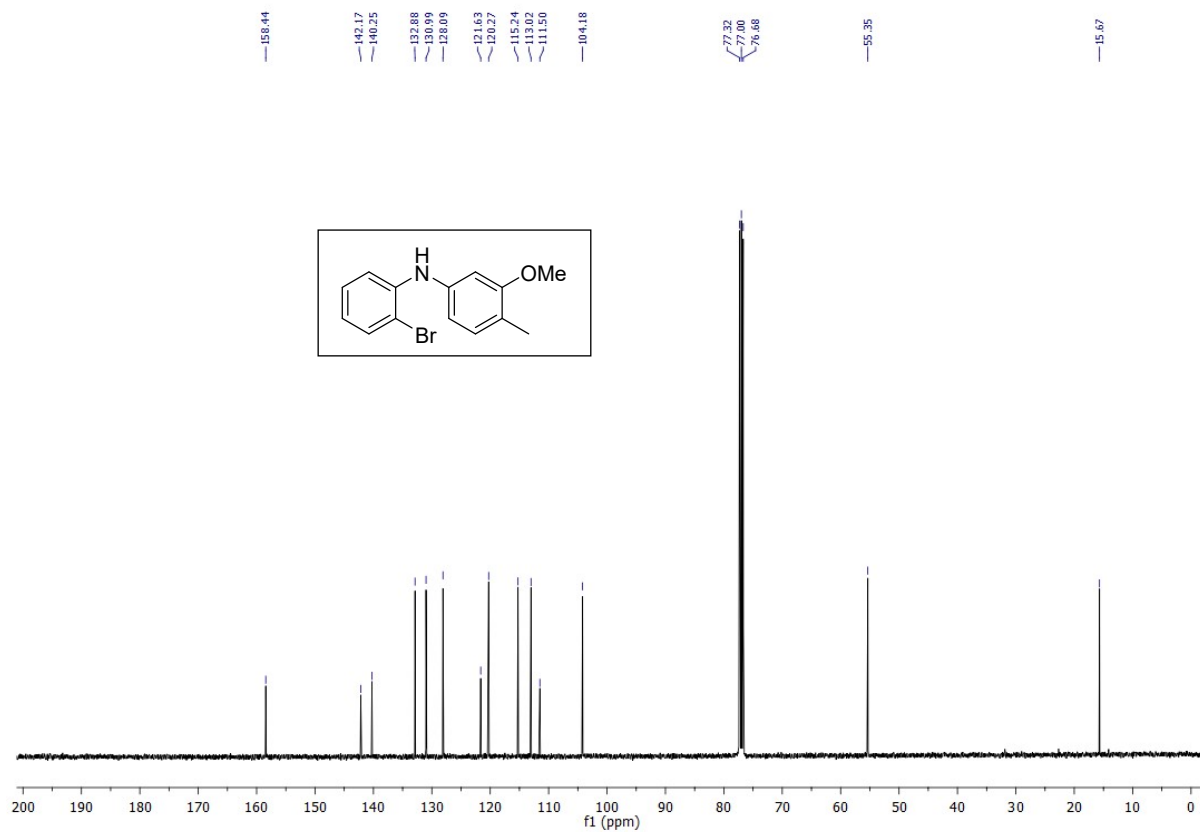


Figure S2. ¹³C NMR of **3** (CDCl₃)

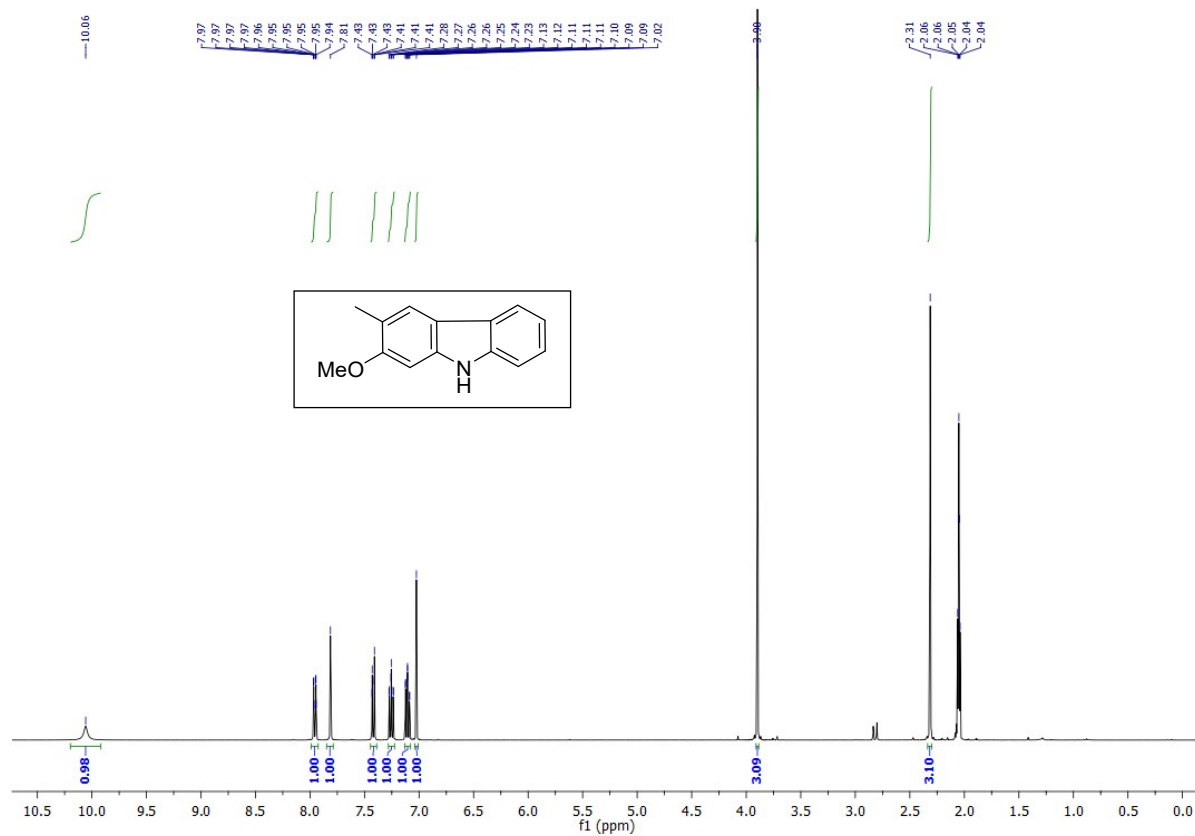


Figure S3. ^1H NMR of 4 (Acetone- d_6)

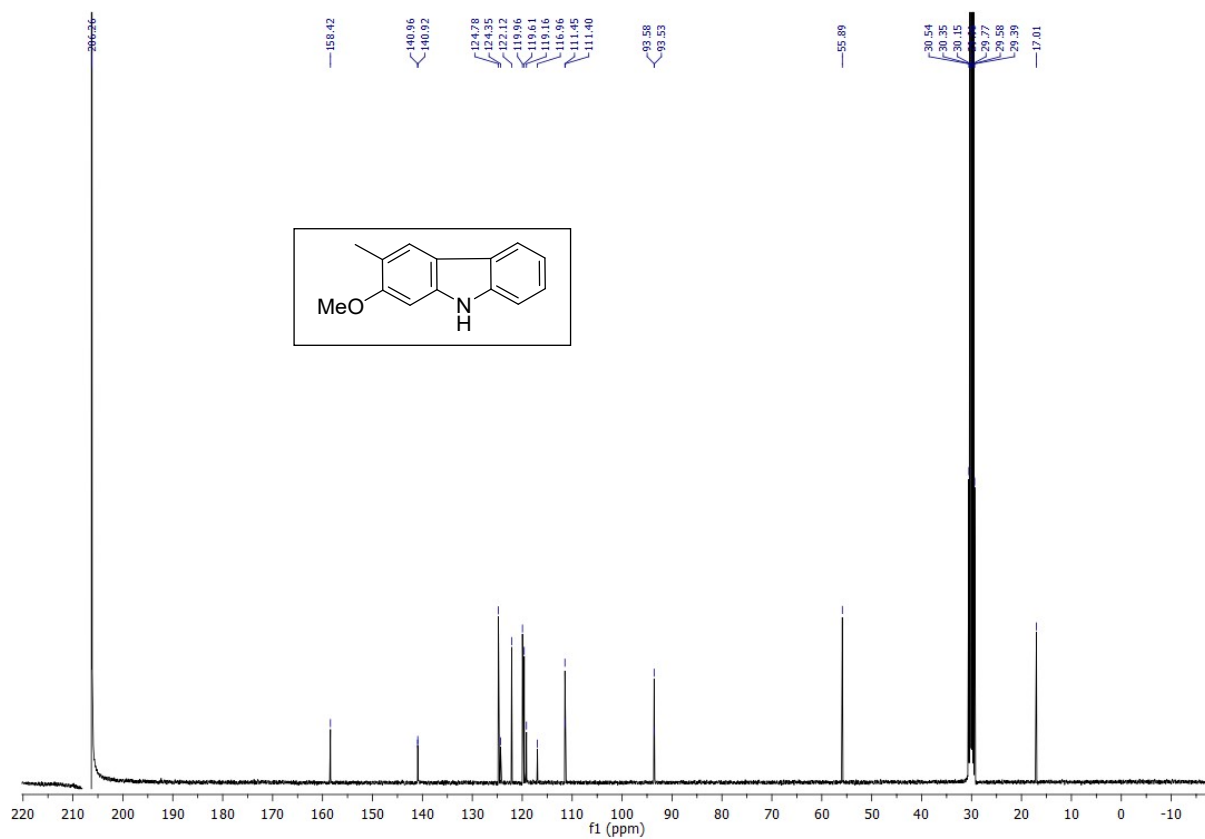


Figure S4. ^{13}C NMR of 4 (Acetone- d_6).

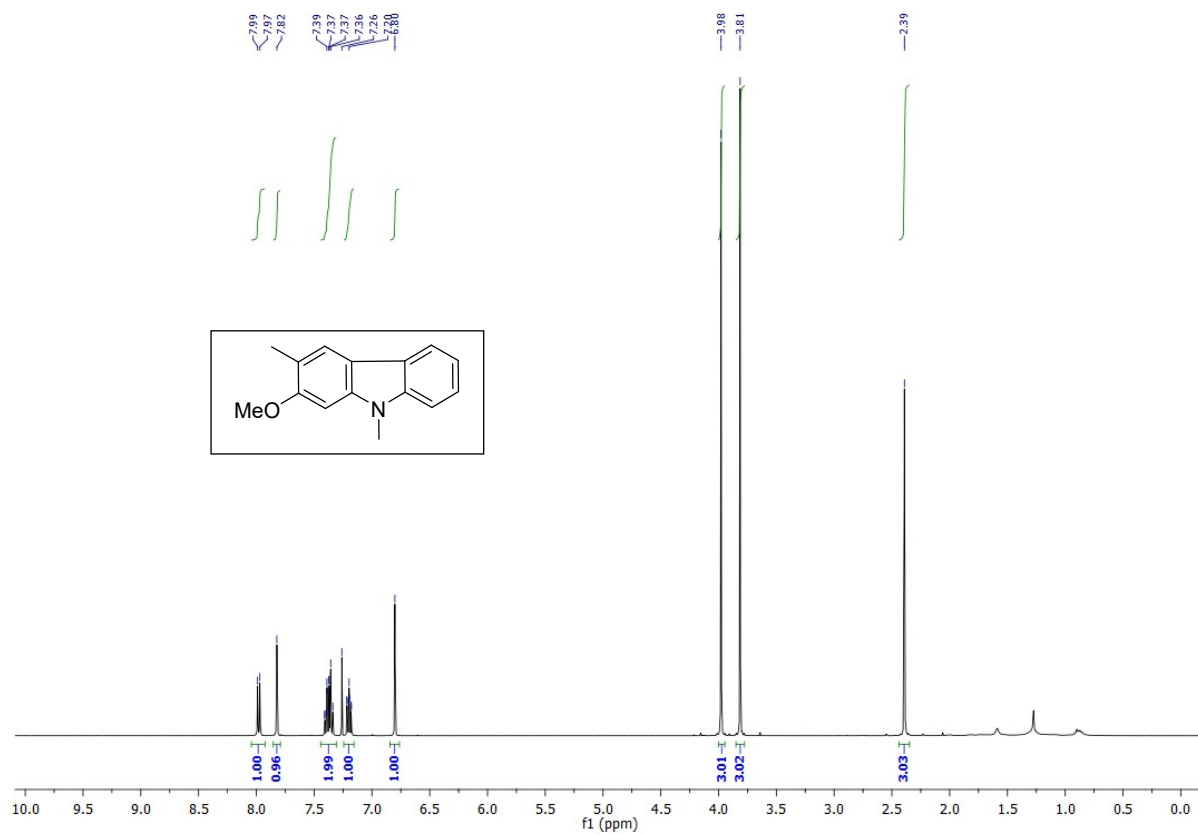


Figure S5. ¹H NMR of 4a (CDCl₃).

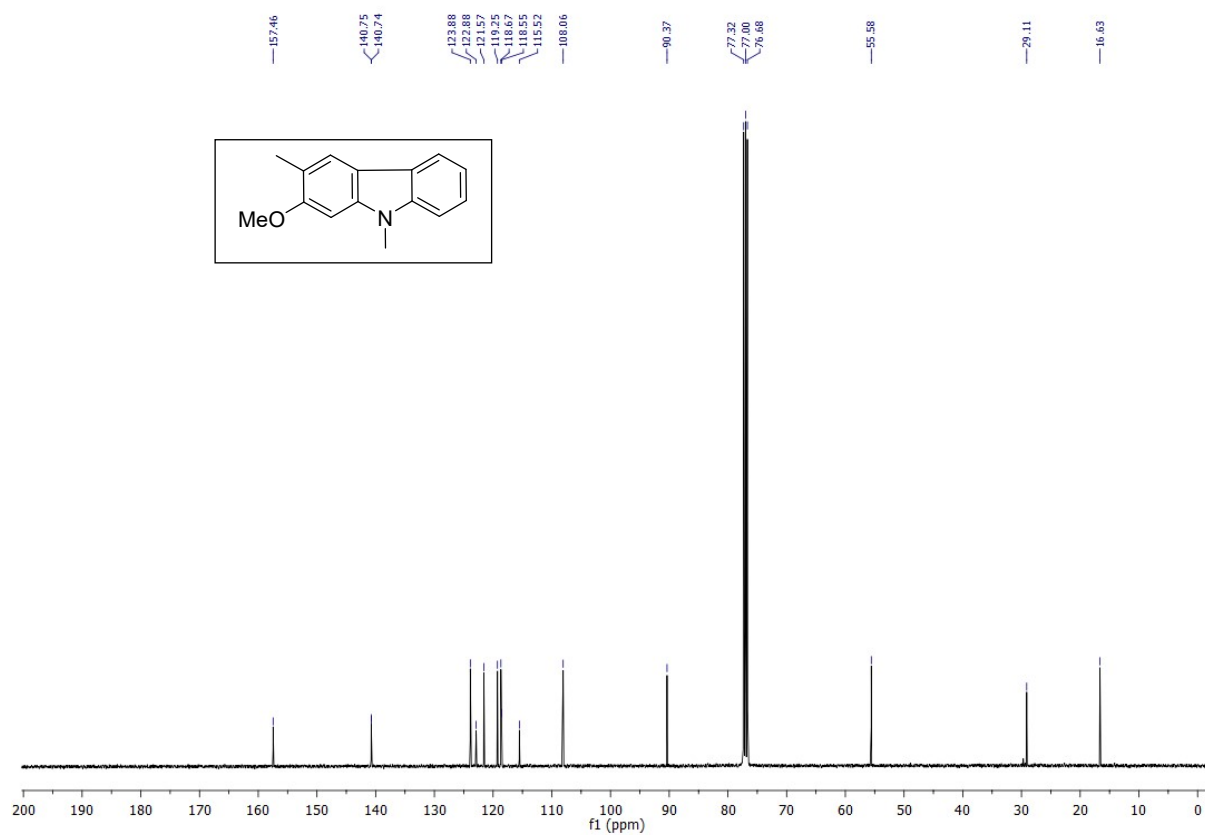


Figure S6. ¹³C NMR of 4a (CDCl₃).

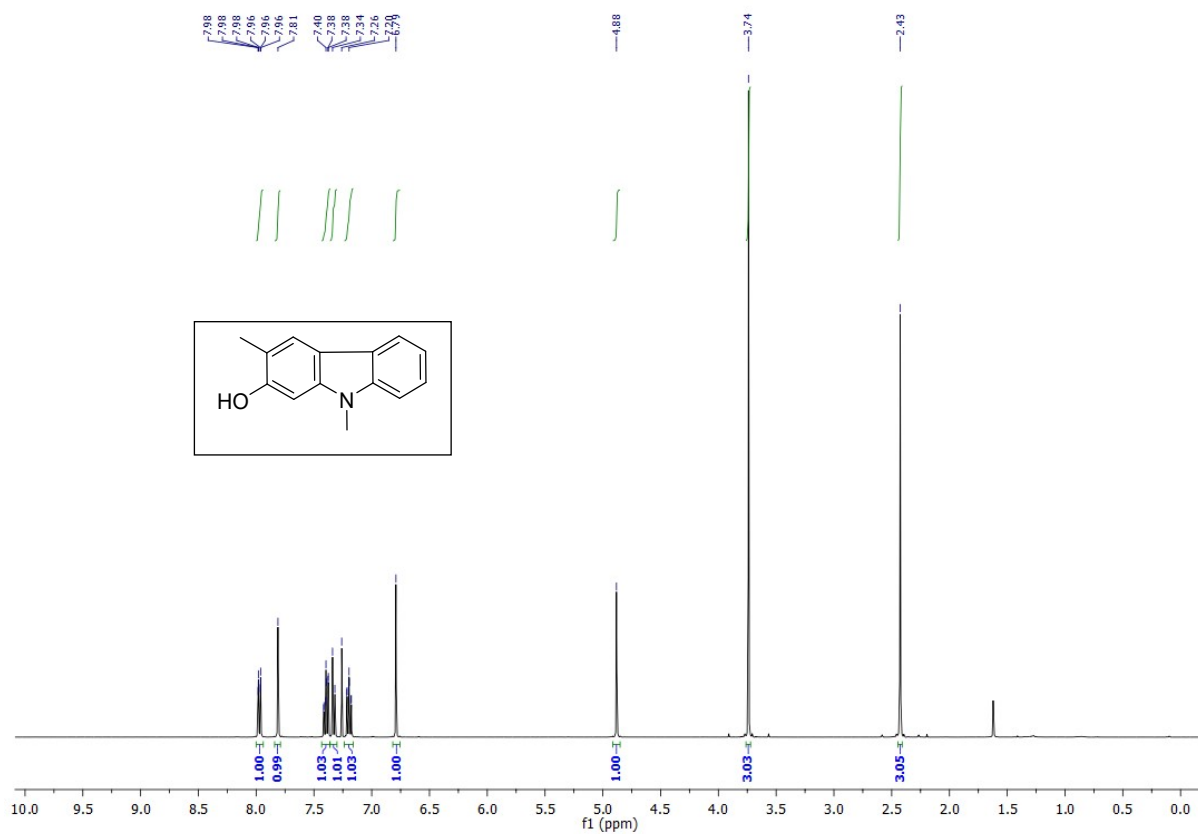


Figure S7. ¹H NMR of 5 (CDCl₃)

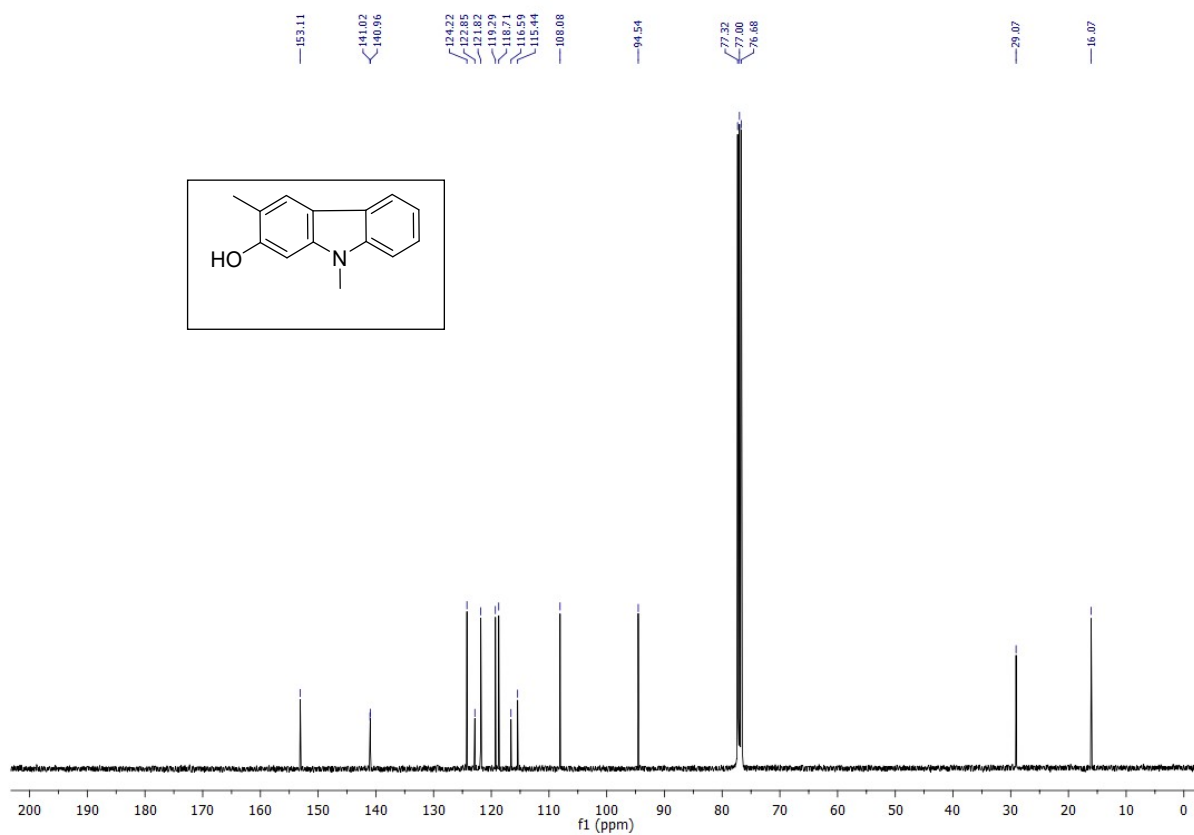


Figure S8. ¹³C NMR of 5 (CDCl₃)

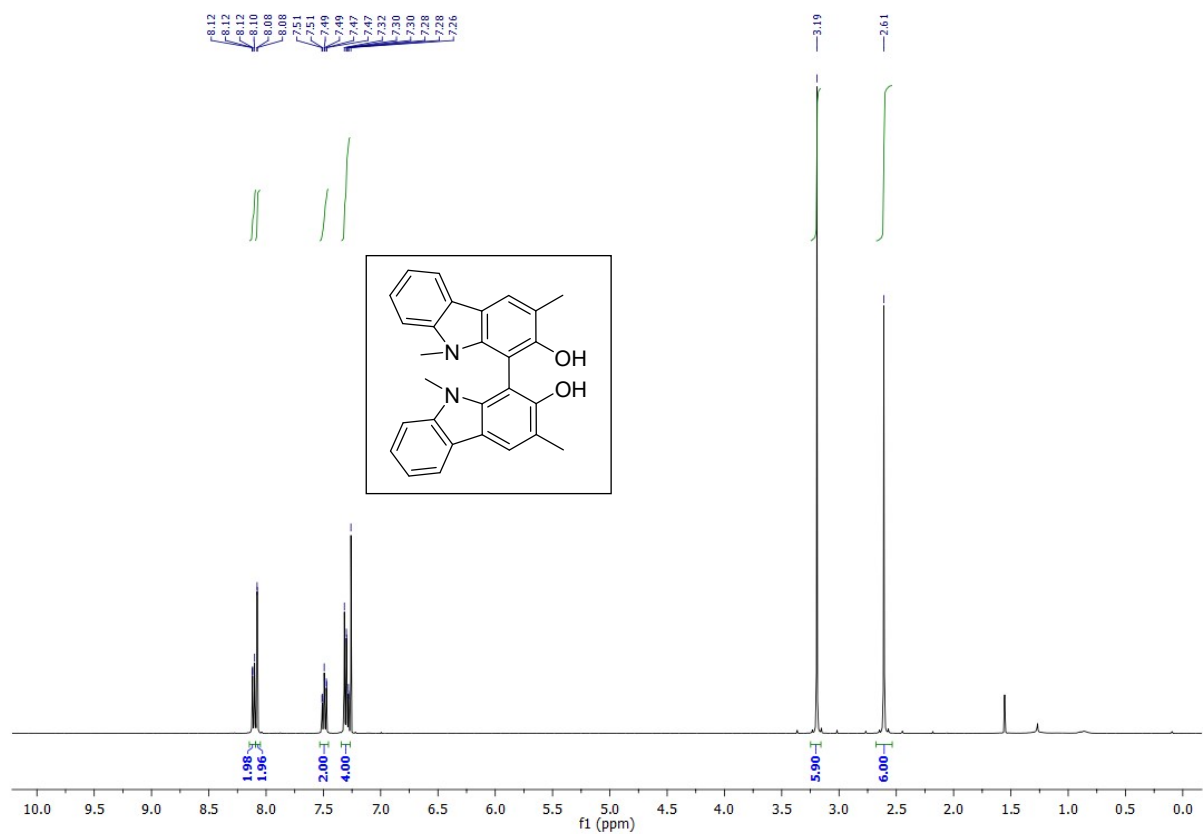


Figure S9. ¹H NMR of **B²** (CDCl₃)

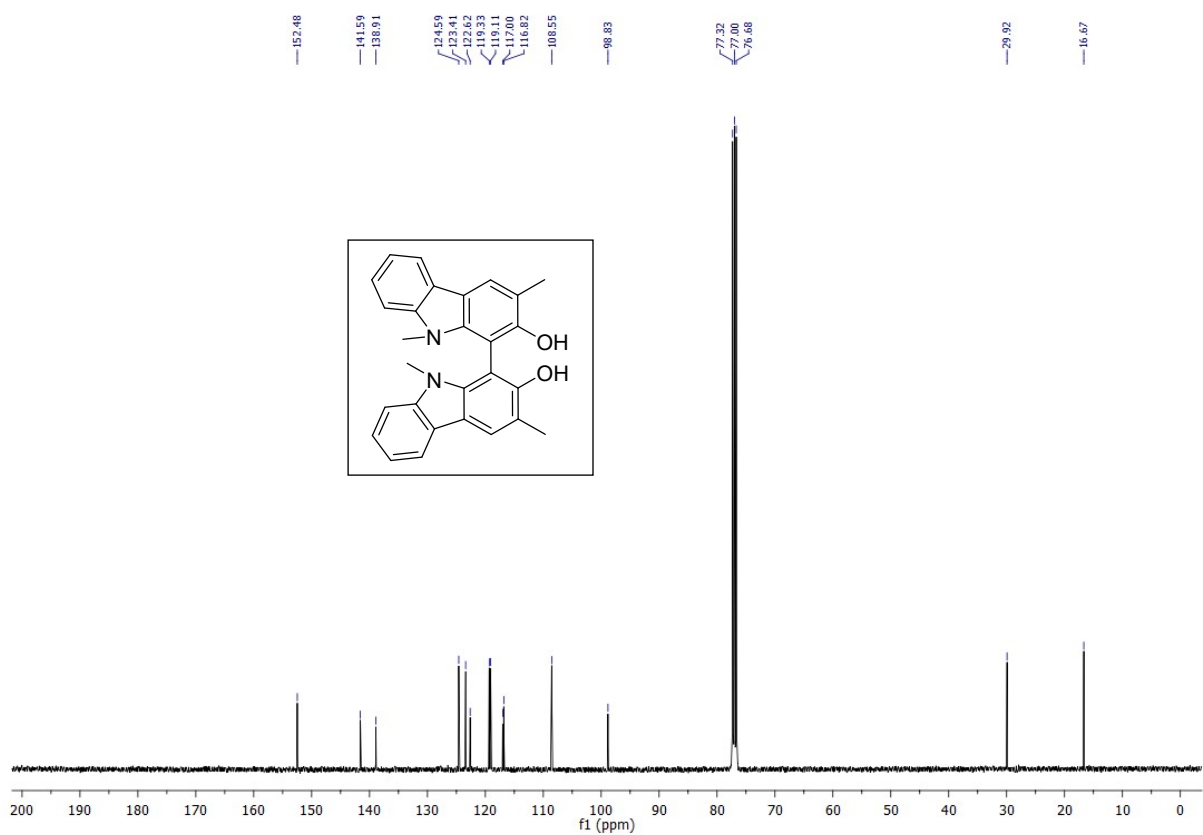


Figure S10. ¹³C NMR of **B²** (CDCl₃)

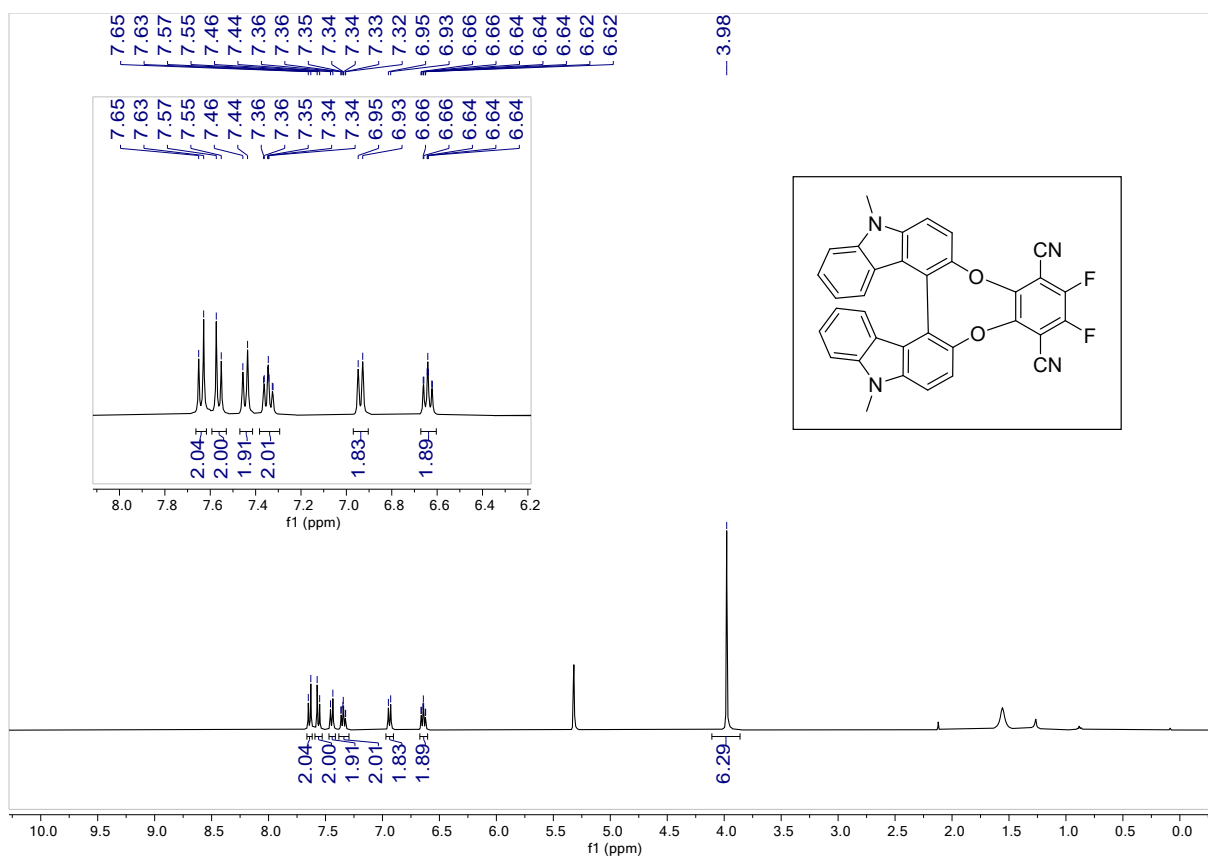


Figure S11. ¹H NMR of **B¹TPNF₂** (CD₂Cl₂).

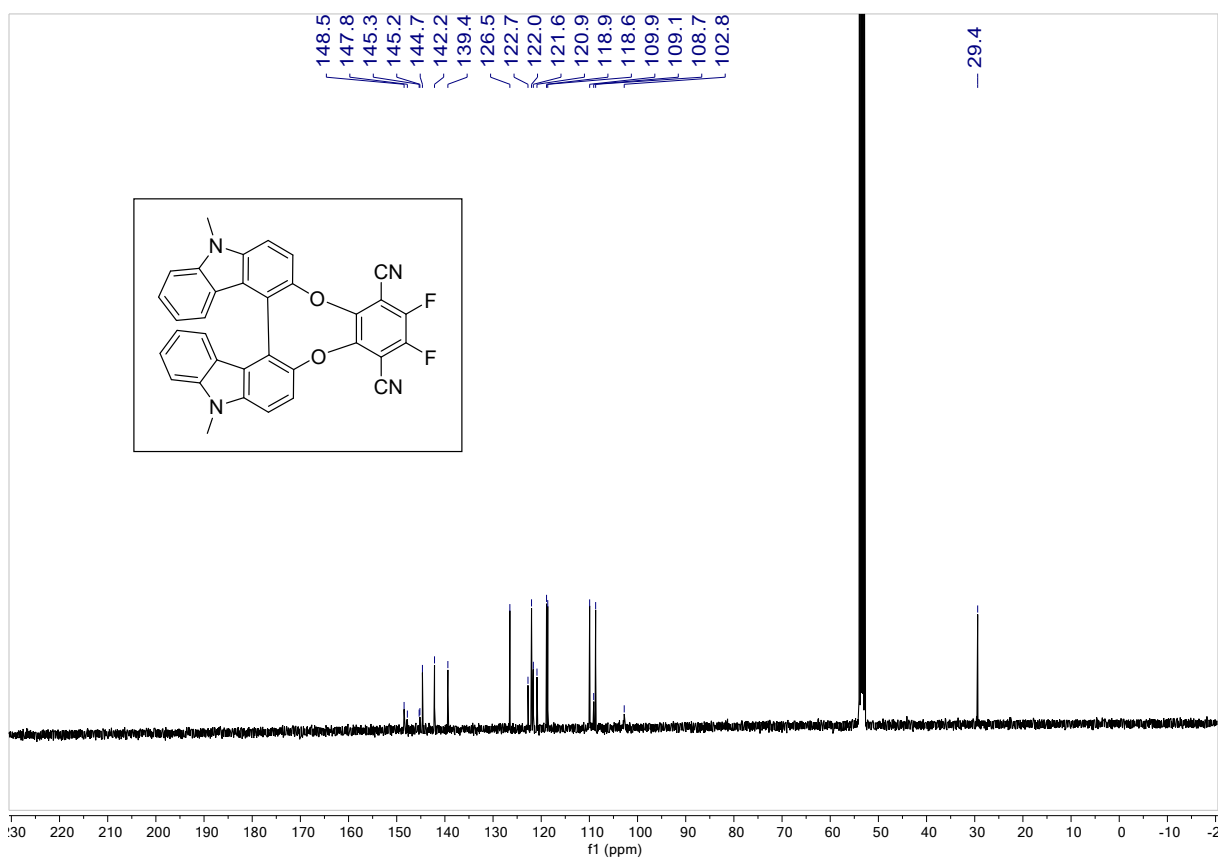


Figure S12. ¹³C NMR of **B¹TPNF₂** (CD₂Cl₂).

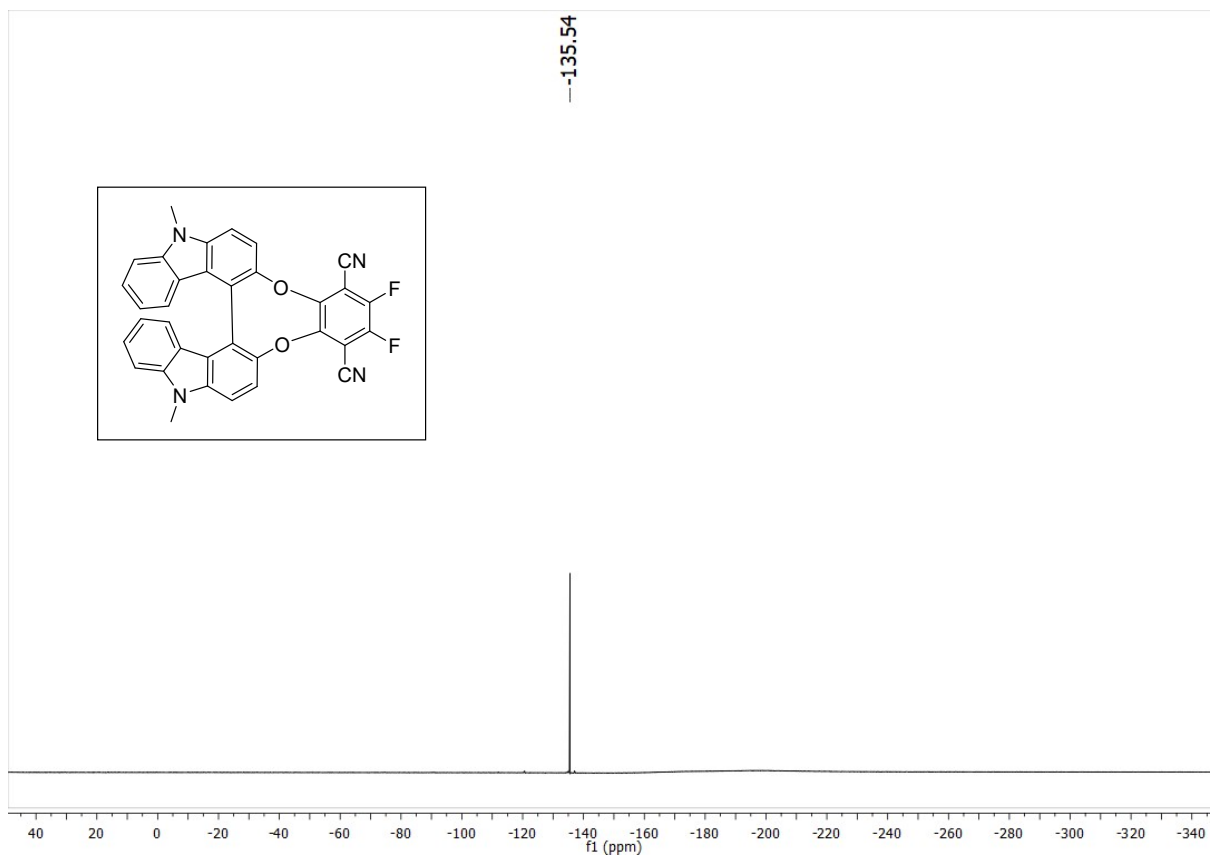


Figure S13. ^{19}F NMR of B^1TPNF_2 (CD_2Cl_2)

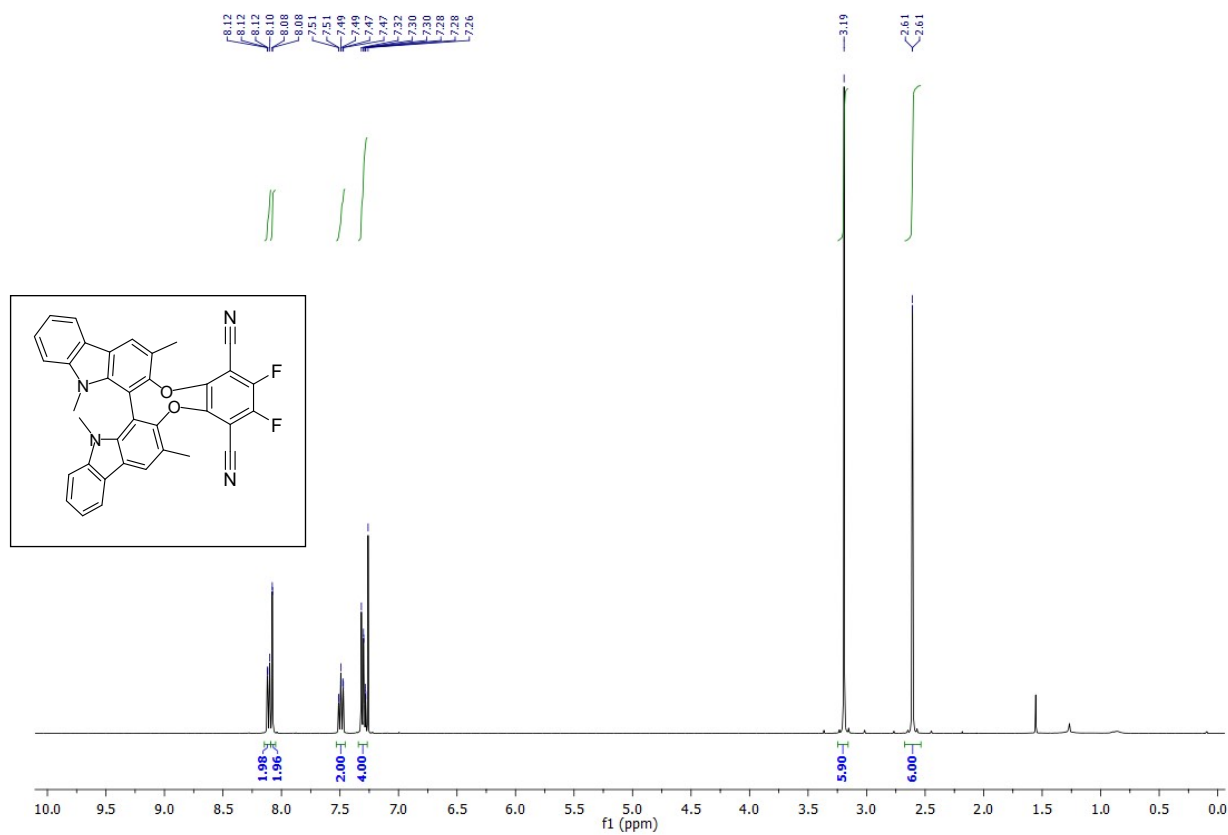


Figure S14. ^1H NMR of B^2TPNF_2 (CDCl_3)

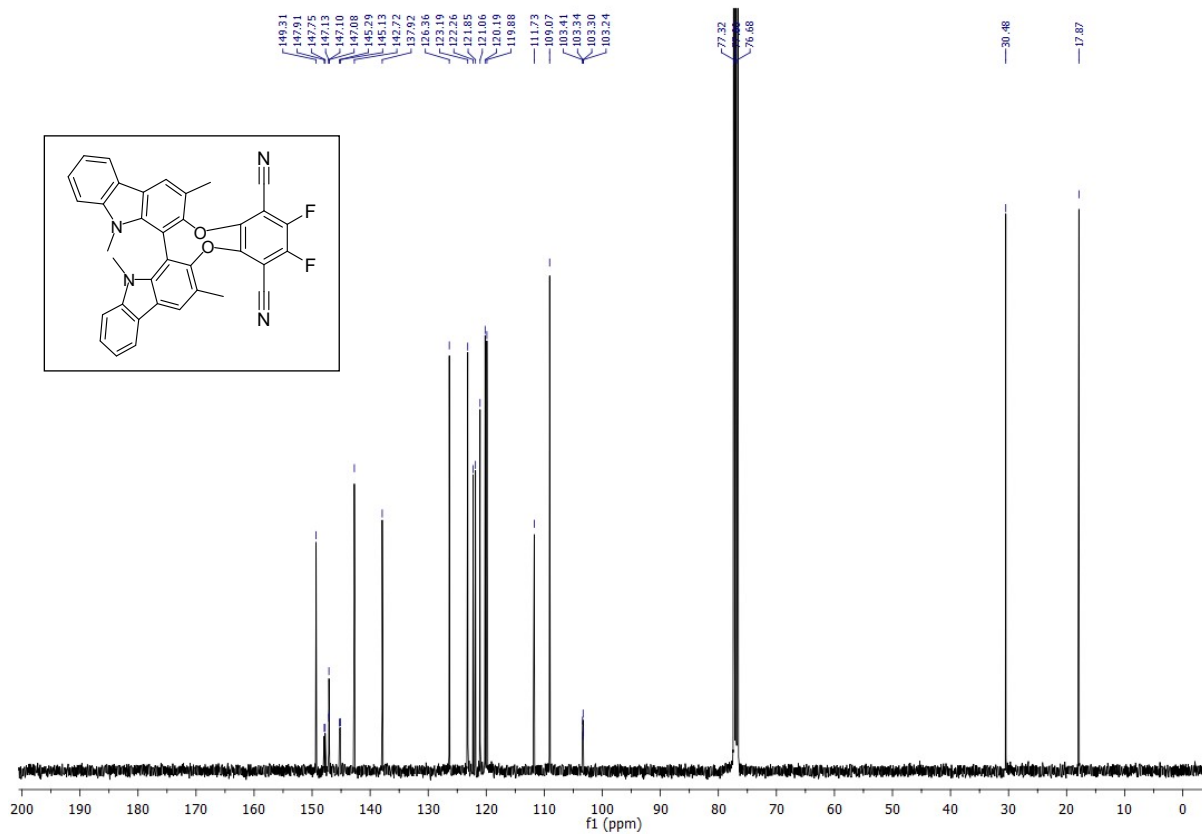


Figure S15. ¹³C NMR of **B²TPNF₂** (CDCl₃)

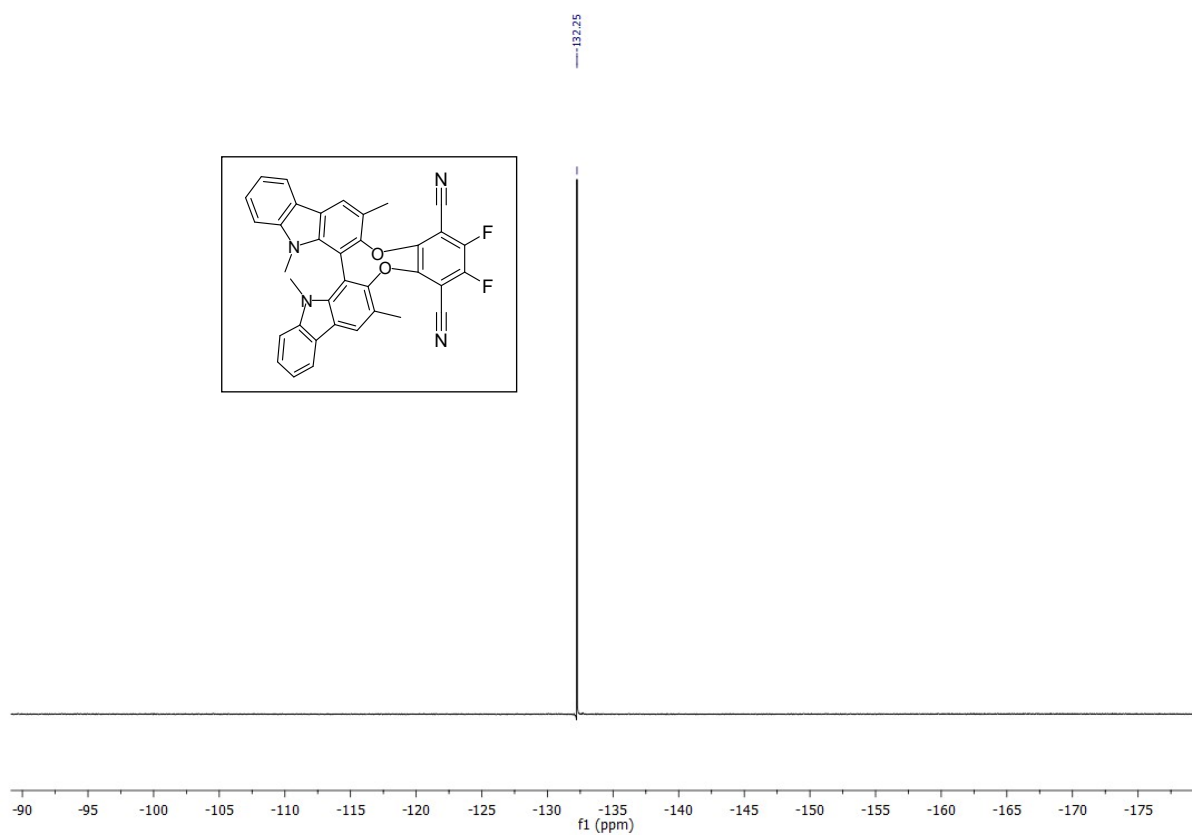


Figure S16. ¹⁹F NMR of **B²TPNF₂** (CDCl₃)

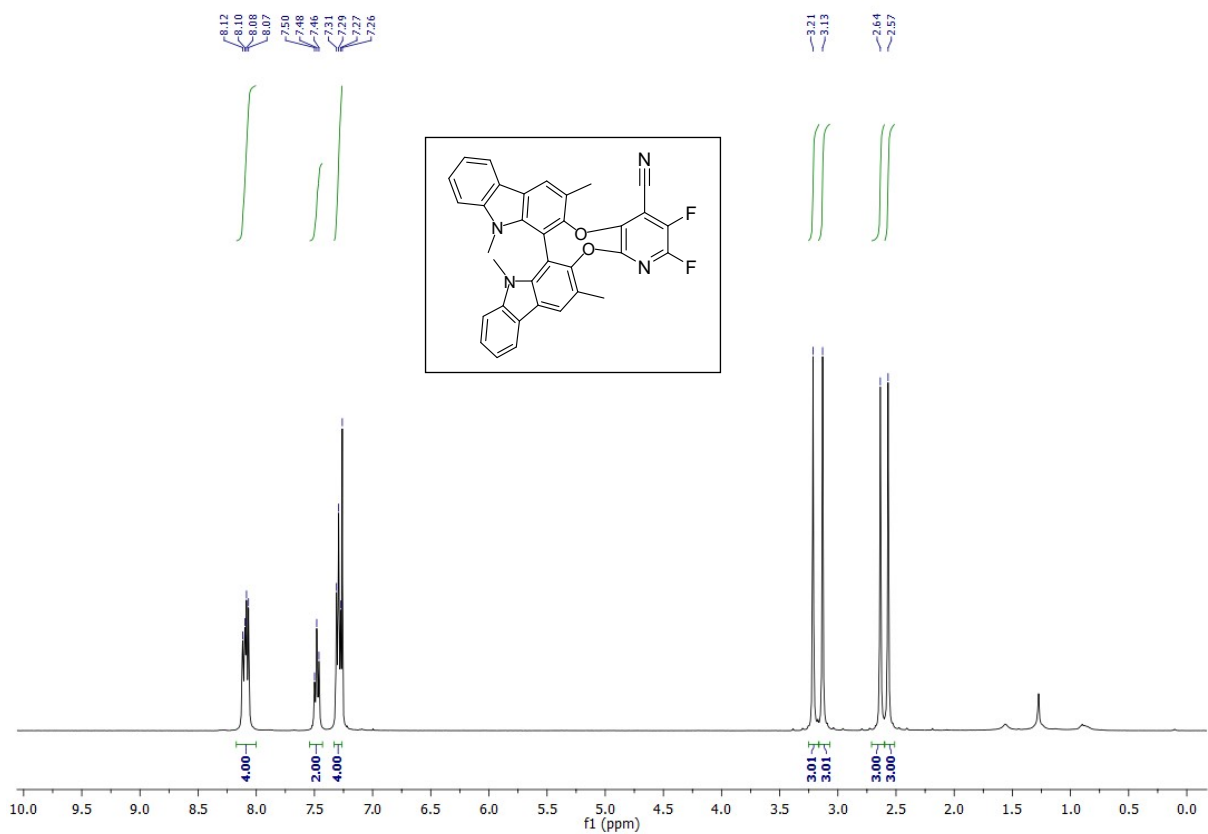


Figure S17. 1H NMR of $B^2CNPYRF_2$ (CDCl₃)

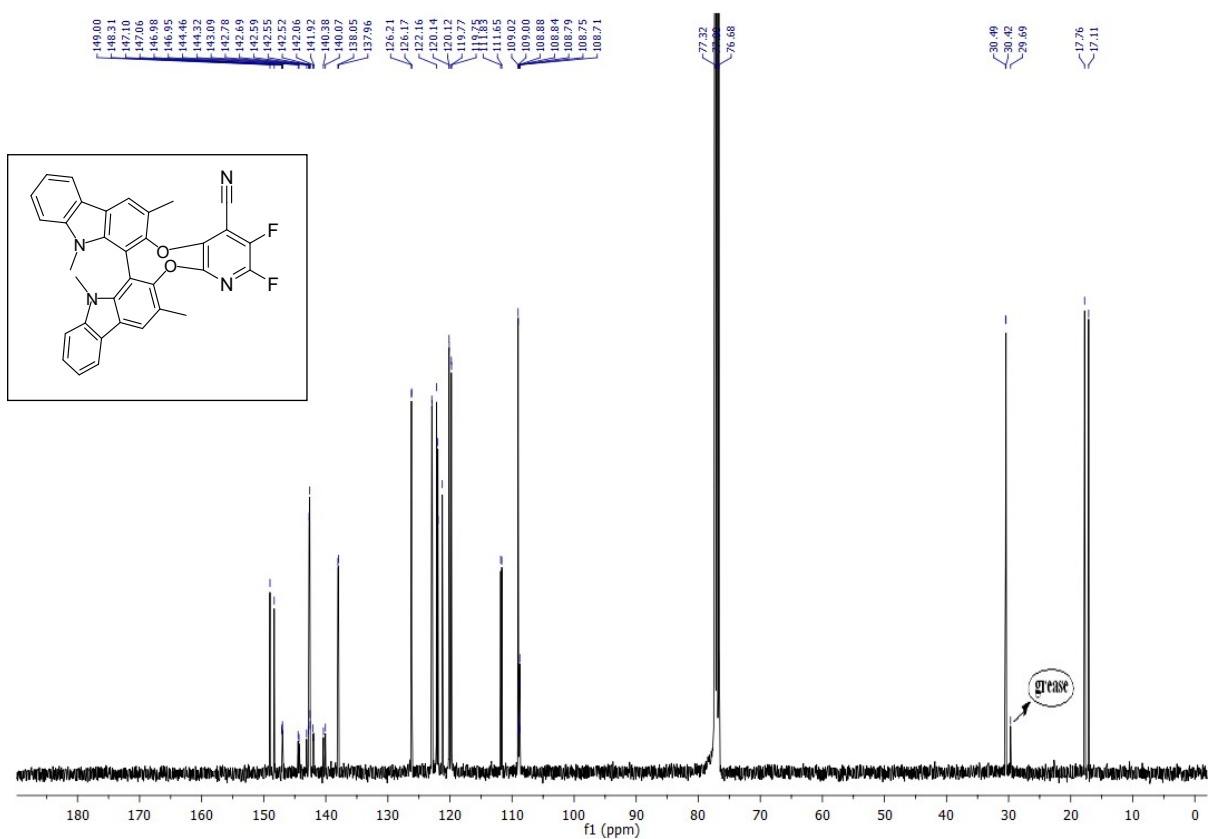


Figure S18. ^{13}C NMR of $B^2CNPYRF_2$ (CDCl₃)

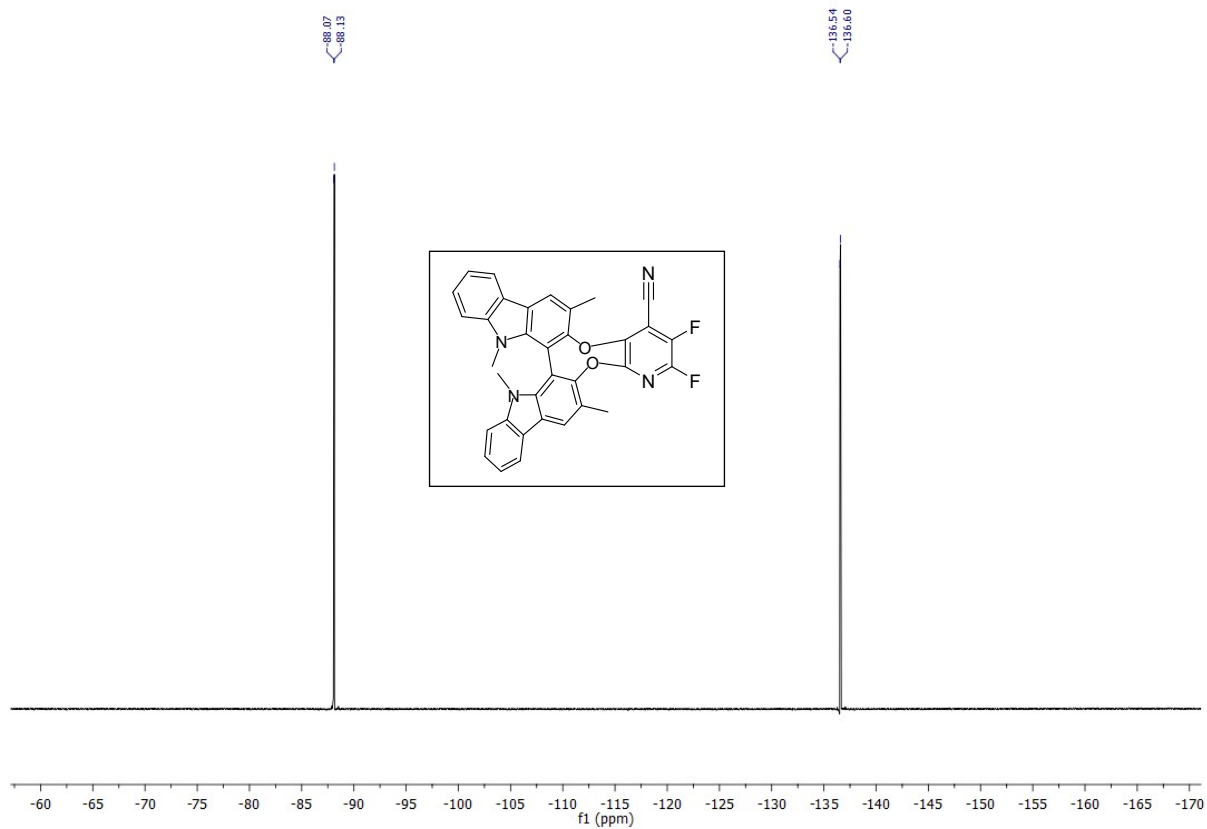


Figure S19. ^{19}F NMR of $\text{B}^2\text{CNPYRF}_2$ (CDCl_3)

SFC purification

B²TPNF₂

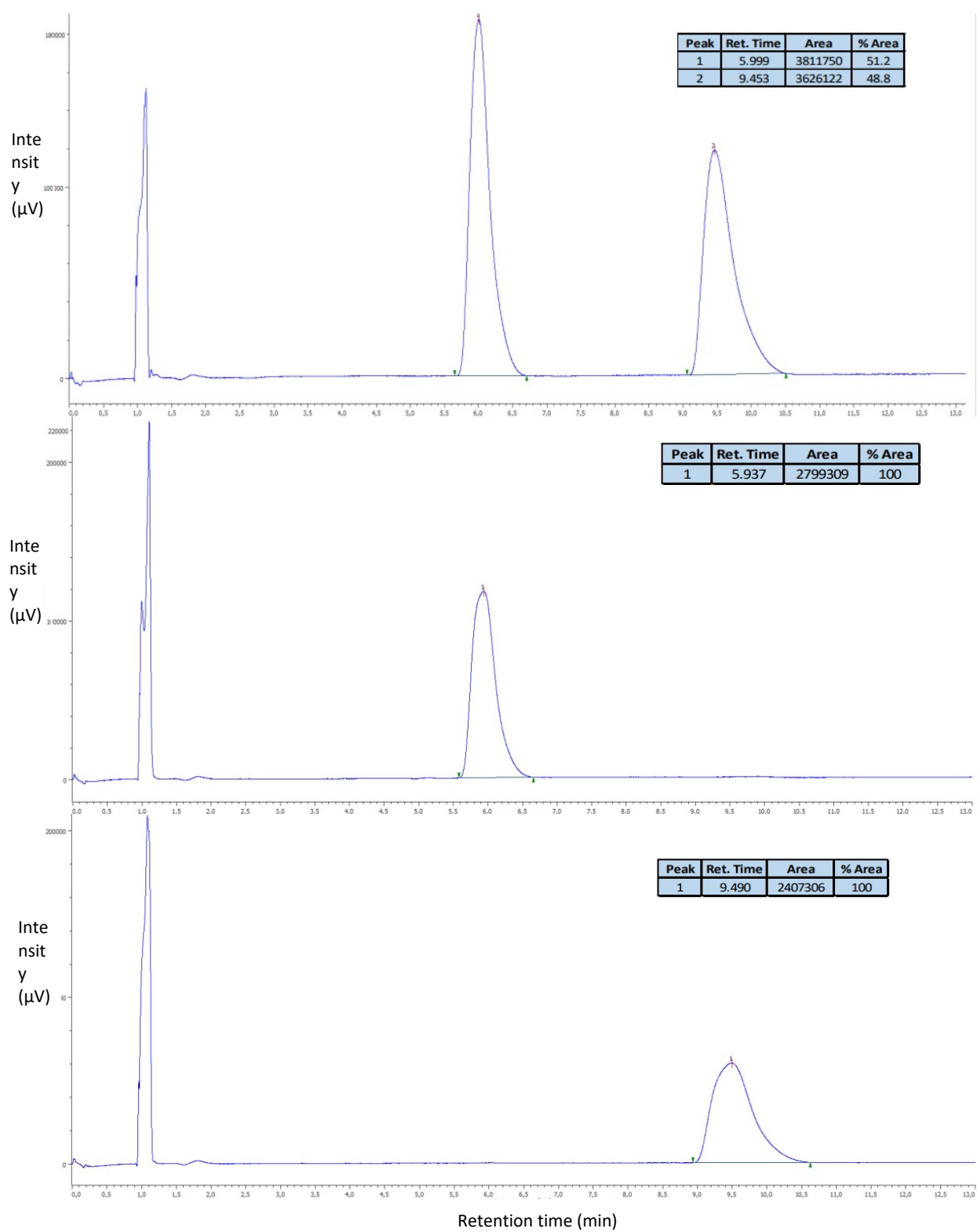


Figure S20. Chiral SFC analysis of B²TPNF₂. Racemic (top) first fraction (middle) and second fraction (bottom).

B²CNPyrF₂

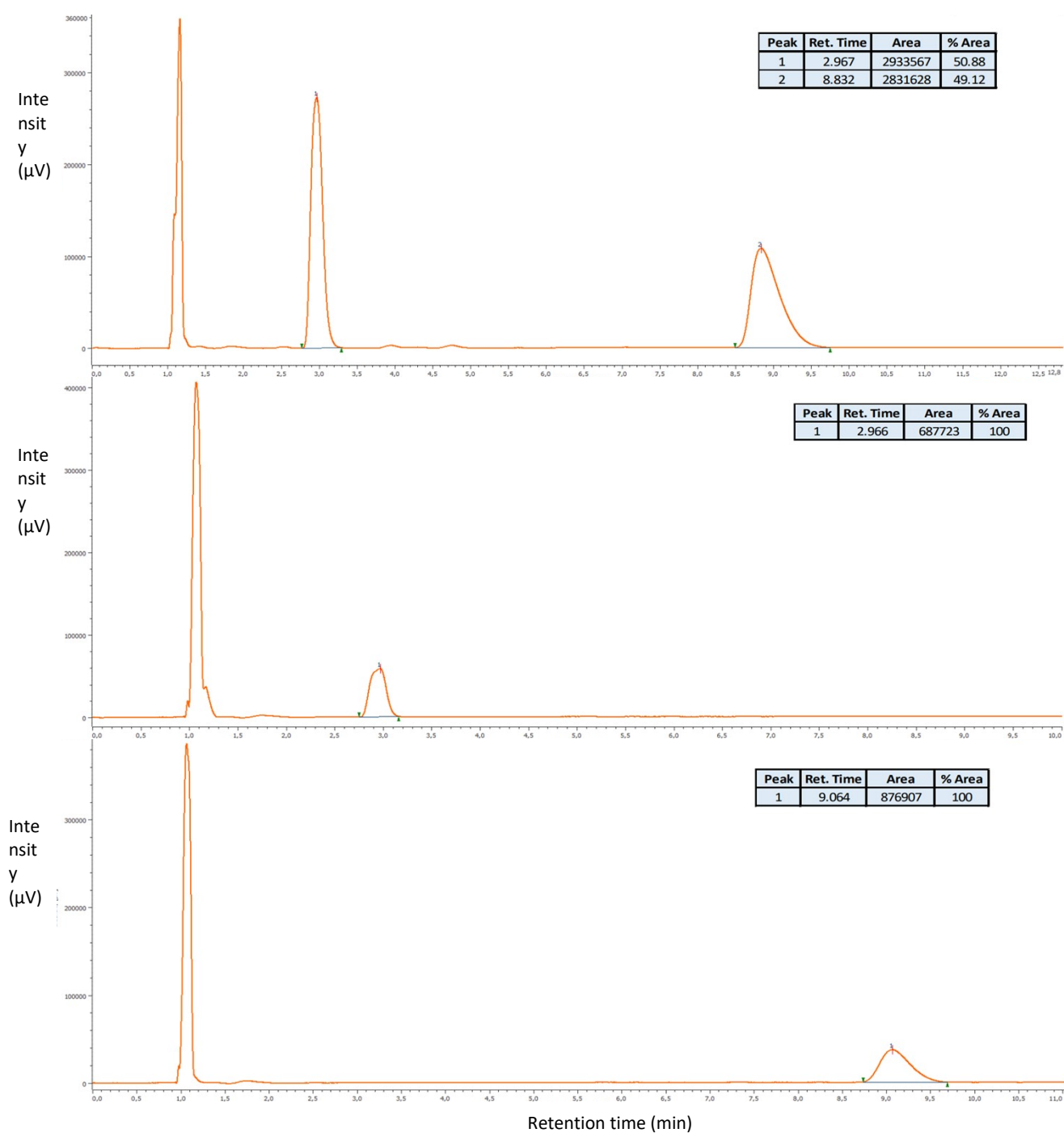


Figure S21. Chiral SFC analysis of B²CNPyrF₂. Racemic (top) first fraction (middle) and second fraction (bottom).

UV-vis spectra

Absorption spectra in DCM

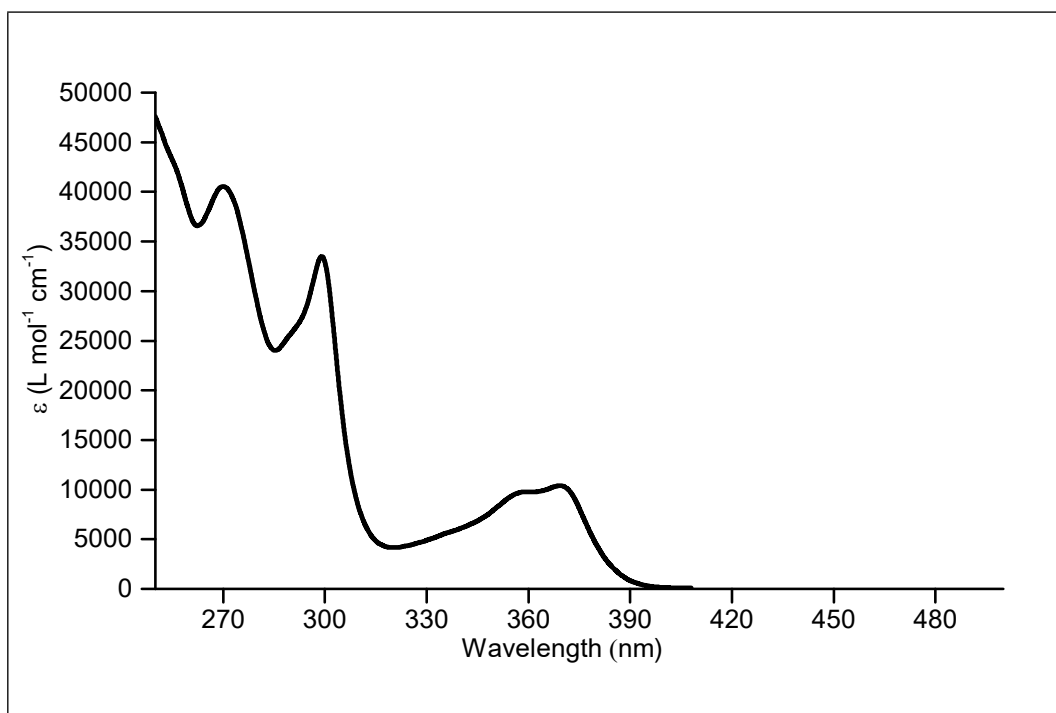


Figure S22. UV-vis absorption spectrum of B¹ recorded in DCM solution.

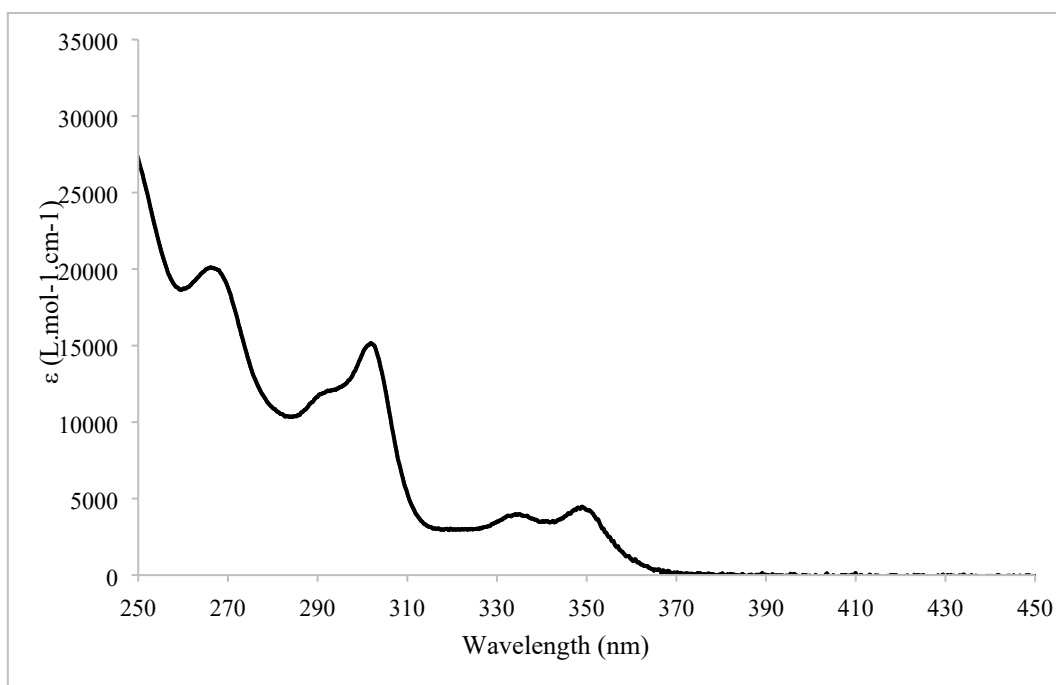


Figure S23. UV-vis absorption spectrum of B² recorded in DCM solution.

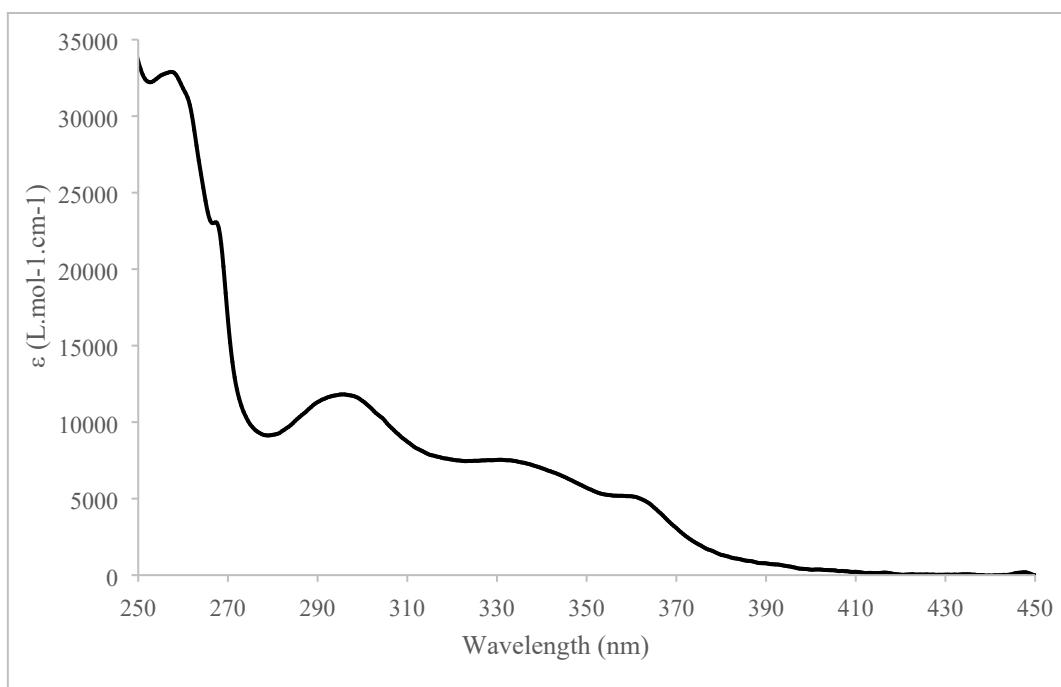


Figure S24. UV-vis absorption spectrum of B¹TPNF₂ recorded in DCM solution.

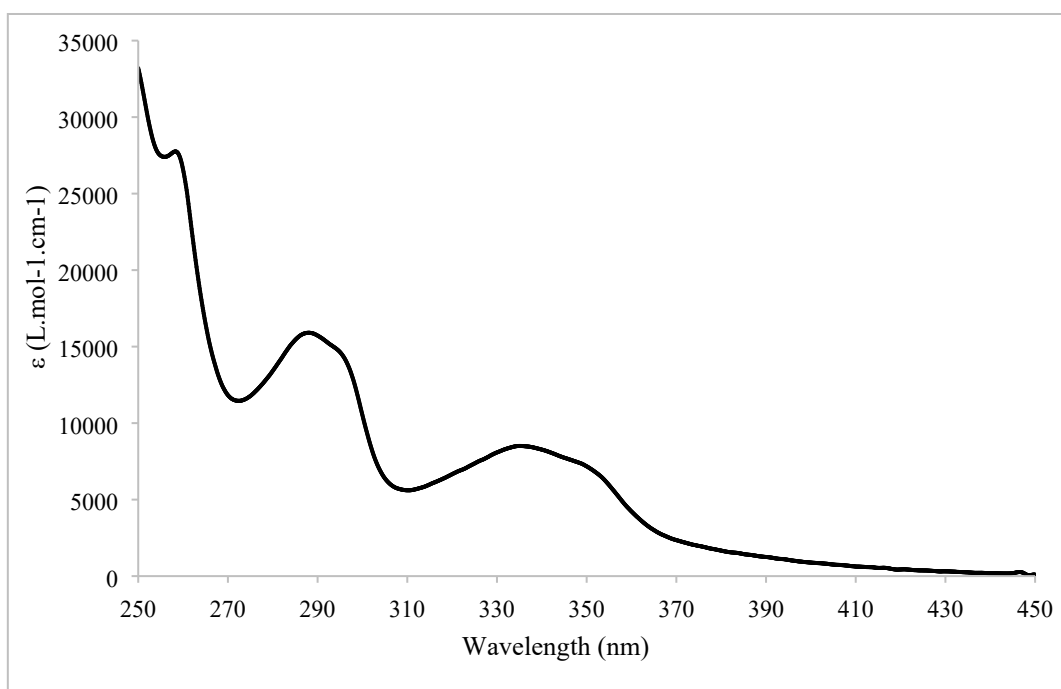


Figure S25. UV-vis absorption spectrum of B²TPNF₂ recorded in DCM solution.

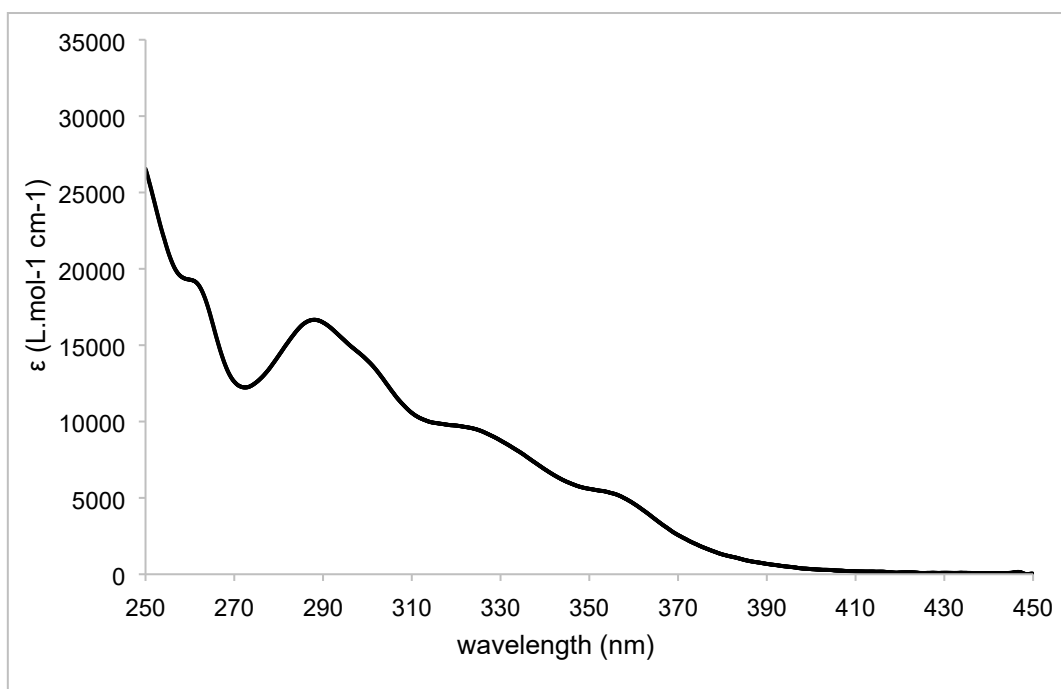


Figure S26. UV-vis absorption spectrum of **B¹CNPyrF₂** recorded in DCM solution.

Absorption spectra in toluene

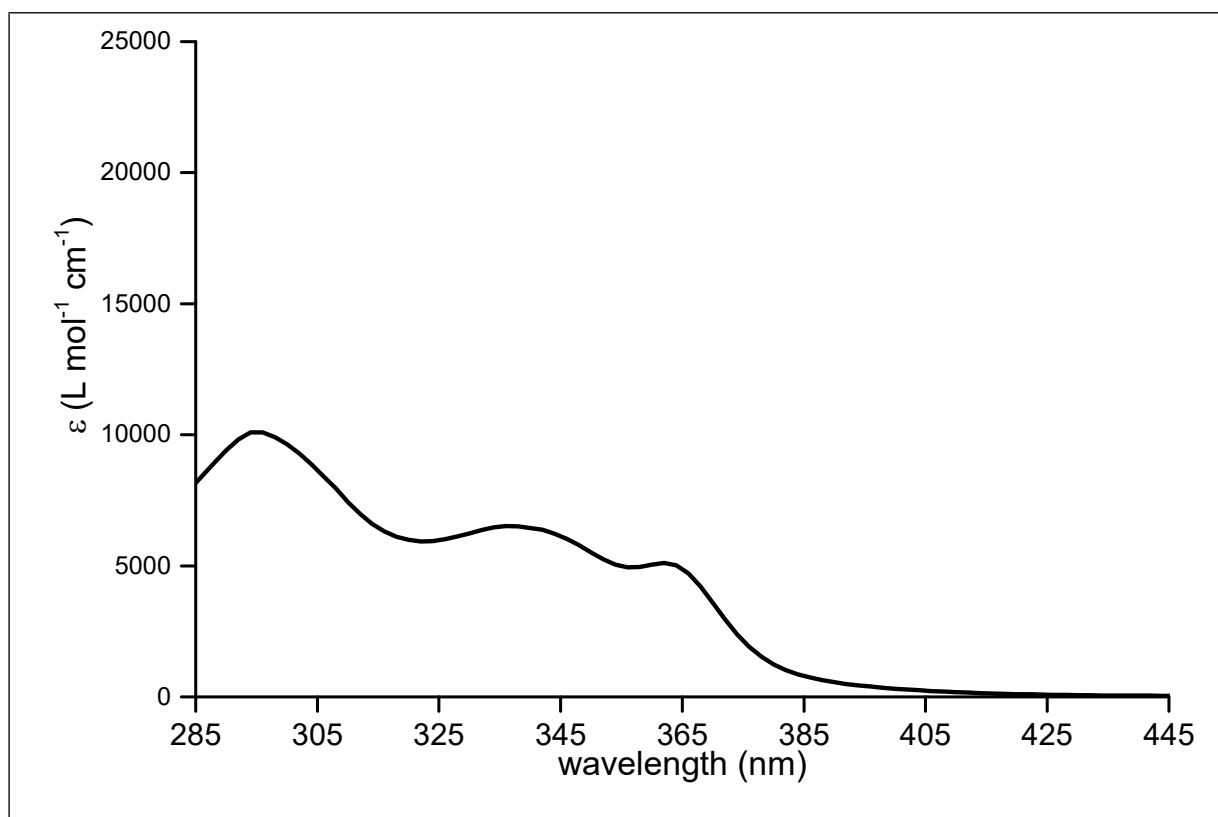


Figure S27. UV-vis absorption spectrum of **B¹TPNF₂** recorded in toluene solution.

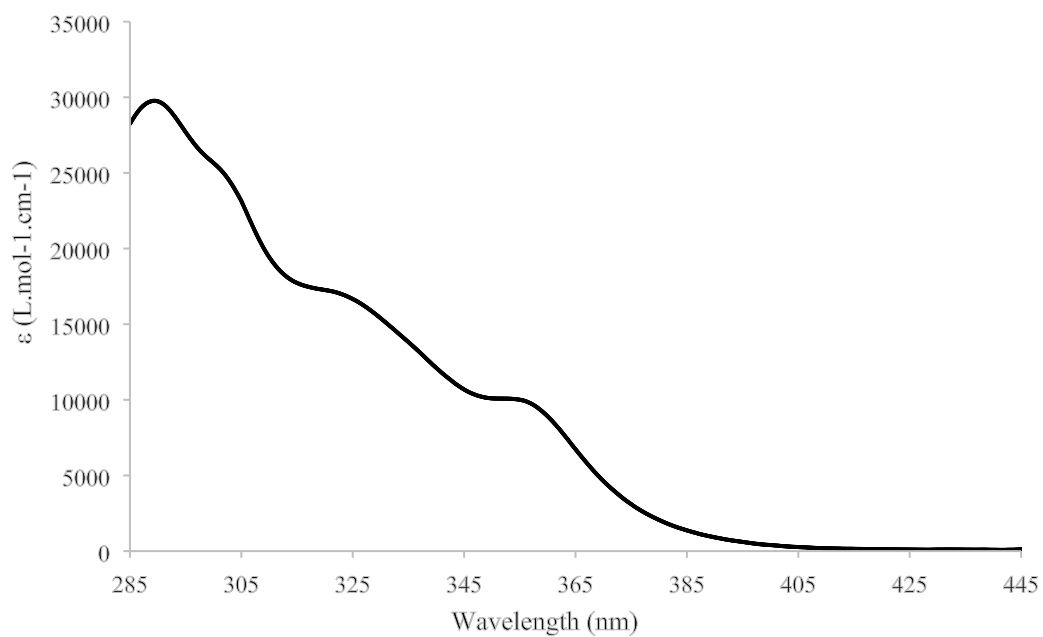


Figure S28. UV-vis absorption spectrum of B¹CNPyrF₂ recorded in toluene solution.

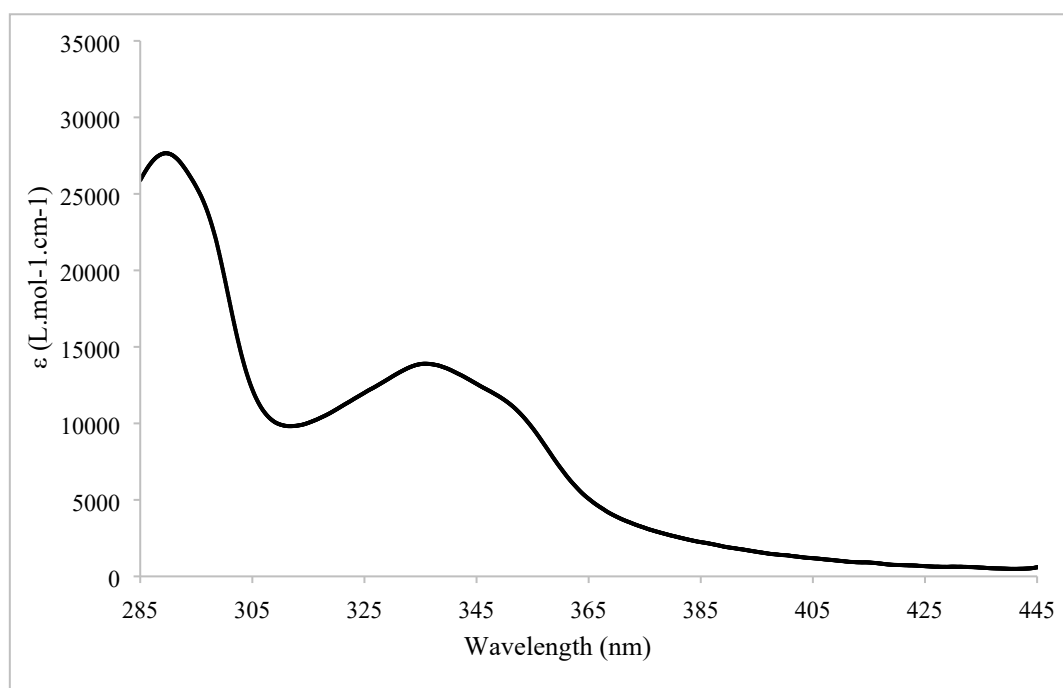


Figure S29. UV-vis absorption spectrum of B²TPNF₂ recorded in toluene solution.

Emission spectra

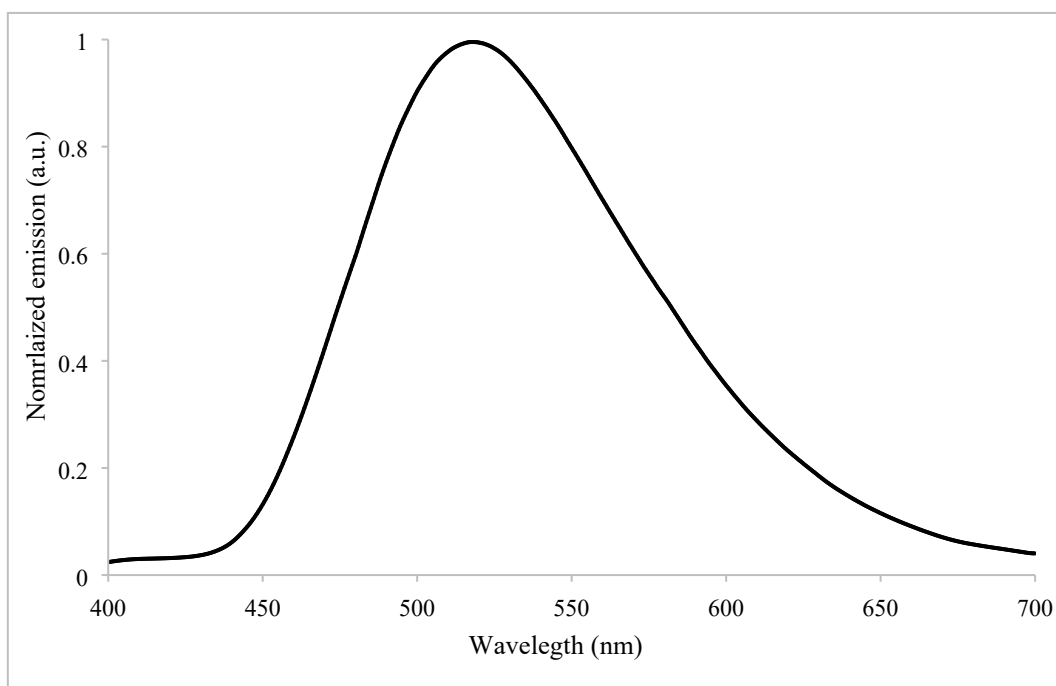


Figure S30. Emission spectra in toluene for **B¹TPNF₂**. [C] = 1×10^{-5} M. λ_{exc} = 375 nm.

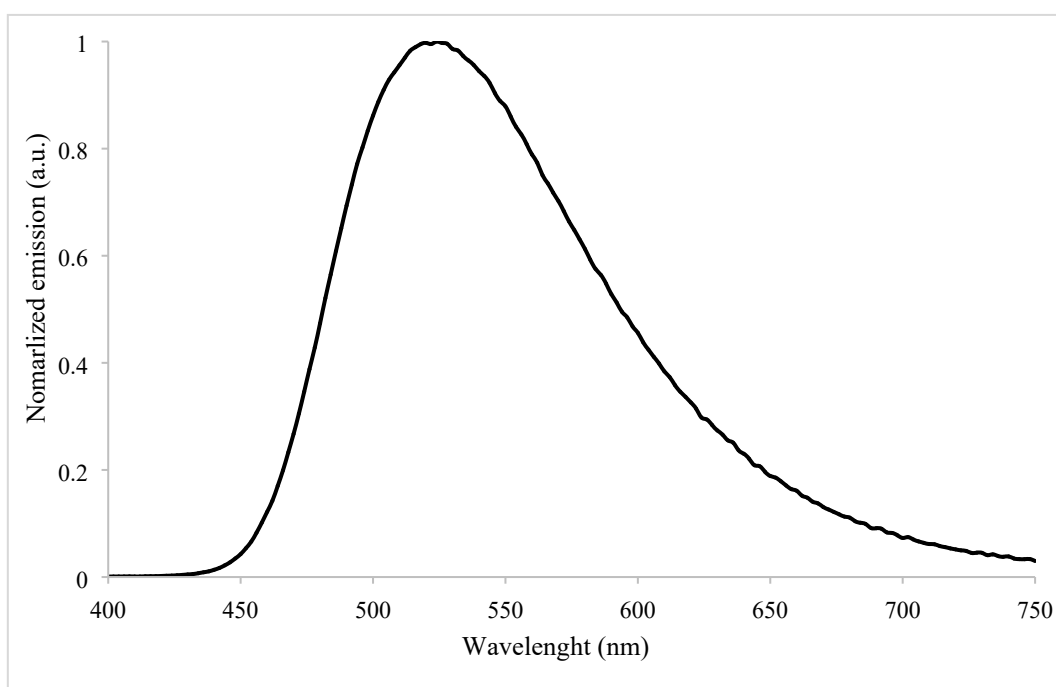


Figure S31. Emission spectra in toluene for **B²TPNF₂**. [C] = 1×10^{-5} M. λ_{exc} = 330 nm.

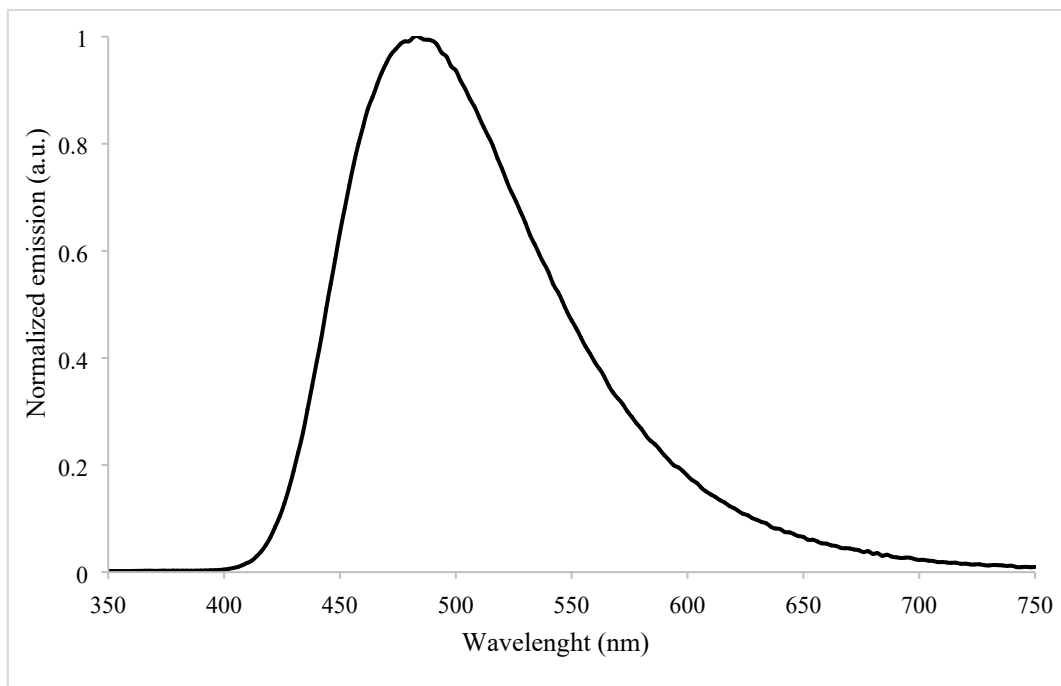


Figure S32. Emission spectra in toluene for **B²CNPyrF₂**. [C] = 1×10^{-5} M. λ_{exc} = 305 nm.

CV and DPV

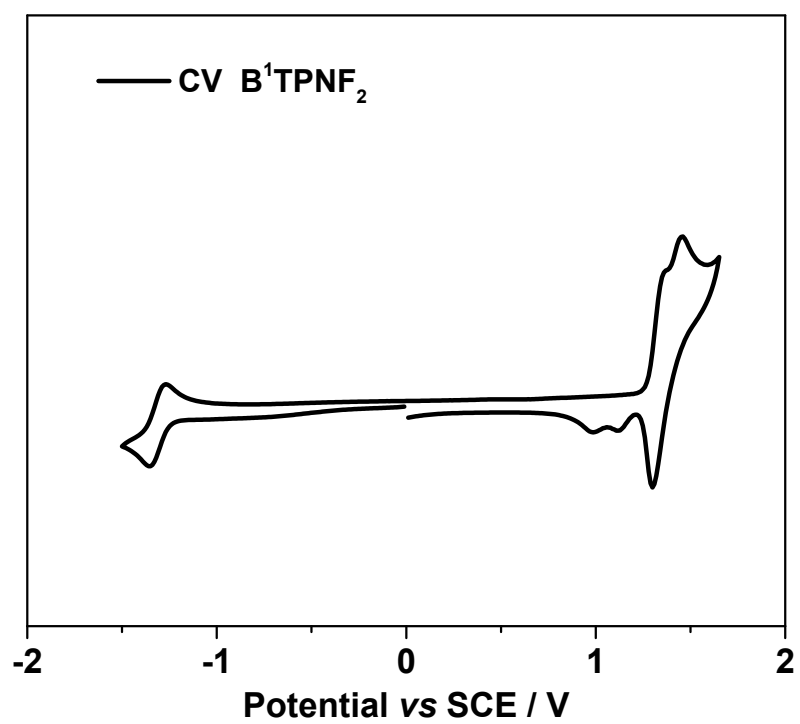


Figure S33. CV of B¹TPNF₂ in DCM.

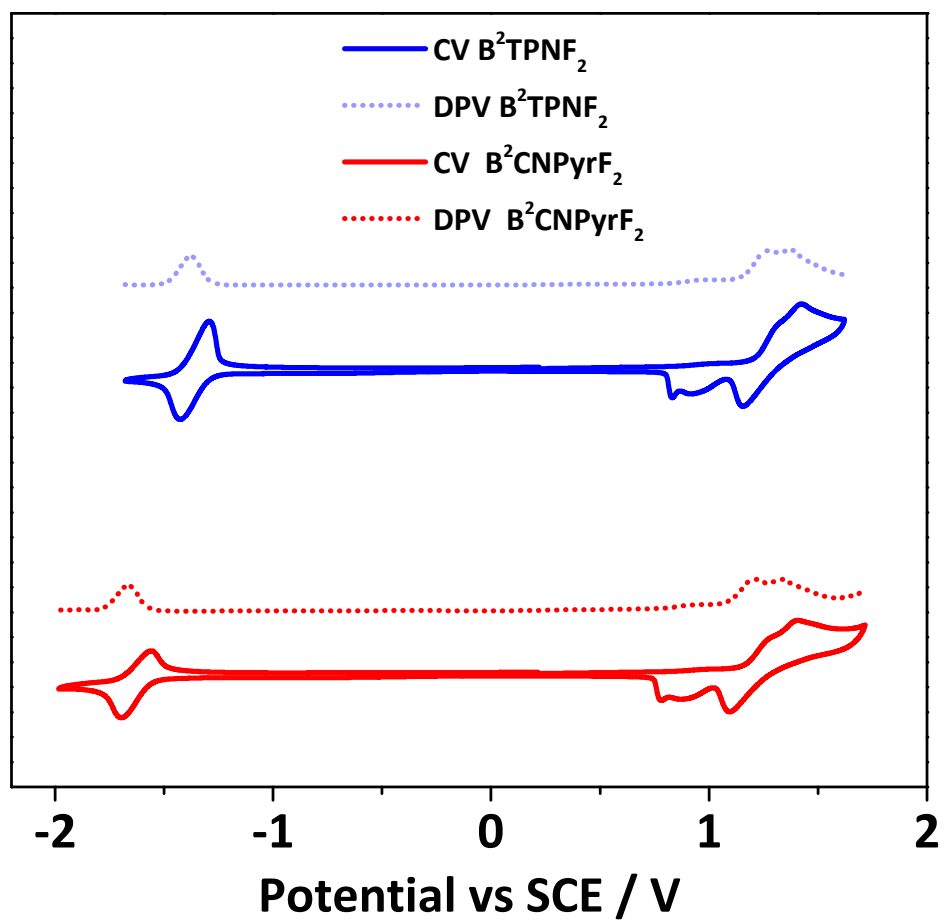


Figure S34. CV and DPV of B²TPNF₂ and B²CNPyrF₂ in DCM.

TCSPC experiments

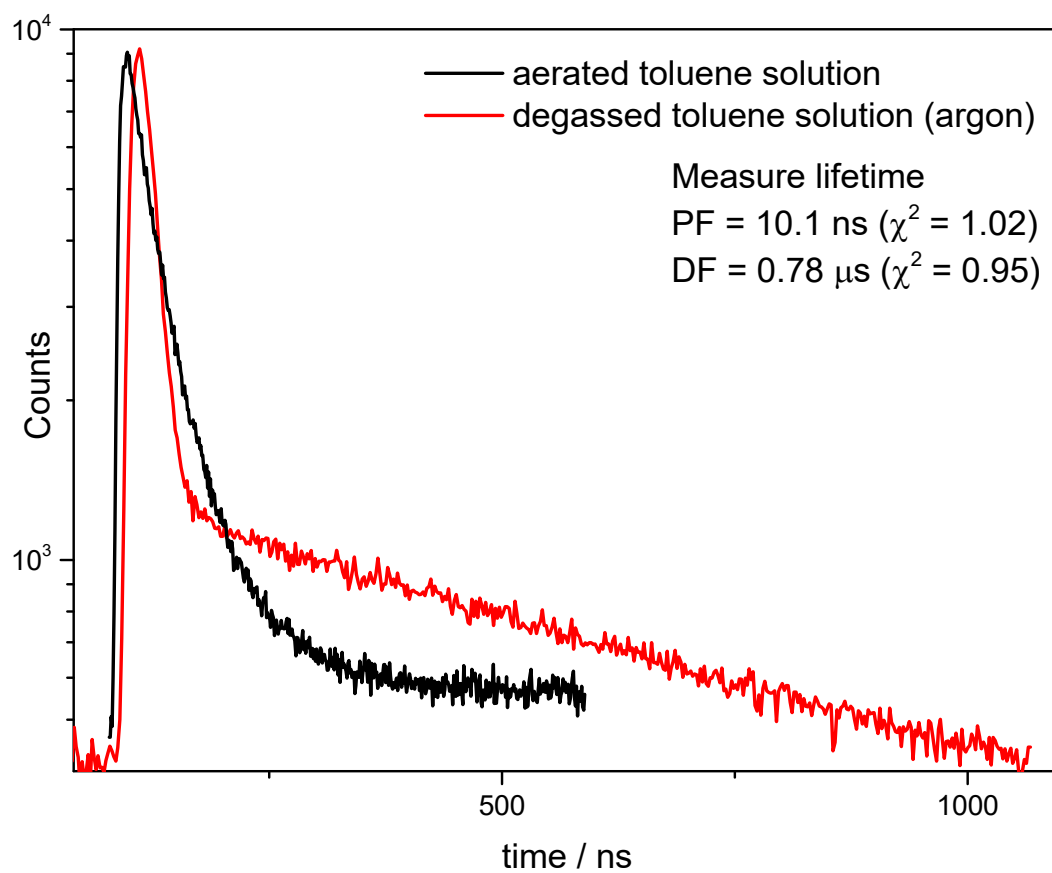


Figure S35. TCSPC experiments in aerated toluene solution (black) and degassed toluene solution (argon) for B^1TPNF_2 . $[\text{C}] = 1 \times 10^{-5} \text{ M}$, $\lambda_{\text{exc}} = 375 \text{ nm}$.

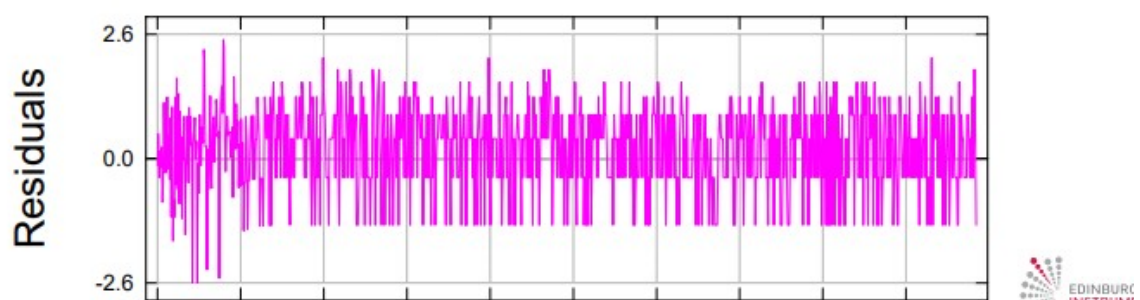
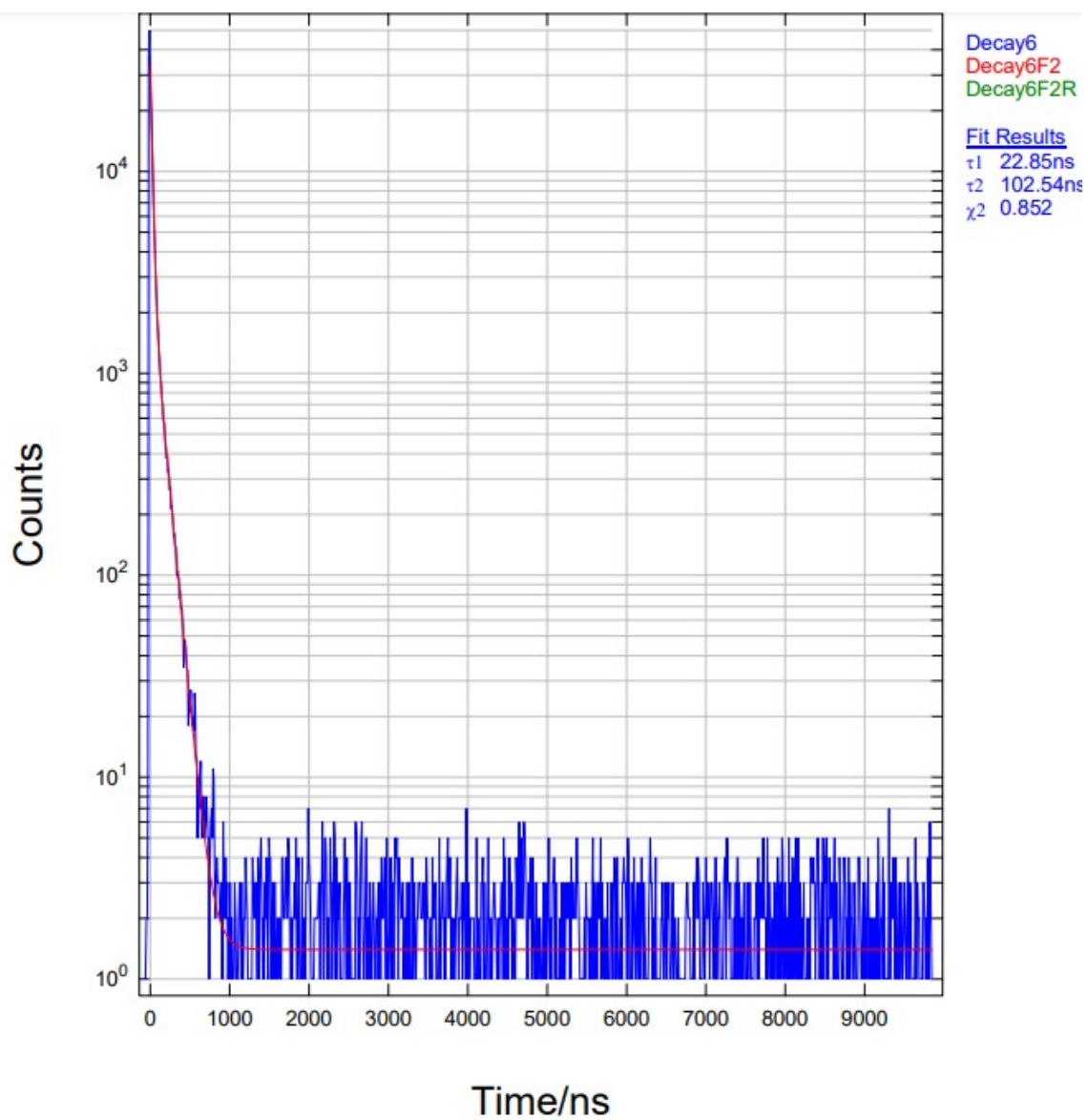


Figure S36. TCSPC experiments in aerated toluene solution for B^2TPNF_2 . $[\text{C}] = 1 \times 10^{-5} \text{ M}$. $\lambda_{\text{exc}} = 365 \text{ nm}$.

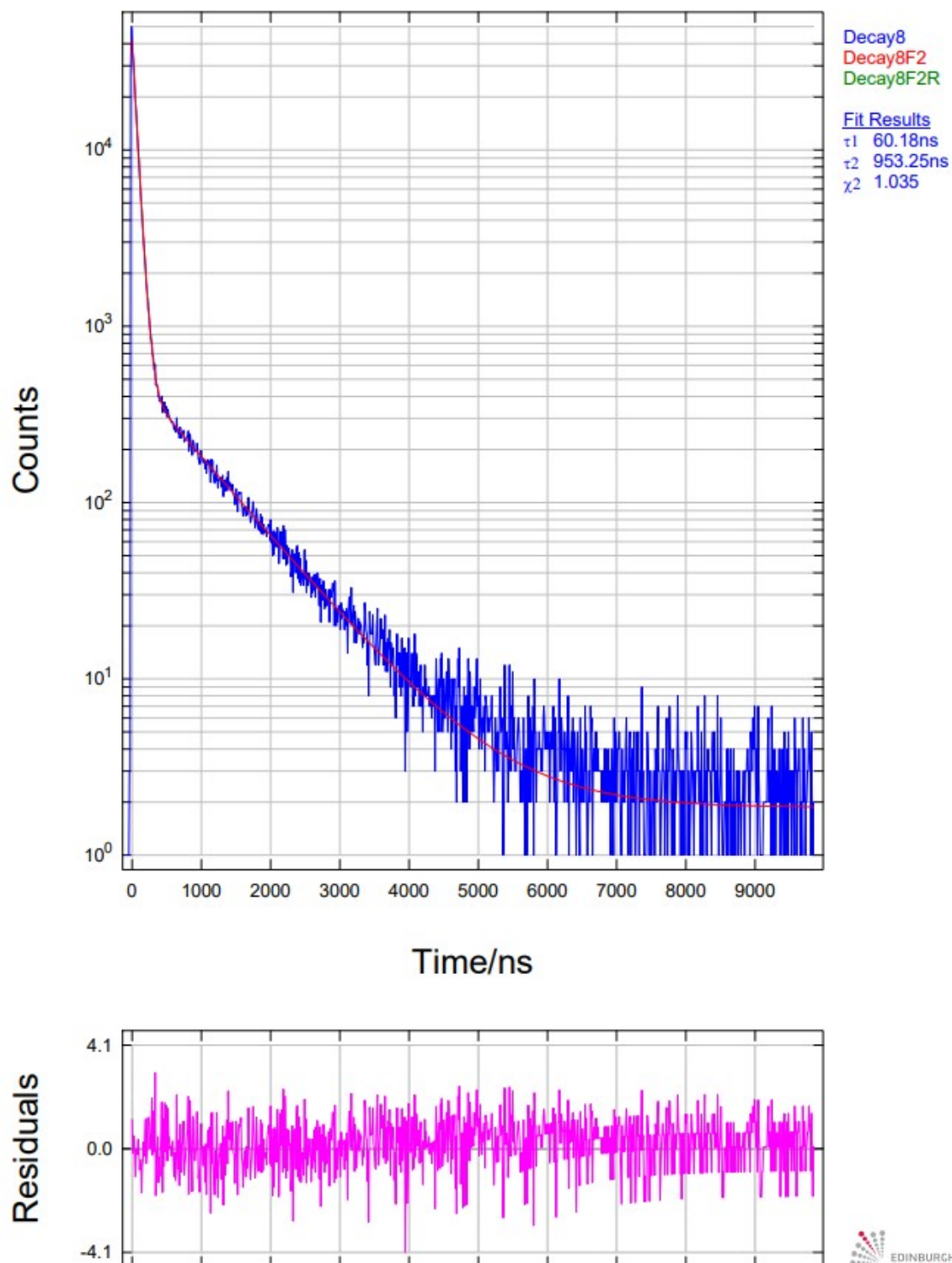


Figure S37. TCSPC experiments in degassed toluene solution (argon) for **B²TPNF₂**. [C] = 1×10^{-5} M. λ_{exc} = 365 nm.

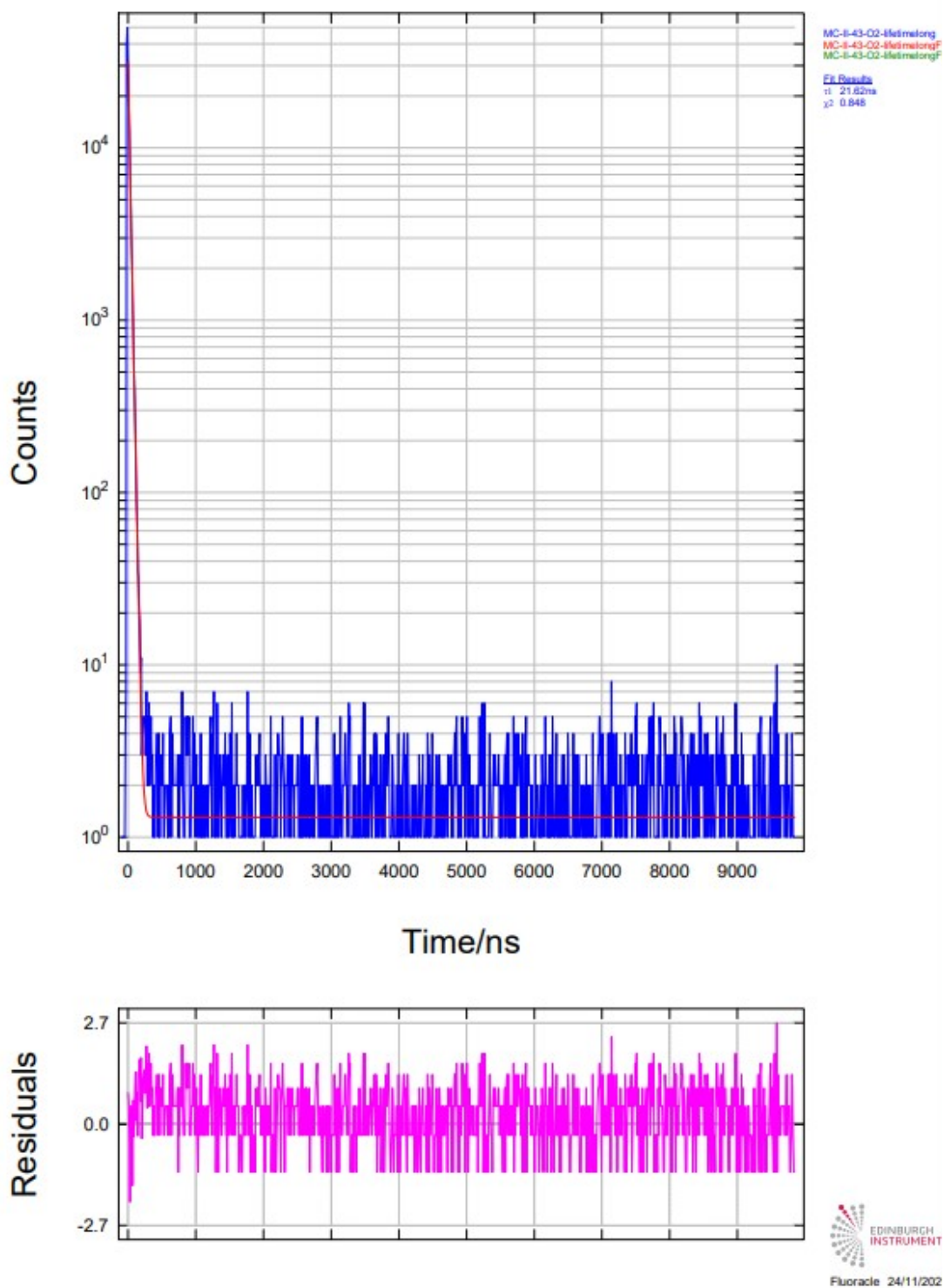


Figure S38. TCSPC experiments in aerated toluene solution for **B²CNPyrF₂**. [C] = 1 × 10⁻⁵ M. λ_{exc} = 365 nm.

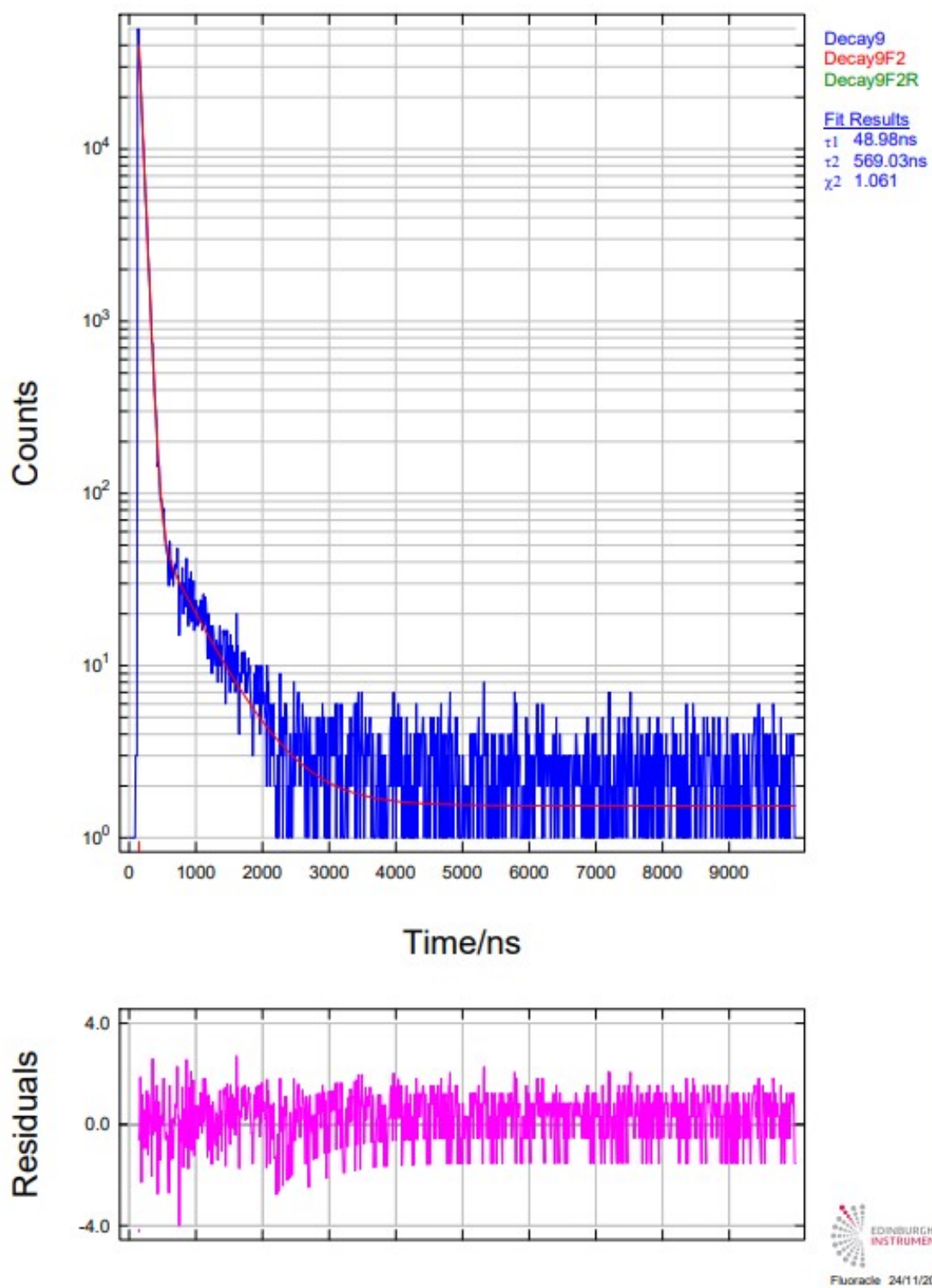


Figure S39. TCSPC experiments in degassed toluene solution (argon) for **B²CNPyrF₂**. $[C] = 1 \times 10^{-5}$ M. $\lambda_{\text{exc}} = 365$ nm.

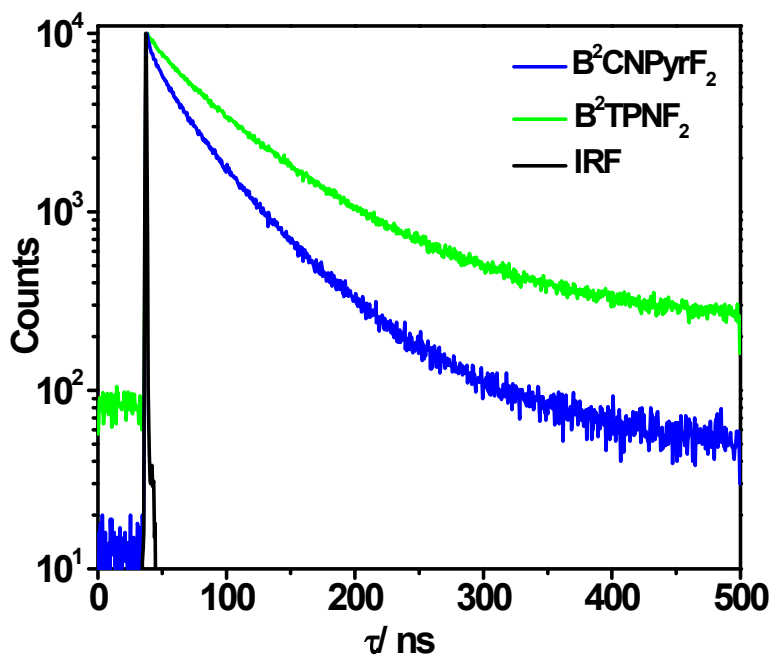


Figure S40. TCSPC experiments of 1 wt% doped mCP films in 500 ns for B^2TPNF_2 and $B^2CNPyrF_2$ at 300 K ($\lambda_{exc} = 379$ nm).

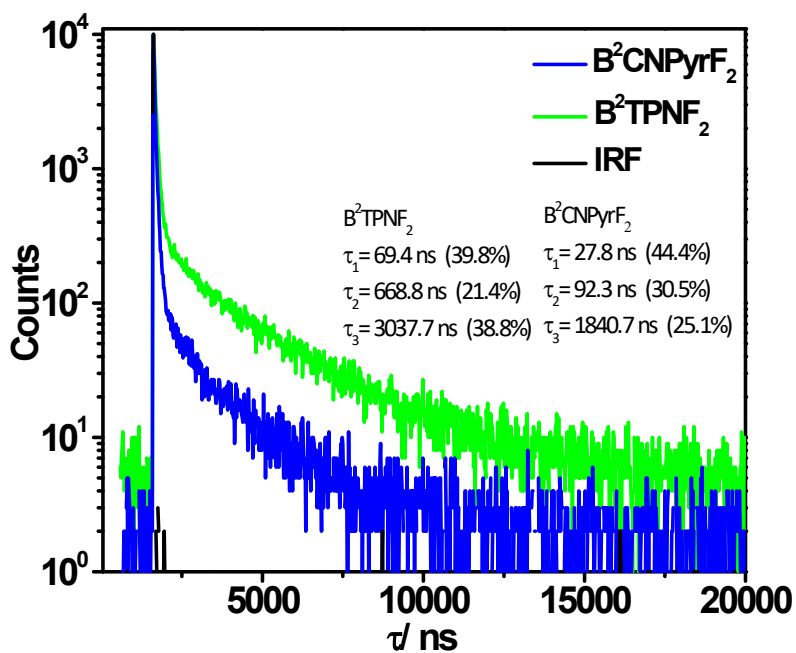


Figure S41. TCSPC experiments of 1 wt% doped mCP films in 20 μ s for B^2TPNF_2 and $B^2CNPyrF_2$ at 300 K ($\lambda_{exc} = 379$ nm).

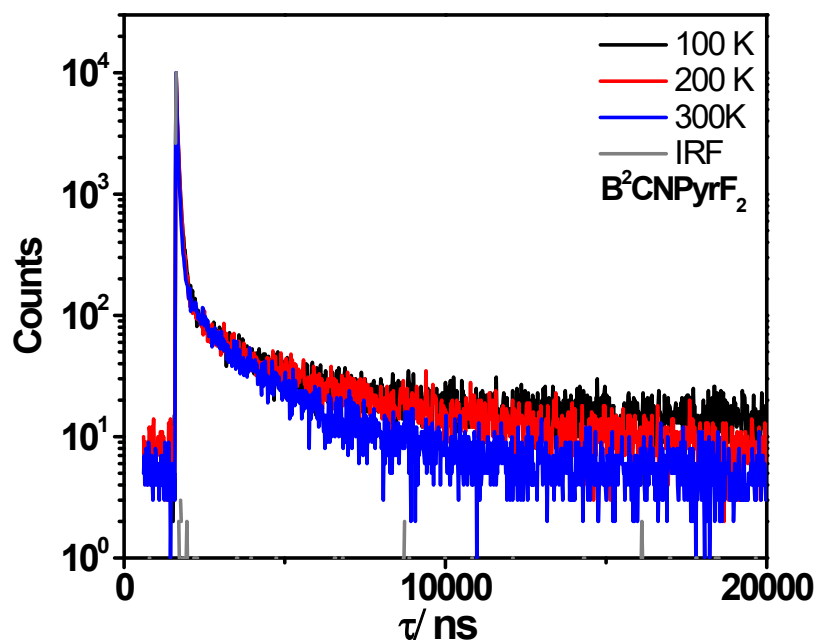


Figure S42. Temperature-dependent time-resolved PL decay for $B^2CNPyrF_2$ in 1 wt% mCP, $\lambda_{exc} = 379$ nm.

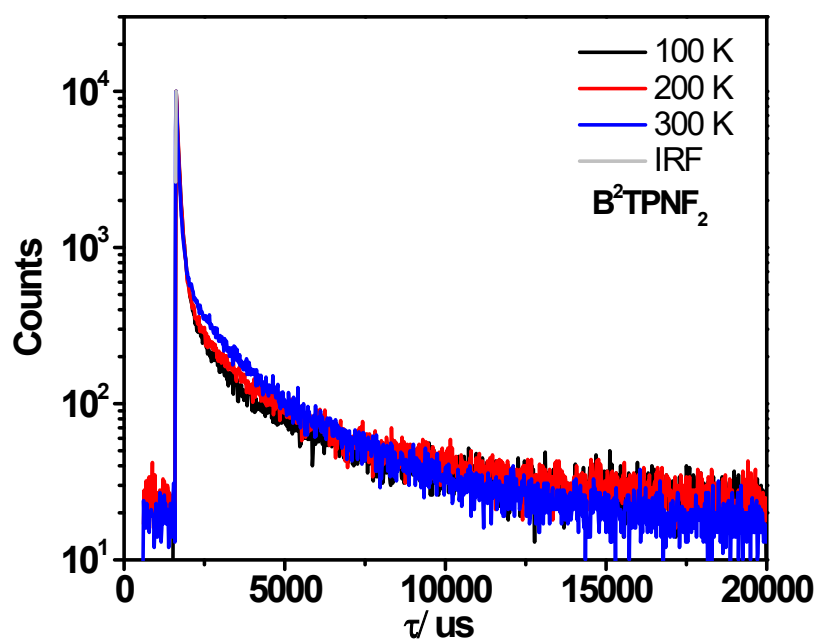


Figure S43. Temperature-dependent time-resolved PL decay for B^2TPNF_2 in 1 wt% mCP, $\lambda_{exc} = 379$ nm.

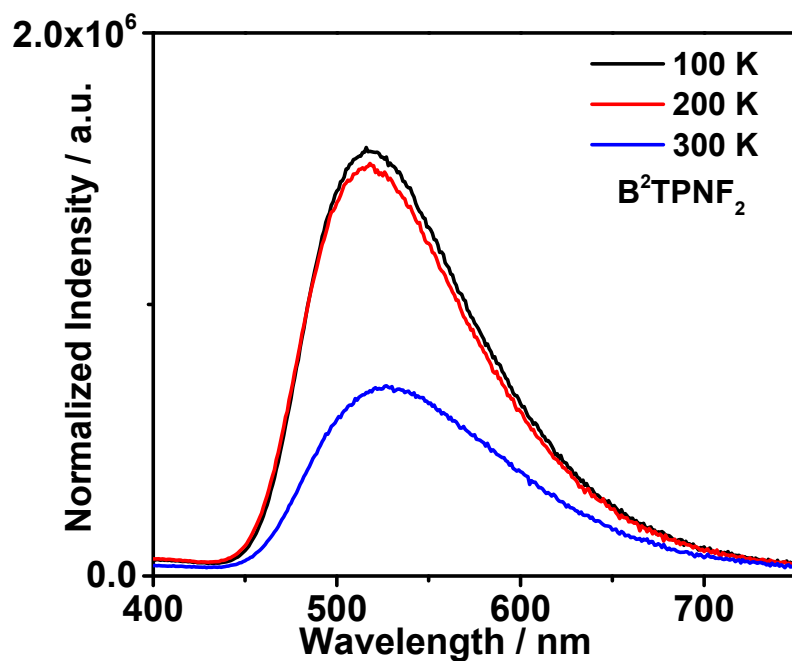


Figure S44. Temperature-dependent steady-state PL spectra in 1 wt% mCP, $\lambda_{exc} = 341$ nm, B^2TPNF_2 .

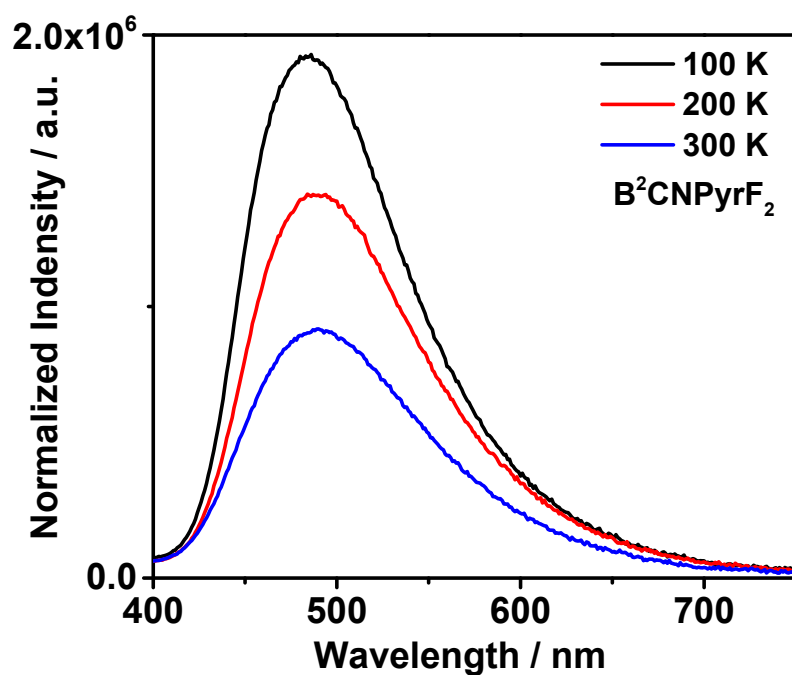


Figure S45. Temperature-dependent steady-state PL spectra in 1 wt% mCP, $\lambda_{exc} = 341$ nm, $B^2CNPyrF_2$.

Rate constants

Table S1: photophysical properties of the CP-TADF emitters with rate constants for **B¹TPNF₂**, **B²TPNF₂** and **B²CNPyrF₂**

Compound	λ_{obs} (nm) ^a	λ_{em} (nm) ^a	PLQY (Air/Ar) in % ^a	τ_{PL} (PF in ns/DF in μ s)	ΔE_{ST} ^c (eV)	k_r [10 ⁵ s ⁻¹]	k_{nr} [10 ⁶ s ⁻¹]	k_{ISC} [10 ⁶ s ⁻¹]	k_{rISC} [10 ⁵ s ⁻¹]
B ¹ TPNF ₂	363	529	5/11	10.1 ^a / 0.78 ^a	0.00	2.48	2.00	2.70	1.69
B ² TPNF ₂	341	530 ^a /527 ^b	11/29	60.2 ^a (69.4) ^b / 0.953 ^a (2.17) ^b	0.00	2.01	0.49	1.13	4.98
B ² CNPyrF ₂	358	492 ^a /488 ^b	9/23	49.0 ^a (54.1) ^b / 0.569 ^a (1.84) ^b	0.22	1.65	0.55	1.12	6.29

ΔE_{ST} determination

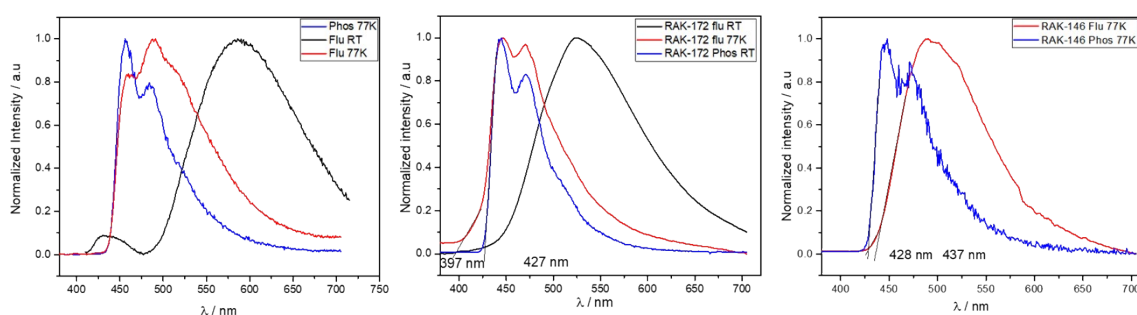


Figure S46. Prompt fluorescence spectra (at RT in black and at 77K in red) and phosphorescence spectra (in blue) of **B¹TPNF₂** (left), **B²TPNF₂** (middle) and **B²CNPyrF₂** (right) in MeTHF at 77 K ($\lambda_{exc} = 360$ nm).

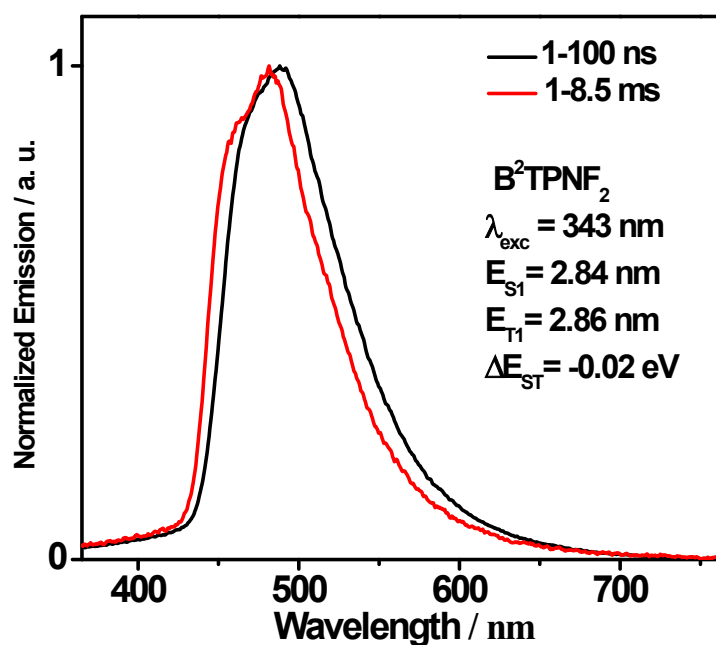


Figure S47. Prompt fluorescence spectra and phosphorescence spectra of **B²TPNF₂** in toluene at 77 K ($\lambda_{\text{exc}} = 343$ nm).

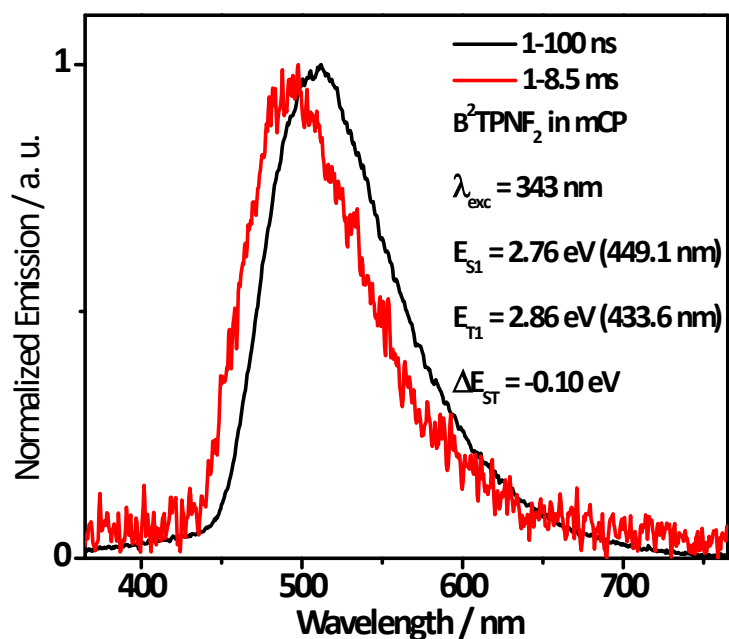


Figure S48. Prompt fluorescence spectra and phosphorescence spectra of 1 wt% **B²TPNF₂** in mCP film at 77 K ($\lambda_{\text{exc}} = 343$ nm).

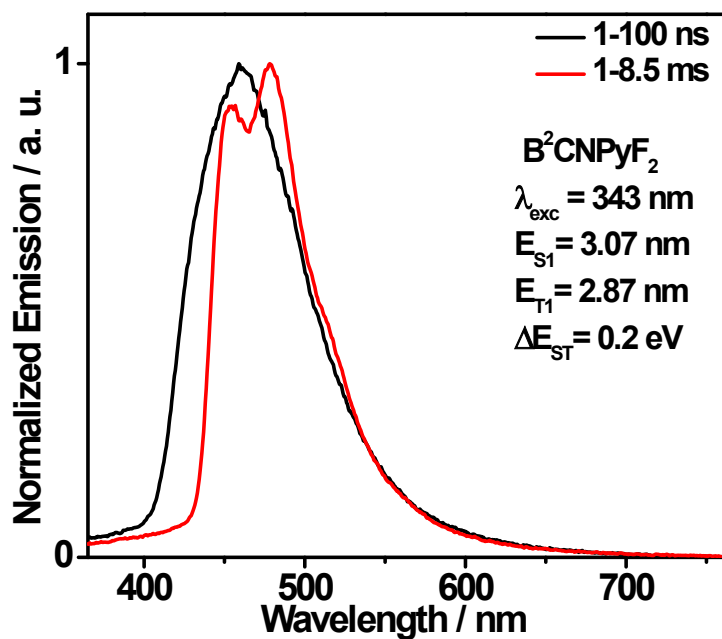


Figure S49. Prompt fluorescence spectra and phosphorescence spectra of **B²CNPyrF₂** in toluene at 77 K ($\lambda_{\text{exc}} = 343$ nm).

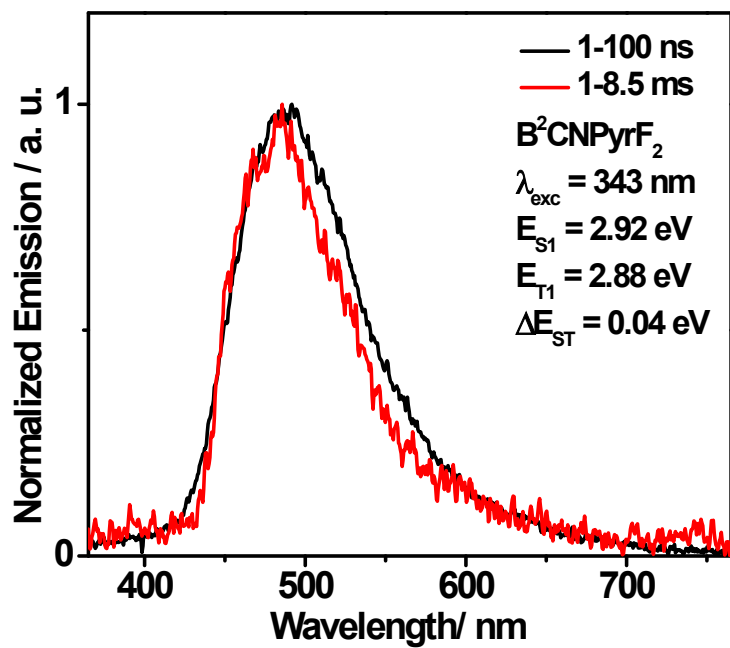


Figure S50. Prompt fluorescence spectra and phosphorescence spectra of 1wt% **B²CNPyrF₂** in mCP film at 77 K ($\lambda_{\text{exc}} = 343 \text{ nm}$).

ECD spectra

B¹TPNF₂

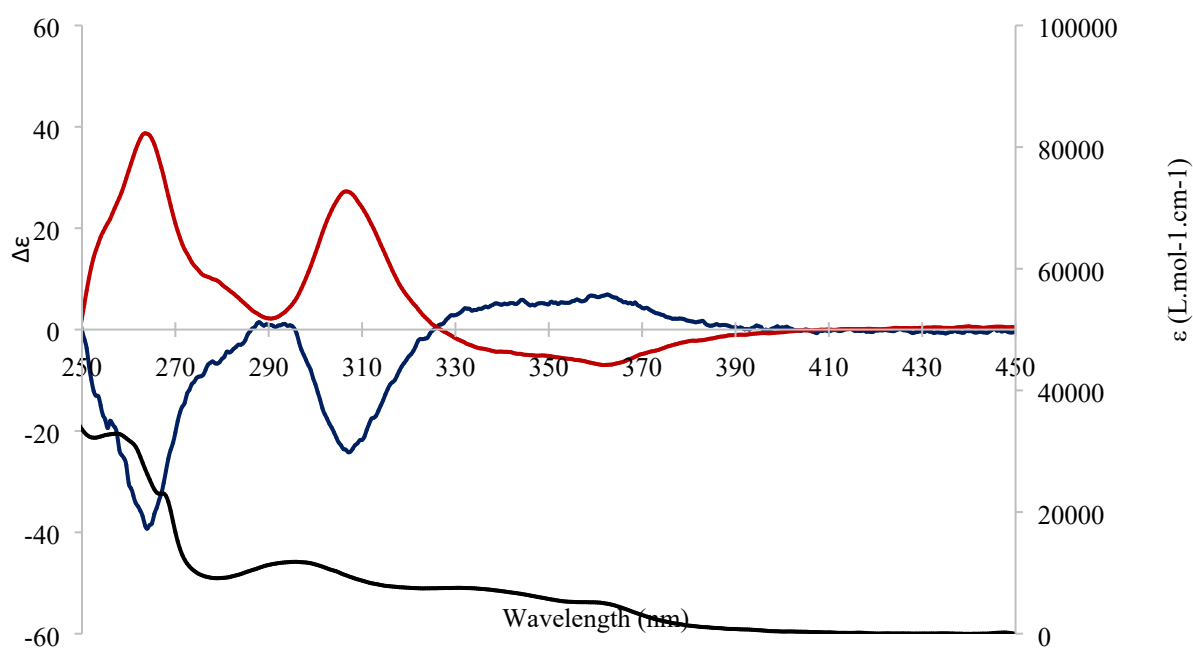


Figure S51. Top: ECD spectra in dichloromethane solution for **B¹TPNF₂**. (*S*)-enantiomer is depicted in red and (*R*) in blue. Bottom: Absorption spectrum is depicted in dotted black line. [C] = 5×10^{-6} M, 1 cm optical pathway.

B²TPNF₂

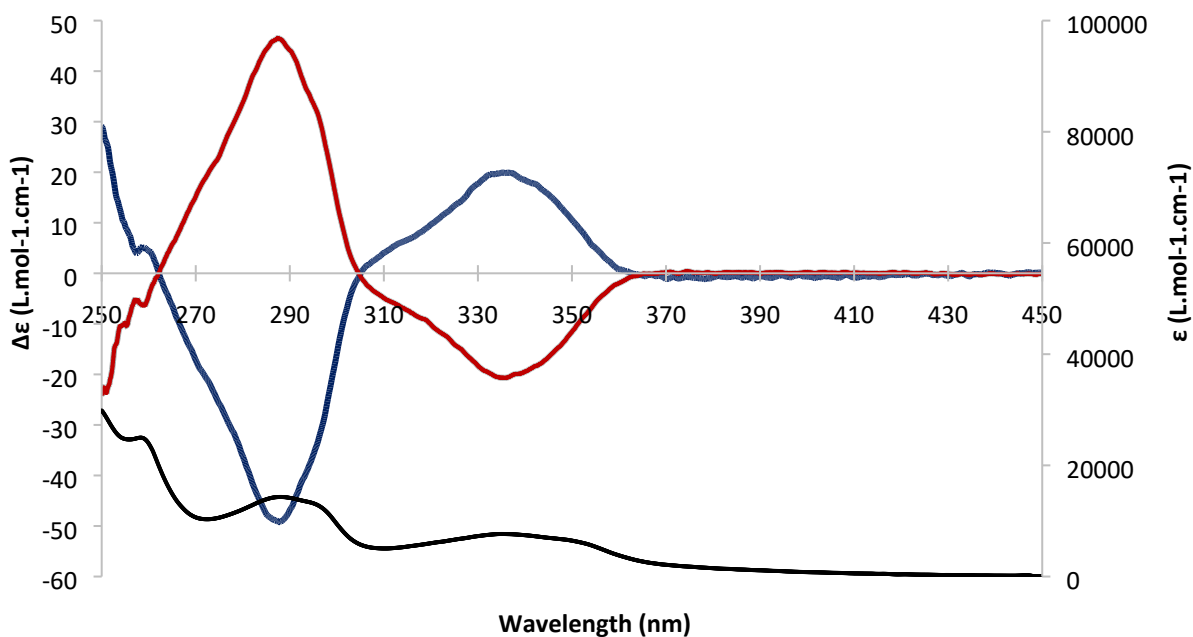


Figure S52. ECD spectra in dichloromethane solution for **B²TPNF₂**. (*S*)-enantiomer is depicted in red and (*R*) in blue. Absorption spectrum is depicted in dotted black line. [C] = 1×10^{-3} M, 1 mm optical pathway.

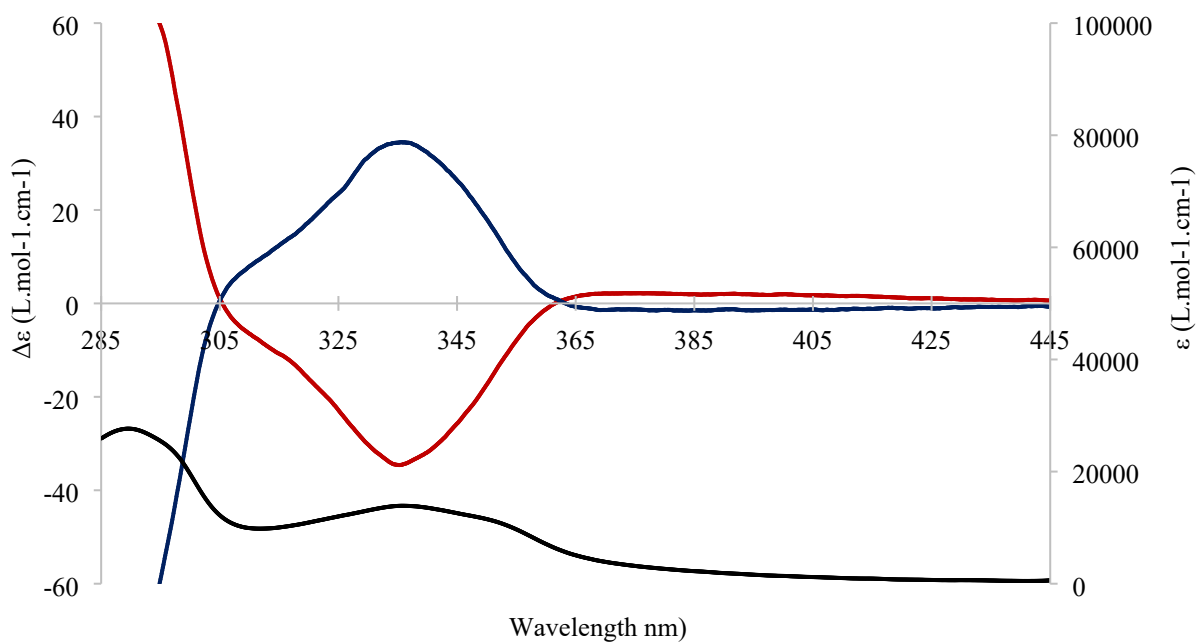


Figure S53. ECD spectra in toluene solution for **B²TPNF₂**. (*S*)-enantiomer is depicted in red and (*R*) in blue. Absorption spectrum is depicted in dotted black line. [C] = 1×10^{-3} M, 1 mm optical pathway.

B²CNPyrF₂

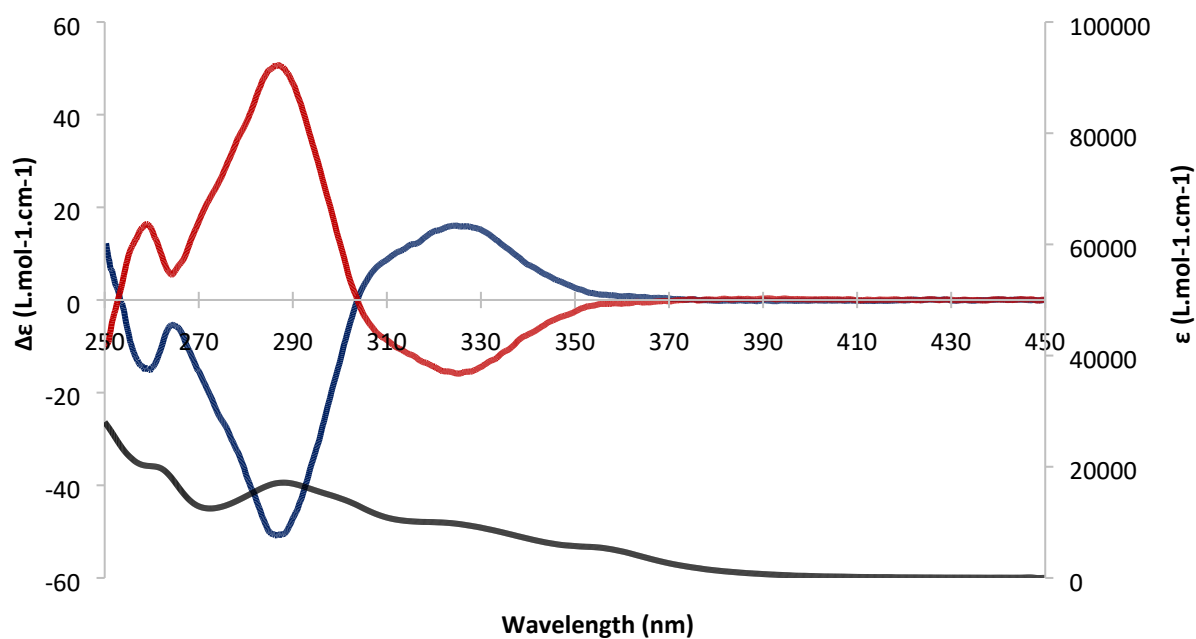


Figure S54. ECD spectra in dichloromethane solution for **B²CNPyrF₂**. (*S*)-enantiomer is depicted in red and (*R*) in blue. Absorption spectrum is depicted in dotted black line. [C] = 1×10^{-3} M, 1 mm optical pathway.

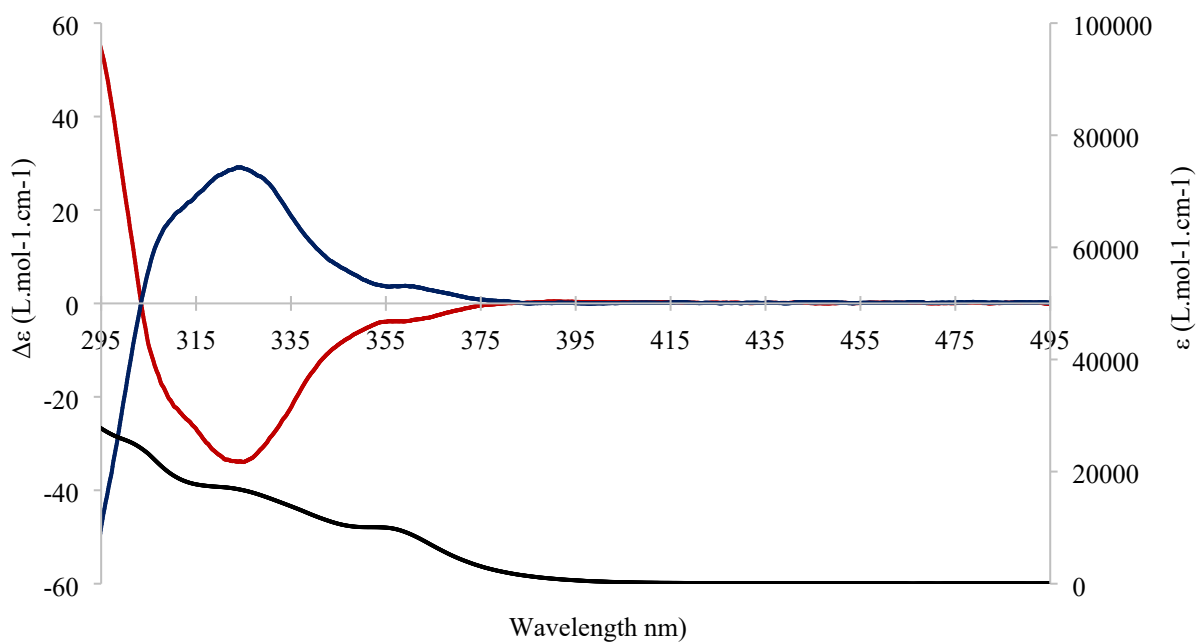


Figure S55. ECD spectra in toluene solution for **B²CNPyrF₂**. (*S*)-enantiomer is depicted in red and (*R*) in blue. Absorption spectrum is depicted in dotted black line. [C] = 1×10^{-3} M, 1 mm optical pathway.

Circularly polarized luminescence spectra

B¹TPNF₂

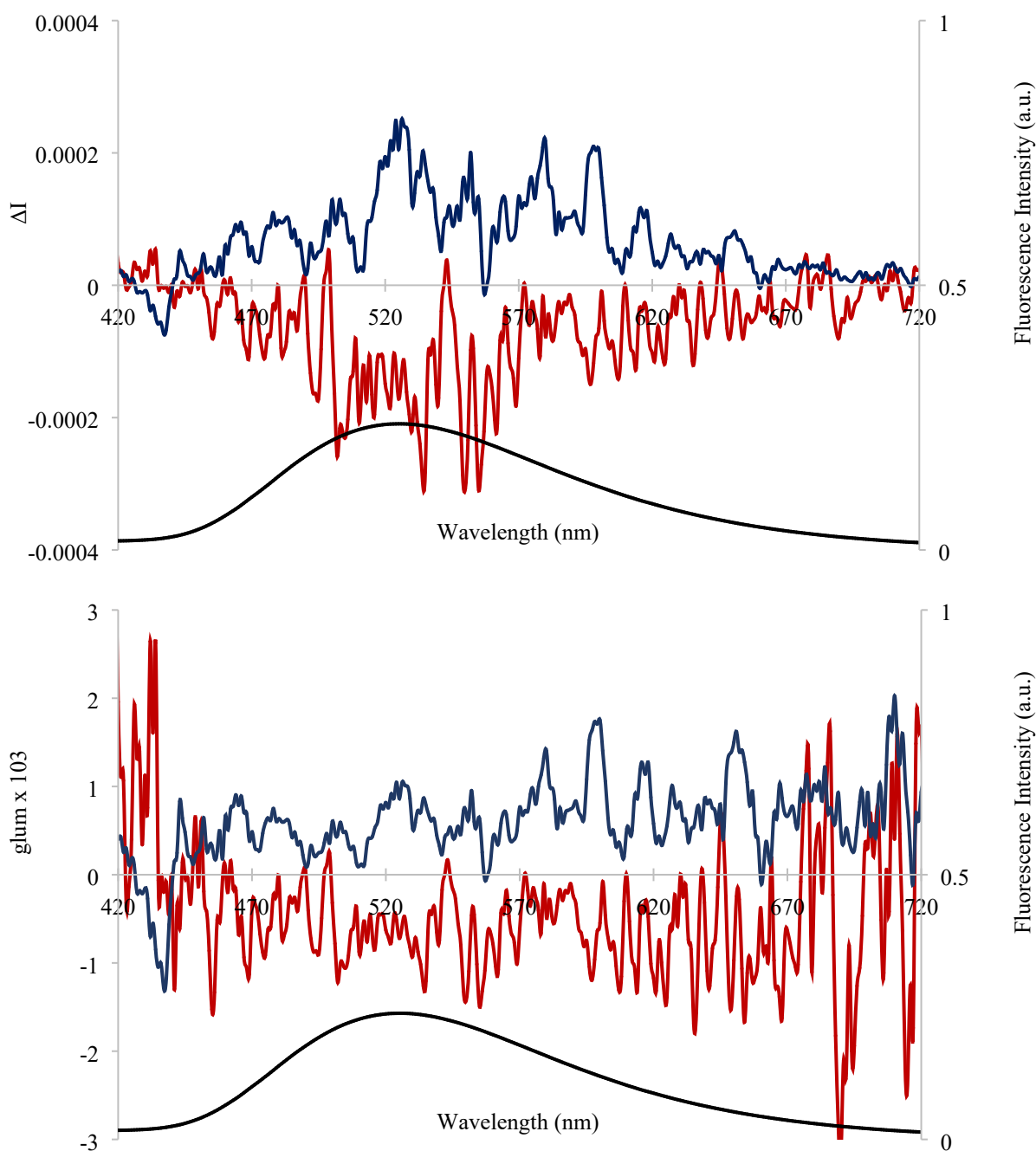


Figure S56. CPL spectra (top) and $g_{lum} = f(\lambda)$ (bottom) in toluene solution for **B¹TPNF₂**. (*S*)-enantiomer is depicted in red and (*R*) in blue. Fluorescence spectra is depicted in black. $[C] = 1 \times 10^{-5}$ M, $\lambda_{exc} = 375$ nm

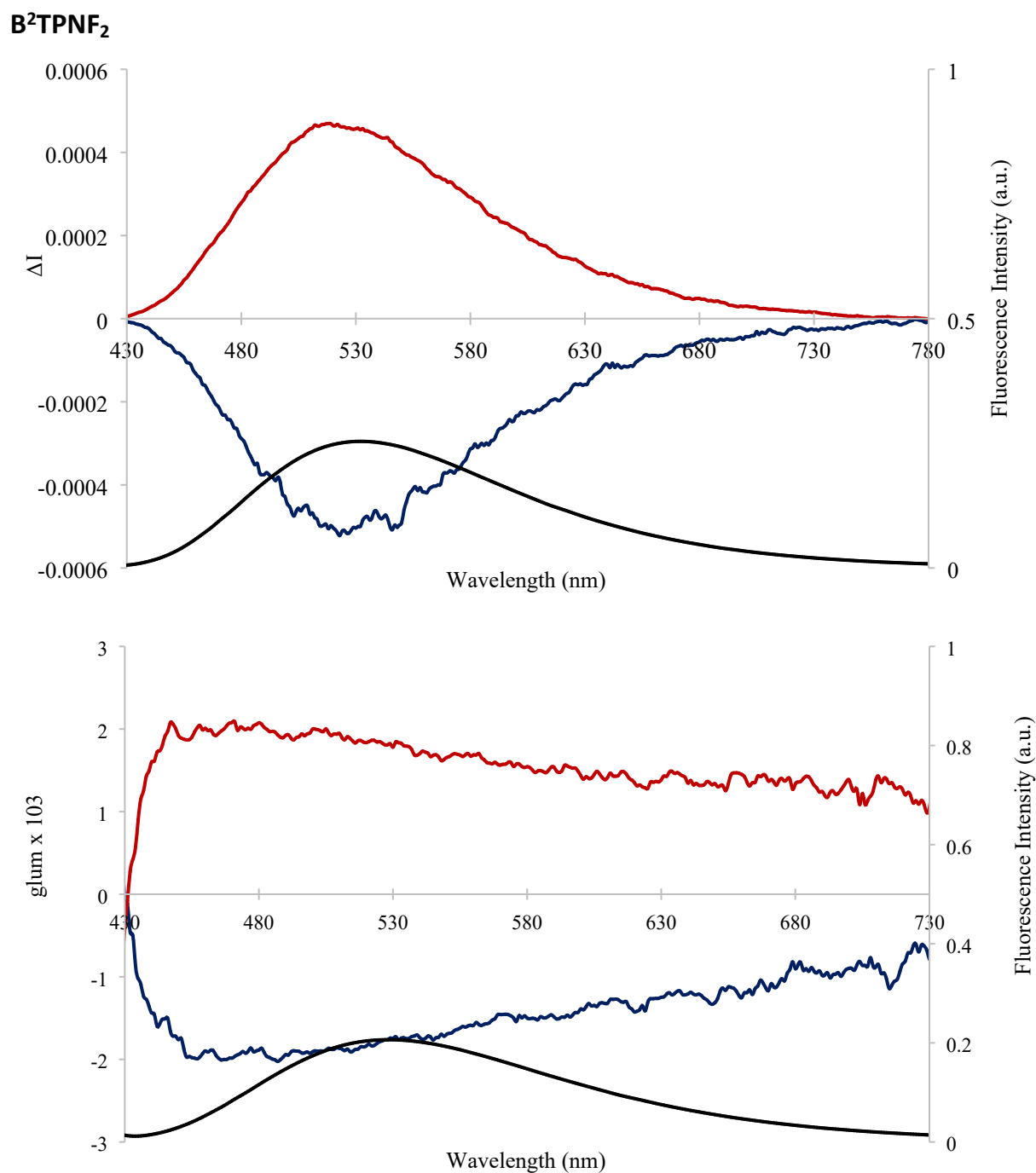


Figure S57. CPL spectra (top) and $g_{lum} = f(\lambda)$ (bottom) in toluene solution for **B₂TPNF₂**. (*S*)-enantiomer is depicted in red and (*R*) in blue. Fluorescence spectra is depicted in black. $[C] = 1 \times 10^{-4}$ M. $\lambda_{exc} = 350$ nm.

B²CNPyrF₂

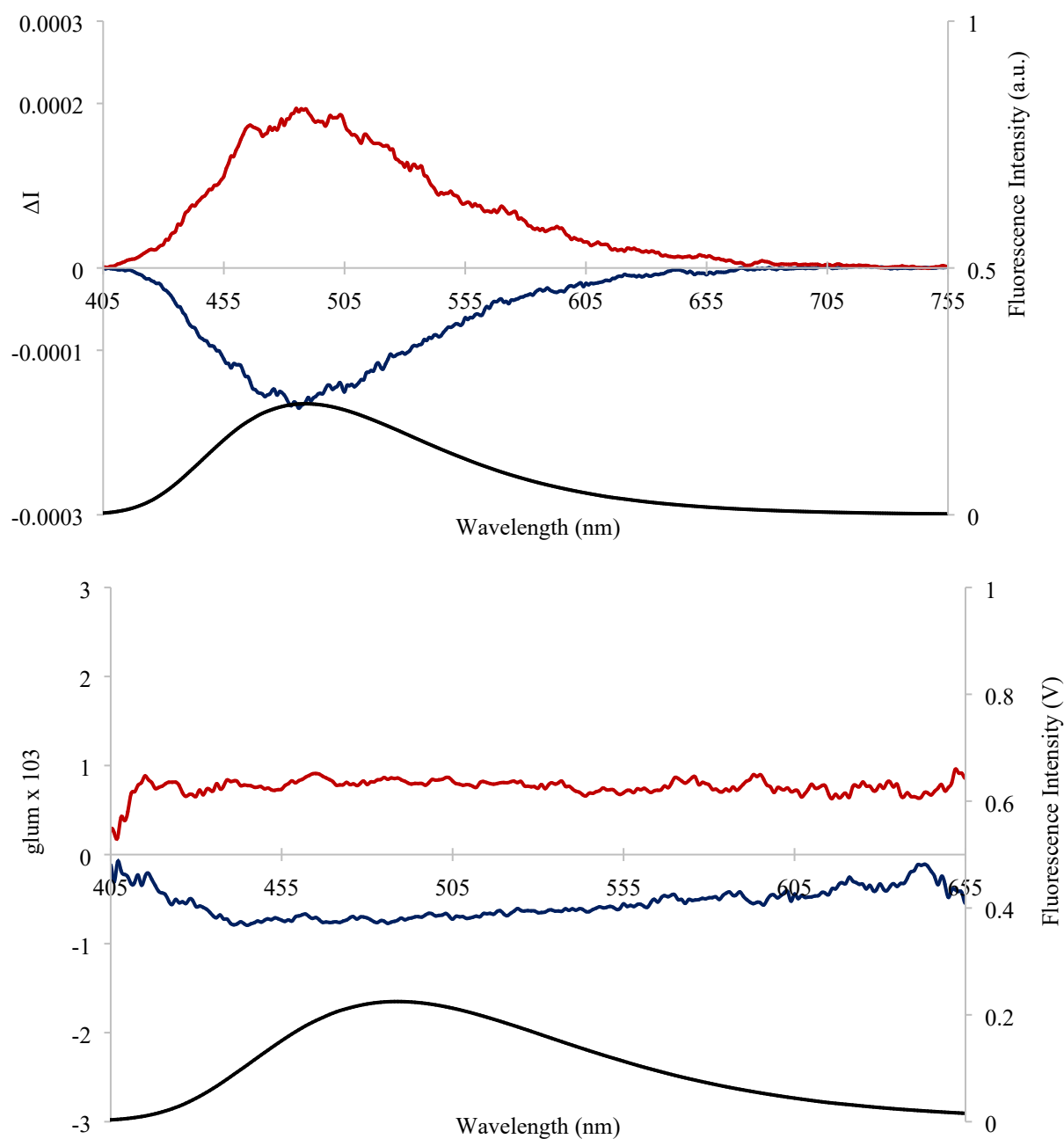


Figure S58. CPL spectra (top) and $g_{lum} = f(\lambda)$ (bottom) in toluene solution for **B₂CNPyrF₂**. (*S*)-enantiomer is depicted in red and (*R*) in blue. Fluorescence spectra is depicted in black. $[C] = 1 \times 10^{-4}$ M. $\lambda_{exc} = 350$ nm.

Theoretical calculations

Cartesian coordinates of the optimized geometry of ground state **B¹TPNF₂** (M06-2X/6-31+G(d,p)/CPCM(DCM)):

C	-3.13328	-0.59637	1.69132
C	-4.29643	-0.91158	2.37599
C	-4.84654	2.20182	-2.30588
C	-2.51014	1.58614	-0.92227
C	-3.08067	2.87965	-0.86257
C	-4.25025	3.20281	-1.55528
C	-1.31487	1.63798	-0.10657
C	-1.22129	2.96383	0.38622
N	-2.30627	3.68924	-0.05602
C	-0.33020	0.70127	0.23460
C	0.72562	1.14740	1.01626
C	0.82722	2.45572	1.48939
C	-0.15160	3.38535	1.17889
C	-0.33021	-0.70129	-0.23459
C	-1.31490	-1.63798	0.10658
C	-1.22134	-2.96383	-0.38622
C	-0.15165	-3.38537	-1.17888
C	0.82718	-2.45575	-1.48937
C	0.72561	-1.14744	-1.01625
C	-2.51017	-1.58612	0.92226
C	-3.08073	-2.87962	0.86257
N	-2.30633	-3.68922	0.05603
C	-4.84658	-2.20175	2.30587
C	-4.25031	-3.20275	1.55527
C	-2.53911	-5.09915	-0.18027
C	-2.53901	5.09918	0.18027
O	1.69804	0.21998	1.42709
O	1.69804	-0.22003	-1.42708
C	2.82951	-0.12637	-0.68836
C	4.05120	-0.23270	-1.36425
C	5.25735	-0.11086	-0.68031
C	5.25735	0.11086	0.68031
C	4.05120	0.23268	1.36425
C	2.82951	0.12632	0.68837
C	4.06190	-0.49857	-2.77016
C	4.06190	0.49859	2.77015
N	4.08073	0.72150	3.89715
N	4.08075	-0.72165	-3.89712
F	6.40805	-0.21865	-1.32891
F	6.40805	0.21868	1.32890
C	-4.29641	0.91164	-2.37601
C	-3.13326	0.59641	-1.69133
H	-2.71278	0.39939	1.75639
H	-4.78701	-0.15553	2.97644
H	-5.75417	2.42304	-2.85500
H	-4.67328	4.19899	-1.51759
H	1.67275	2.72521	2.11140

H	-0.07660	4.40210	1.54179
H	-0.07667	-4.40212	-1.54178
H	1.67271	-2.72527	-2.11138
H	-5.75423	-2.42295	2.85498
H	-4.67336	-4.19893	1.51758
H	-2.07779	-5.38864	-1.12302
H	-3.61073	-5.27983	-0.25985
H	-2.12810	-5.71148	0.62618
H	-3.61062	5.27989	0.25980
H	-2.12794	5.71148	-0.62618
H	-2.07771	5.38866	1.12303
H	-4.78699	0.15560	-2.97647
H	-2.71278	-0.39936	-1.75640

Simulated UV spectrum of **B¹TPNF₂**:

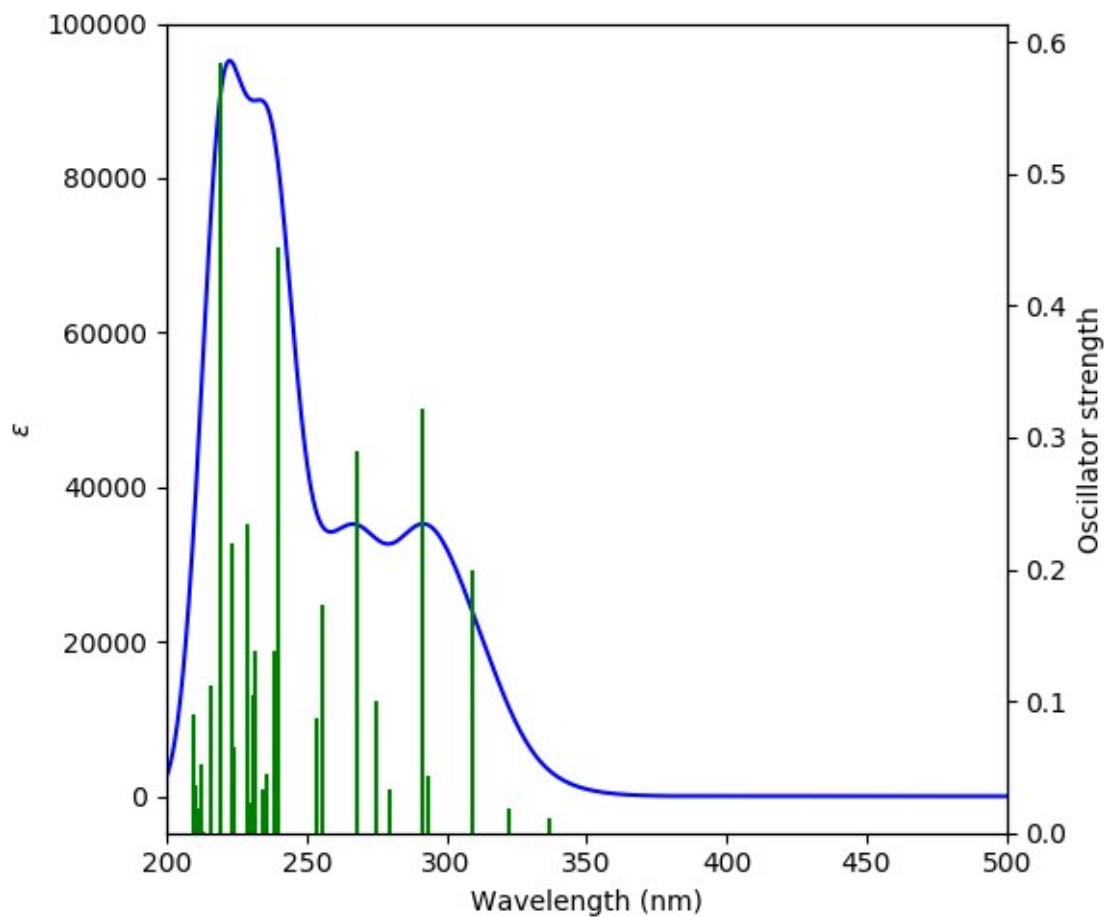


Figure S59. Simulated UV spectrum of **B¹TPNF₂** and oscillator strengths

Cartesian coordinates of the optimized geometry of ground state **B²TPNF₂** (M06-2X/6-31+G(d,p)/CPCM(DCM)):

C	-5.12224	-0.07119	0.68582
C	-5.12224	0.07117	-0.68580
C	-3.91705	0.17200	-1.37334
C	-2.69401	0.12173	-0.68966
C	-2.69401	-0.12171	0.68966
C	-3.91704	-0.17200	1.37335
F	-6.27264	-0.13027	1.34035
F	-6.27265	0.13023	-1.34032
C	-3.93995	-0.33728	2.79437
C	-3.93998	0.33726	-2.79437
O	-1.56194	0.26190	-1.42324
O	-1.56193	-0.26187	1.42323
N	-3.97897	-0.46222	3.93586
N	-3.97901	0.46218	-3.93585
C	-0.60983	-1.19601	0.97373
C	0.43032	-0.71481	0.18893
C	1.40378	-1.64731	-0.19767
C	1.35065	-2.97695	0.27966
C	0.29426	-3.39878	1.08548
C	-0.71852	-2.51565	1.43640
C	0.43031	0.71483	-0.18895
C	-0.60984	1.19603	-0.97373
C	-0.71853	2.51568	-1.43639
C	0.29425	3.39881	-1.08547
C	1.35064	2.97697	-0.27965
C	1.40378	1.64732	0.19766
N	2.52163	-1.49410	-1.00011
C	3.21274	-2.69489	-1.01680
C	2.52018	-3.64841	-0.23990
C	2.52017	3.64842	0.23991
C	3.21274	2.69488	1.01679
N	2.52164	1.49409	1.00008
C	4.40823	-3.01461	-1.66597
C	4.88781	-4.30887	-1.52547
C	4.20599	-5.26882	-0.76037
C	3.02241	-4.94533	-0.11468
C	3.02240	4.94535	0.11471
C	4.20599	5.26882	0.76041
C	4.88782	4.30885	1.52548
C	4.40824	3.01459	1.66596
C	2.89567	-0.33796	-1.79910
C	2.89568	0.33792	1.79902
C	-1.87094	2.93401	-2.30835
C	-1.87093	-2.93397	2.30837
H	0.25734	-4.42170	1.44466
H	0.25733	4.42173	-1.44463
H	4.95348	-2.28417	-2.25019
H	5.81432	-4.58247	-2.01625

H	4.61288	-6.26867	-0.67373
H	2.49570	-5.68468	0.47804
H	2.49569	5.68471	-0.47799
H	4.61287	6.26868	0.67378
H	5.81432	4.58245	2.01626
H	4.95349	2.28414	2.25016
H	2.00258	0.16412	-2.16604
H	3.50068	0.37102	-1.22743
H	3.46776	-0.68300	-2.65895
H	3.46778	0.68293	2.65888
H	2.00259	-0.16417	2.16595
H	3.50069	-0.37104	1.22732
H	-2.82536	2.84222	-1.78175
H	-1.75569	3.97491	-2.60917
H	-1.92976	2.31740	-3.20716
H	-2.82535	-2.84219	1.78177
H	-1.75567	-3.97486	2.60921
H	-1.92975	-2.31734	3.20717

Simulated UV spectrum of **B²TPNF₂**:

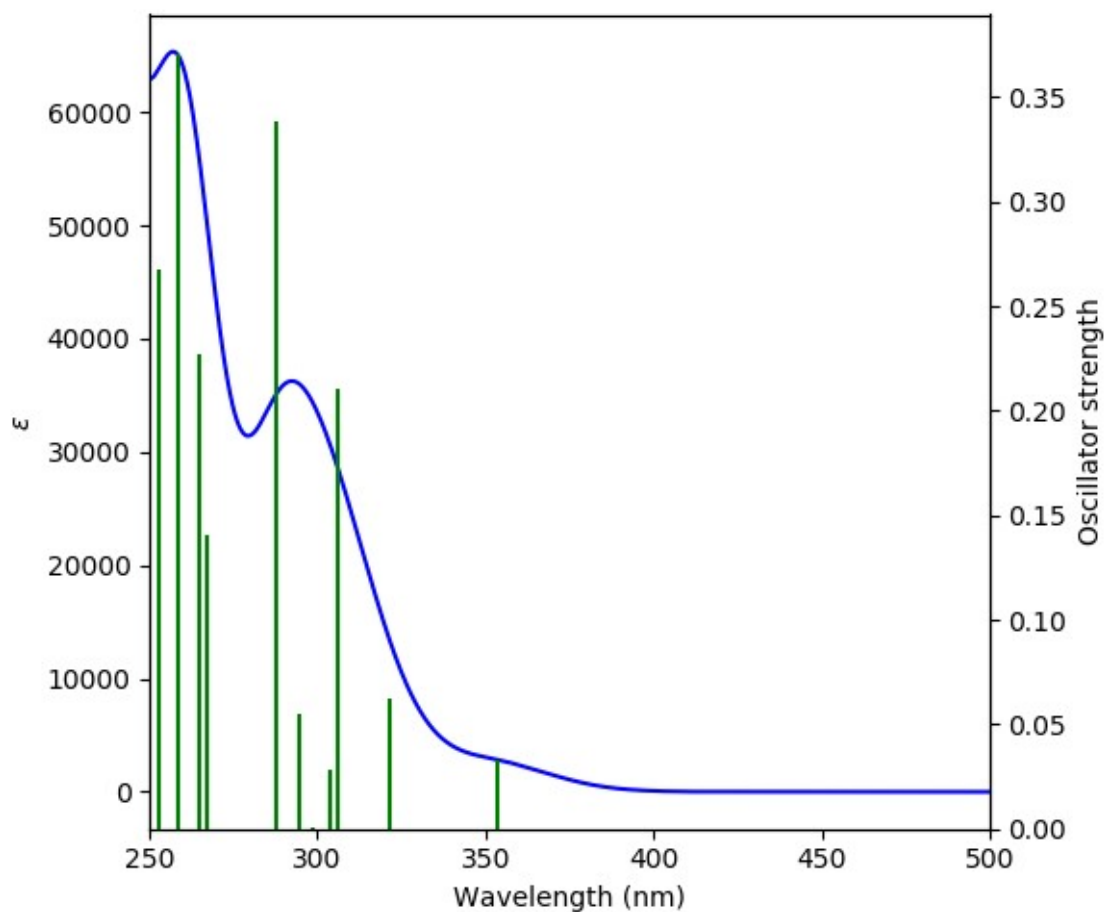


Figure S60. Simulated UV spectrum (blue line) of **B²TPNF₂** and oscillator strengths (green bars)

Cartesian coordinates of the optimized geometry of ground state **B²CNPyrF₂** (M06-2X/6-31+G(d,p)/CPCM(DCM)):

C	-5.08299	0.18801	-1.21965
C	-5.29062	0.01345	0.13761
C	-4.17421	-0.14278	0.94728
C	-2.89863	-0.11330	0.37186
C	-2.82123	0.14840	-1.00541
N	-3.90029	0.26386	-1.76058
F	-6.13816	0.30776	-2.01712
F	-6.51383	-0.01126	0.64511
O	-1.82650	-0.27768	1.18424
O	-1.63378	0.24942	-1.65293
C	-0.71323	1.18400	-1.15687
C	0.27210	0.71460	-0.29680
C	1.21926	1.65303	0.13786
C	1.20155	2.97393	-0.36594
C	0.20258	3.38360	-1.24857
C	-0.78787	2.49618	-1.64818
C	0.25078	-0.71393	0.08825
C	-0.84049	-1.20238	0.79594
C	-0.97725	-2.52335	1.24682
C	0.06057	-3.40261	0.96782
C	1.17020	-2.97436	0.24063
C	1.25216	-1.64345	-0.22986
N	2.28310	1.51195	1.01303
C	2.97590	2.71086	1.05281
C	2.33802	3.65166	0.21556
C	2.37511	-3.64174	-0.19672
C	3.11695	-2.68527	-0.92267
N	2.42314	-1.48649	-0.95285
C	4.12802	3.03958	1.77212
C	4.62061	4.32989	1.63933
C	3.99318	5.27705	0.81427
C	2.85230	4.94466	0.09960
C	2.87138	-4.93742	-0.03880
C	4.09760	-5.25674	-0.60182
C	4.82776	-4.29385	-1.31702
C	4.35516	-3.00068	-1.48845
C	2.60399	0.36717	1.84999
C	2.84868	-0.33253	-1.72923
C	-2.19059	-2.94425	2.03085
C	-1.89209	2.89748	-2.58893
C	-4.33605	-0.33983	2.35634
N	-4.48270	-0.49239	3.48521
H	0.19459	4.39959	-1.62895
H	0.00177	-4.42683	1.32037
H	4.63126	2.31880	2.40418
H	5.51445	4.61020	2.18398
H	4.40858	6.27411	0.73569
H	2.36767	5.67438	-0.53924

H	2.30722	-5.67922	0.51521
H	4.50035	-6.25561	-0.48845
H	5.78661	-4.56415	-1.74328
H	4.93694	-2.26762	-2.03282
H	1.68889	-0.13582	2.15623
H	3.25209	-0.34485	1.33167
H	3.11049	0.72453	2.74536
H	1.98117	0.17432	-2.14695
H	3.42406	0.37334	-1.12400
H	3.46727	-0.68137	-2.55484
H	-3.10305	-2.85568	1.43372
H	-2.09567	-3.98435	2.34155
H	-2.31903	-2.32606	2.92142
H	-1.99315	2.18029	-3.40539
H	-2.85584	2.93733	-2.07432
H	-1.69099	3.88344	-3.00734

Simulated UV spectrum of **B²CNPyrF₂**

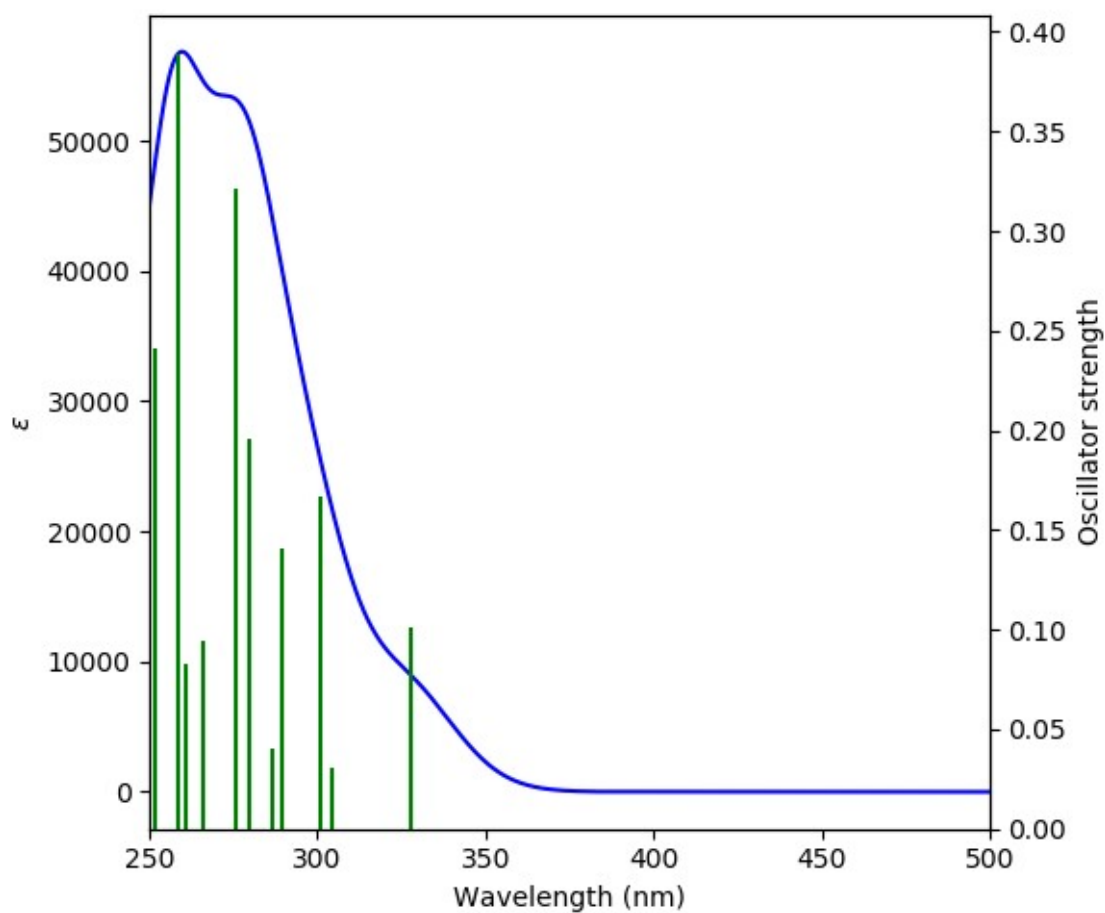


Figure S61. Simulated UV spectrum (blue line) of **B²CNPyrF₂** and oscillator strengths (green bars)

Theoretical calculations of ΔE_{ST}

The energies of the excited state were calculated using time-dependent DFT within the Tamm-Dancoff approximation (TDA-DFT) at the PBE0/6-311G(d,p) level of theory in toluene phase in the Gaussian (G16) package.

The ΔE_{ST} s are calculated as 0.02, 0.02 and 0.05 eV for **B¹TPNF₂**, **B²TPNF₂** and **B²CNPyrF₂**, respectively, which show same tendency and similar values as compared with the experimental data (0.00, 0.00 and 0.22 eV, respectively).

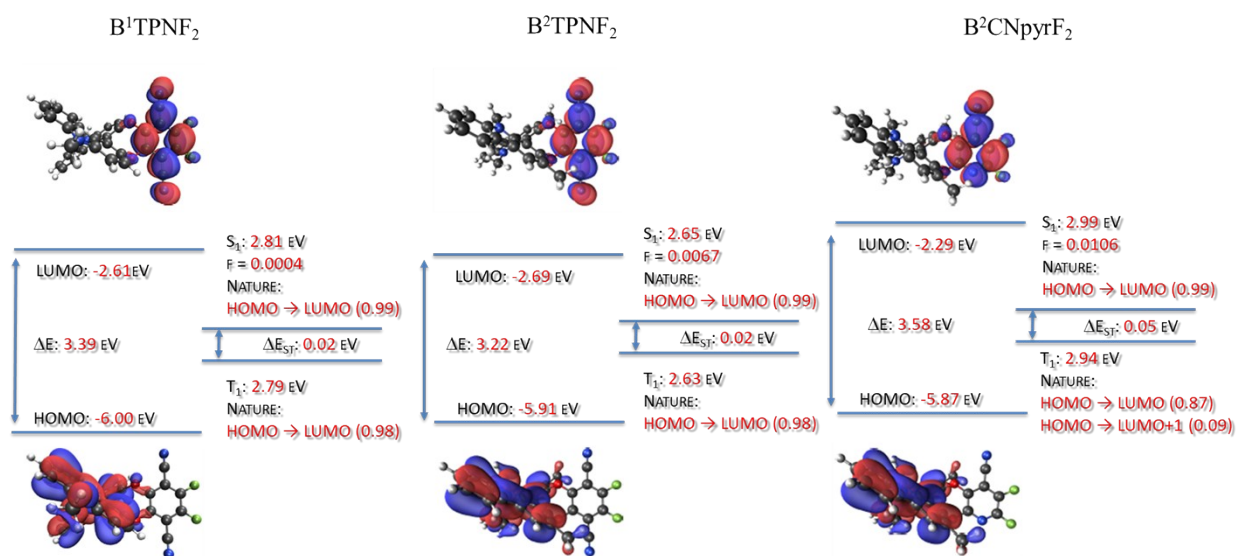


Figure S62: Calculated optical gaps, S_1 and T_1 energy levels and isosurfaces (isovalue 0.02) of HOMO-LUMO orbitals for **B¹TPNF₂**, **B²TPNF₂** and **B²CNPyrF₂**

Theoretical dissymmetry factor calculations

The optimized geometry in the S_1 state and transition electric and magnetic dipole moments were calculated using time-dependent DFT at the M062X/6-311G(d,p) level of theory in toluene phase in the Gaussian (G16) package.

The calculated $|g_{lum}|$ s for **B¹TPNF₂**, **B²TPNF₂** and **B²CNPyrF₂** are 5.40×10^{-4} , 3.12×10^{-3} and 1.84×10^{-4} , respectively. A moderate transition magnetic dipole moment and larger $\cos\theta$ value make **B²TPNF₂** show the largest $|g_{lum}|$, which corresponds to the experimental result. (The experimental values of $|g_{lum}|$ s are 7×10^{-4} , 2.0×10^{-3} and 8×10^{-4} for **B¹TPNF₂**, **B²TPNF₂** and **B²CNPyrF₂** in toluene solutions, respectively.)

Table S2. Transition electric dipole moments (μ) of S_1 - S_0 in optimized S_1 geometry

	μ in atomic units (a.u.)				μ in CGS Units (10^{-20} esu-cm)			
	x	y	z	$ \mu $	x	y	z	$ \mu $
B¹TPNF₂	-0.383	0.037	0.161	0.417	-97.3	9.54	40.8	106
B²TPNF₂	0.000	0.501	-0.099	0.510	0.025	127	-25.1	130
B²CNPyrF₂	-0.036	0.614	-0.092	0.622	-9.11	156	-23.4	158

Table S3. Transition magnetic dipole moments (m) of S_1 - S_0 in optimized S_1 geometry

	m in atomic units (a.u.)				m in CGS Units (10^{-20} erg/Gauss)			
	x	y	z	$ m $	x	y	z	$ m $
B¹TPNF₂	0.106	-0.058	0.306	0.329	-0.098	0.054	-0.283	0.305
B²TPNF₂	0	0.136	0.127	0.187	0	-0.126	-0.118	0.173
B²CNPyrF₂	0.024	0.014	0.034	0.044	-0.022	-0.013	-0.031	0.041

Table S4. Summary of chiroptical properties of S_1 - S_0 in optimized S_1 geometry

	$ \mu $ (10^{-20} esu-cm)	$ m $ (10^{-20} erg/Gauss)	θ	$ \cos\theta $	$ g $
B¹TPNF₂	106	0.305	93	0.047	5.40×10^{-4}
B²TPNF₂	130	0.173	126	0.585	3.12×10^{-3}
B²CNPyrF₂	158	0.041	100	0.180	1.84×10^{-4}

Cartesian coordinates of the optimized geometry in S_1 state **B¹TPNF₂** (M06-2X/6-31G(d,p)/CPCM(Toluene)):

```

C      -3.25122100 -0.65740500  1.55655600
C      -4.42745500 -1.03446600  2.20486700
C      -4.98015100  2.18746300 -2.21647000
C      -2.60873200  1.58055500 -0.88822600
C      -3.17459700  2.87742400 -0.83110200
C      -4.36359900  3.19367100 -1.49440400
C      -1.38941600  1.64102000 -0.11121600
C      -1.27050900  2.97601100  0.34617300
N      -2.36992500  3.69693400 -0.07049900
C      -0.37715300  0.72407100  0.20345400
C      0.72360800  1.18290500  0.93746900
  
```

C	0.83710600	2.50335100	1.36314700
C	-0.16250300	3.41788600	1.07186800
C	-0.35376700	-0.68618900	-0.21301000
C	-1.30045300	-1.63974900	0.09857100
C	-1.09513800	-2.99623000	-0.30879900
C	0.06428400	-3.41621800	-1.00833700
C	1.01061600	-2.46971500	-1.30204700
C	0.79858100	-1.12680100	-0.93749400
C	-2.53827000	-1.62852300	0.86420200
C	-3.01674300	-2.95326200	0.84907800
N	-2.12416800	-3.75215900	0.13132500
C	-4.88980200	-2.35099000	2.16748300
C	-4.18690700	-3.34098300	1.48798300
C	-2.29174700	-5.18601800	-0.02870400
C	-2.58081300	5.11458000	0.13508700
O	1.66140300	0.24923800	1.34049800
O	1.65869000	-0.17731000	-1.34655600
C	2.87675400	-0.08976500	-0.67602000
C	4.07666100	-0.25816400	-1.41866700
C	5.28463200	-0.07661700	-0.67749700
C	5.27832300	0.22135500	0.64681100
C	4.06689600	0.37276000	1.38956100
C	2.86012000	0.20295700	0.65890800
C	4.06168700	-0.64703900	-2.76319600
C	4.06152500	0.70364400	2.75229200
N	4.04180400	0.98934000	3.87539500
N	4.01900700	-0.98650200	-3.87196800
F	6.44923600	-0.21749300	-1.32425900
F	6.43881000	0.38834100	1.29449300
C	-4.43087100	0.89710200	-2.29112100
C	-3.25161000	0.58759200	-1.63620700
H	-2.90465800	0.36611300	1.59851300
H	-4.99254300	-0.28885900	2.74898200
H	-5.90105400	2.40356700	-2.74429600
H	-4.78113500	4.19203000	-1.46090400
H	1.70625800	2.78686700	1.94415100
H	-0.07463200	4.44495700	1.40144100
H	0.20589100	-4.44705600	-1.30165500
H	1.91240100	-2.71591900	-1.84789300
H	-5.80690800	-2.61025300	2.68048200
H	-4.53626800	-4.36542200	1.46902400
H	-1.56041900	-5.56405600	-0.73643200
H	-3.29243100	-5.38649800	-0.41128600
H	-2.16124200	-5.68240700	0.93425000
H	-3.64780400	5.30750100	0.24307900
H	-2.18866200	5.70057300	-0.69970400
H	-2.08839000	5.42322000	1.05568800
H	-4.93475200	0.13797800	-2.87583300
H	-2.82982600	-0.40597900	-1.71697700

Cartesian coordinates of the optimized geometry in S_1 state in toluene B^2TPNF_2 :

C	-5.15592200	-0.08484400	0.67323900
C	-5.15587700	0.08463600	-0.67336000
C	-3.94600300	0.19962500	-1.41928700
C	-2.73279200	0.12035000	-0.67302600
C	-2.73283000	-0.12085700	0.67304300
C	-3.94610200	-0.19994600	1.41924100
F	-6.31807900	-0.16557300	1.33507500
F	-6.31798900	0.16558400	-1.33524900
C	-3.95044800	-0.35473200	2.81147200
C	-3.95022800	0.35460000	-2.81149900
O	-1.54393300	0.23526200	-1.37399700
O	-1.54399300	-0.23578800	1.37406600
N	-3.93581900	-0.49755200	3.96254300
N	-3.93545300	0.49762200	-3.96254300
C	-0.64408100	-1.18036700	0.92896100
C	0.45622600	-0.70390200	0.19168300
C	1.45048800	-1.64824200	-0.14851500
C	1.35949900	-2.99072800	0.29684200
C	0.26181300	-3.40487200	1.02313200
C	-0.76885800	-2.50193500	1.35034400
C	0.45613900	0.70373900	-0.19151700
C	-0.64416900	1.17997600	-0.92892300
C	-0.76914900	2.50146800	-1.35043100
C	0.26136700	3.40459600	-1.02326900
C	1.35908100	2.99068800	-0.29688000
C	1.45025400	1.64826000	0.14864400
N	2.57330600	-1.50685900	-0.92320800
C	3.25403100	-2.72421200	-0.95678900
C	2.53241100	-3.67650100	-0.21057100
C	2.53186800	3.67670100	0.21049500
C	3.25359300	2.72462100	0.95687200
N	2.57304800	1.50716400	0.92343800
C	4.45208900	-3.03634900	-1.59573600
C	4.91207500	-4.34039500	-1.47652200
C	4.20182700	-5.30066300	-0.74549300
C	3.00895300	-4.97868800	-0.10880800
C	3.00822000	4.97894600	0.10858100
C	4.20101500	5.30118500	0.74528200
C	4.91136700	4.34112200	1.47647700
C	4.45156700	3.03702400	1.59584400
C	2.96466300	-0.35669400	-1.71845900
C	2.96454300	0.35721500	1.71893300
C	-1.94583500	2.93050400	-2.17276000
C	-1.94547500	-2.93128800	2.17259900
H	0.18298200	-4.43363100	1.35674200
H	0.18239600	4.43330800	-1.35699000
H	5.01366700	-2.29951400	-2.15520600
H	5.84061000	-4.61874500	-1.95863800
H	4.59073000	-6.30849500	-0.67531500
H	2.46401400	-5.72615600	0.45487200

H	2.46319700	5.72625700	-0.45522500
H	4.58977000	6.30906600	0.67498900
H	5.83983400	4.61967600	1.95860700
H	5.01322200	2.30034800	2.15544900
H	2.07338900	0.16473300	-2.06566400
H	3.58465300	0.33774100	-1.14355200
H	3.52414700	-0.70849800	-2.58239000
H	3.52393700	0.70928300	2.58281400
H	2.07333900	-0.16427700	2.06621200
H	3.58466700	-0.33723800	1.14419400
H	-2.86870200	2.85898800	-1.59074100
H	-1.82561400	3.95932800	-2.50907600
H	-2.07327700	2.28089700	-3.04092500
H	-2.86834500	-2.85988400	1.59057600
H	-1.82505900	-3.96013000	2.50878800
H	-2.07305000	-2.28181800	3.04084400

Cartesian coordinates of the optimized geometry in S_1 state in toluene **B²CNPyrF₂**:

C	-5.10422200	0.17991700	-1.19804900
C	-5.30843700	-0.01864000	0.13307400
C	-4.19540300	-0.17016300	1.01710300
C	-2.92650100	-0.11176800	0.35995800
C	-2.86726200	0.13812400	-0.98711500
N	-3.91554700	0.27328700	-1.80253600
F	-6.17424800	0.30731100	-1.99954300
F	-6.55066600	-0.08415000	0.63863100
O	-1.78115300	-0.23343600	1.13139700
O	-1.62206600	0.21347200	-1.60345100
C	-0.75944200	1.16412600	-1.11809800
C	0.30357700	0.70221300	-0.31271700
C	1.27029900	1.65879900	0.07024800
C	1.19763300	2.99428200	-0.39734100
C	0.13840200	3.39377400	-1.18867600
C	-0.86869000	2.48099000	-1.55783800
C	0.28776300	-0.70151800	0.08039400
C	-0.86226700	-1.17996800	0.74179700
C	-1.01722600	-2.50155300	1.15105300
C	0.03640200	-3.40187300	0.90389500
C	1.18629200	-2.98521200	0.26034100
C	1.30626100	-1.64549800	-0.18268900
N	2.34467600	1.53555200	0.91449400
C	3.01494200	2.75700100	0.97217500
C	2.33418900	3.69387600	0.16898500
C	2.39281600	-3.67042900	-0.15831700
C	3.16386900	-2.72088300	-0.85833700
N	2.48099600	-1.50563500	-0.87916300
C	4.16963000	3.08680900	1.67885900
C	4.62886400	4.39177600	1.56845300
C	3.95935500	5.33644500	0.78043100
C	2.80952300	4.99757800	0.07727600

C	2.86526500	-4.97092300	-0.01418300
C	4.09984800	-5.29387900	-0.56362900
C	4.85744000	-4.33665000	-1.25088400
C	4.40412400	-3.03487200	-1.41051000
C	2.68611000	0.40025500	1.75278300
C	2.91937500	-0.36261500	-1.65964300
C	-2.25344300	-2.92609700	1.88442900
C	-2.01715700	2.89455700	-2.42842600
C	-4.32836400	-0.34299300	2.39470500
N	-4.41596800	-0.50601900	3.54314300
H	0.07348500	4.41851100	-1.53814800
H	-0.06318000	-4.43037000	1.23306600
H	4.69958900	2.36223700	2.28345200
H	5.52441100	4.68334100	2.10242400
H	4.34632500	6.34565600	0.71897000
H	2.29558000	5.73310900	-0.52962700
H	2.28425600	-5.71554900	0.51646700
H	4.48564700	-6.29993600	-0.45855100
H	5.81804100	-4.61582200	-1.66501200
H	5.00172000	-2.29979500	-1.93398400
H	1.77435500	-0.11588700	2.05183900
H	3.34047100	-0.30405500	1.23065500
H	3.19008400	0.76808700	2.64379600
H	2.05046600	0.15373500	-2.06619700
H	3.50147900	0.33961700	-1.05554400
H	3.53213500	-0.72183000	-2.48366300
H	-3.13101200	-2.84553500	1.23720600
H	-2.16459100	-3.95661200	2.22571800
H	-2.44092300	-2.27744300	2.74262800
H	-2.26726800	2.10740500	-3.14058000
H	-2.91318300	3.05304000	-1.82138200
H	-1.78839300	3.81916300	-2.95751800

Isosurfaces of LUMO+1 for **B¹TPNF₂**, **B²TPNF₂** and **B²CNPyrF₂**

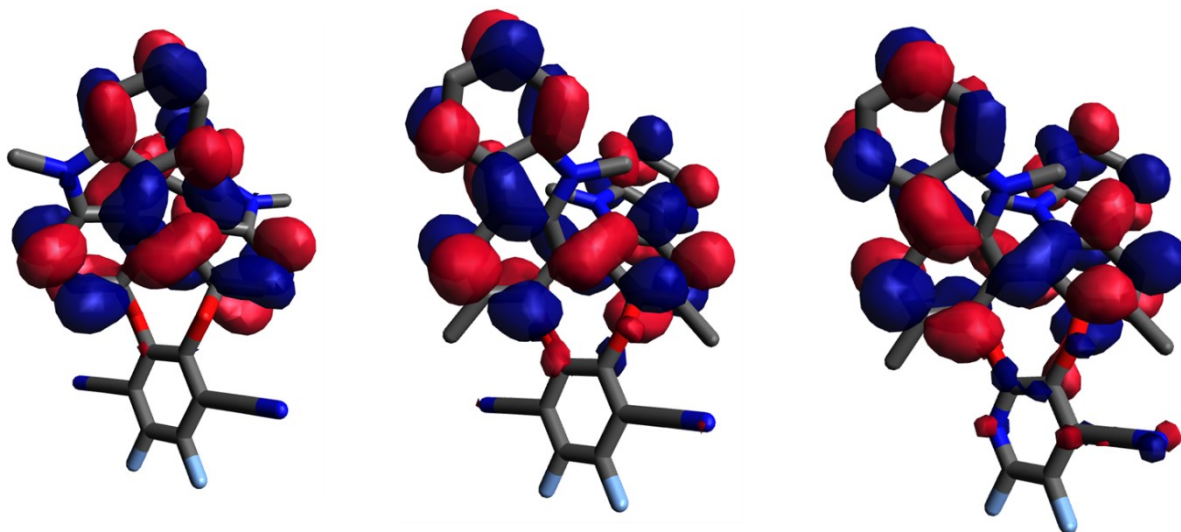


Figure S63. Isosurfaces (isovalue 0.02) of LUMO+1 for **B¹TPNF₂**, **B²TPNF₂** AND **B²CNPyrF₂**
 UV-Vis spectra and computational details regarding the first excitations and oscillator strengths for each compound

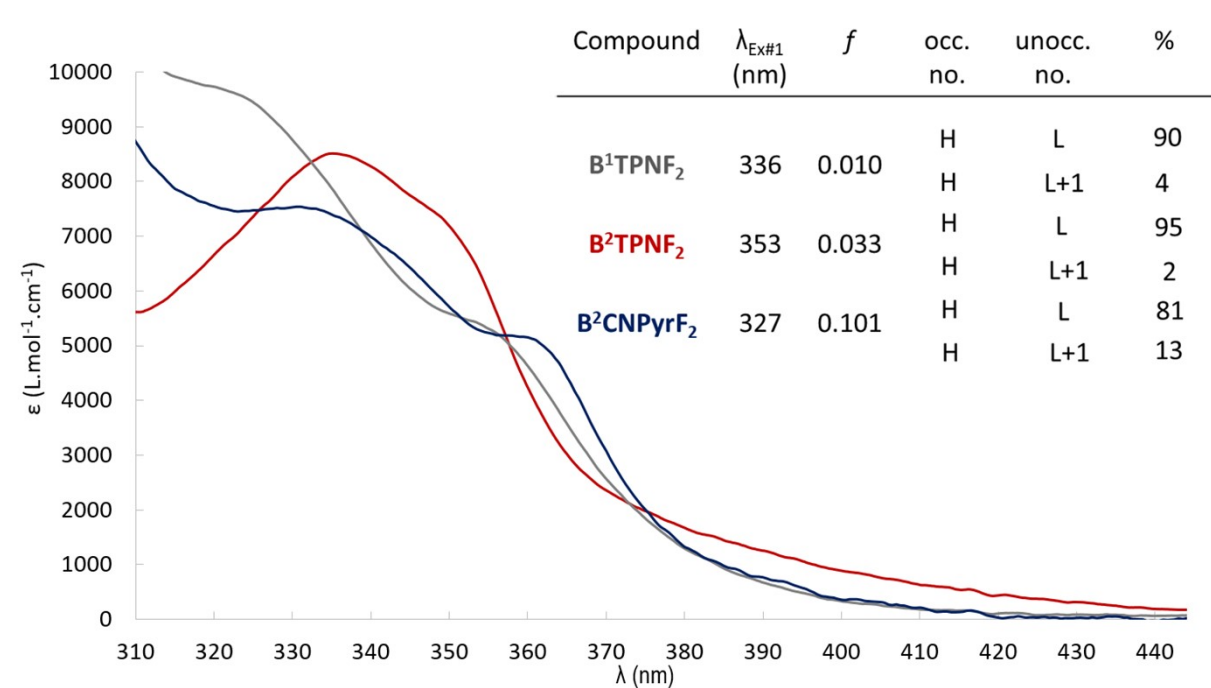


Figure S64. UV-vis spectra of **B¹TPNF₂** (grey line), **B²TPNF₂** (red line) and **B²CNPyrF₂** (blue line) in DCM and computational details regarding the first excitations and oscillator strengths for each compound.

References:

- [S1] C. Würth, M. Grabolle, J. Pauli, M. Spieles, U. resch-Genger, *Nature protocols*, 2013, **8**, 1535-1550
- [S2]. V. V. Pavlishchuk, A. W Addison, *Inorganica Chim. Acta*. 2000, **298**, 97-102
- [S3]: Gaussian 16, Revision B.01, M. J. Frisch, G. W. Trucks, H. B. Schlegel, G. E. Scuseria, M. A. Robb, J. R. Cheeseman, G. Scalmani, V. Barone, G. A. Petersson, H. Nakatsuji, X. Li, M. Caricato, A. V. Marenich, J. Bloino, B. G. Janesko, R. Gomperts, B. Mennucci, H. P. Hratchian, J. V. Ortiz, A. F. Izmaylov, J. L. Sonnenberg, D. Williams-Young, F. Ding, F. Lipparini, F. Egidi, J. Goings, B. Peng, A. Petrone, T. Henderson, D. Ranasinghe, V. G. Zakrzewski, J. Gao, N. Rega, G. Zheng, W. Liang, M. Hada, M. Ehara, K. Toyota, R. Fukuda, J. Hasegawa, M. Ishida, T. Nakajima, Y. Honda, O. Kitao, H. Nakai, T. Vreven, K. Throssell, J. A. Montgomery, Jr., J. E. Peralta, F. Ogliaro, M. J. Bearpark, J. J. Heyd, E. N. Brothers, K. N. Kudin, V. N. Staroverov, T. A. Keith, R. Kobayashi, J. Normand, K. Raghavachari, A. P. Rendell, J. C. Burant, S. S. Iyengar, J. Tomasi, M. Cossi, J. M. Millam, M. Klene, C. Adamo, R. Cammi, J. W. Ochterski, R. L. Martin, K. Morokuma, O. Farkas, J. B. Foresman, and D. J. Fox, Gaussian, Inc., Wallingford CT, 2016.
- [S4] H. Kubo, T. Hirose, T. Nakashima, T. Kawai, J.Y. Hasegawa, K. Matsuda, *J. Phys. Chem. Lett.*, 2021, **12**, 686-695
- [S5] S. Kasemthaveechok, L. Abella, M. Jean, M. Cordier, T. Roisnel, N. Vanthuyne, T. Guizouarn, O. Cador, J. Autschbach, J. Crassous and L. Favereau, *J. Am. Chem. Soc.*, 2020, **142**, 20409-20418
- [S6]. J. Dai, D. Fu and S. Ma, *Eur. J. Org. Chem.* 2015, 5655– 5662
- [S7]. H. Kang, M. Herling, K.A. Niedered, Y.E. Lee, P.V.G. Reddy, S. Dey, D.E. Allen, P. Sung, K. Hewwit, C. Torruellas, G.J. Kin and M.C. Kozlowski, *J. Org. Chem.* 2018, **83**, 14362– 14384